INFLUENCE OF WOOD SPECIES ON PROPERTIES OF WOOD/HDPE COMPOSITES

By

WILLIAM GACITUA ESCOBAR

A dissertation/thesis submitted in partial fulfillment of
The requirements for the degree of

DOCTOR OF PHILOSOPHY

WASHINGTON STATE UNIVERSITY
Department of Civil and Environmental Engineering

May 2008

To the Faculty of Washington State University:

The members of the committee appointed to examine the dissertation/thesis of WILLIAM GACITUA ESCOBAR find it satisfactory and recommended that it be accepted.

Chair

ACKNOWLEDGMENT

I would like to thank my major professor, Dr. Michael P. Wolcott, and my committee members; Dr. David Bahr, Dr. William Cofer and Dr. Vikram Yadama.

Thanks to the staff at Wood Material and Engineering Laboratory for their kind help. To all my good friends here in US, my gratitude especially to Brent, Karl and Eduarcito. I would also like to extend a special thanks to my friend at University of Bio-Bio, Dr. Aldo Ballerini.

To my great family, to Luis and Nelly, to Dany and Jacqueline, to my brother Marcelo and his family…

INFLUENCE OF WOOD SPECIES ON PROPERTIES OF WOOD/HDPE COMPOSITES

Abstract

by William Gacitua Escobar, Ph.D.
Washington State University
May 2008

Chair: Michael P. Wolcott

Methodologies were developed to analyze the wood species effect on performance of wood plastic composites (WPC). In an experiment designed to analyze the physical interaction between a molten thermoplastic and solid wood, results showed a high correlation between the potential area for transverse flow and the interaction between HDPE and wood species. Cell collapse in specific wood species was identified as a probable mechanism impeding mobility of the thermoplastic and thus the interpenetration and interfacial area. It was possible to quantify the mechanical interlocking type of adhesion using a numerical factor; this factor represents the slippage between phases, which is determined by using a viscoelastic model and its parameters as an analogy. Another associated factor contributing to the final strength and variability of WPCs was the void content. A poor interpenetration of the molten thermoplastic into the cell lumens generates conditions for the free buckling of cell walls during extrusion, which finally results in an important source of void generation. We also proposed an adapted rule of mixture. In the new model for predicting the modulus in the 1-Direction, it was assumed that the TCL (transcrystalline layer) and bulk matrix had similar mechanical properties. The new model also introduced a modification factor affecting filler properties. This factor represents the modulus reduction in wood cells due to

processing, and is expressed as a reduction in modulus in the 1-Direction, where the modulus of the natural filler in a composite was evaluated with nanoindentations. A model was developed a more detailed prediction model based on these measurements, which provided very good approximations to experimental results in the modulus of elasticity for lodgepole pine and grand fir composites in coupled and uncoupled systems.

TABLE OF CONTENTS

LIST OF TABLES

LIST OF FIGURES

Dedication

To my parents… Luis Arnoldo and Rosa Nelly

CHAPTER 1
INTRODUCTION

Wood plastic composites (WPCs) are hybrid materials with the properties of both plastics (polyethylene, polypropylene, PVC, etc.) and wood (natural polymer). These natural polymers are generally used as wood flour. Many studies show significant effects related to variables such as the size and amount of fillers, coupling agents, types of thermoplastic matrix and additives (Dalvag et al. 1985; Harper 2003; Matuana et al. 1998; Stark 1997; Stark and Rowlands 2003). Little research has been conducted on the influence of wood species on the engineering properties of WPCs, although wood comprises a majority of the material. Important unanswered questions include:

- How the use of different wood species affects the mechanical properties of WPCs
- How wood flour size affects the performance of a WPC made with a specific wood species
- Whether the same extrusion conditions (temperature, pressure and speed) can be used for all wood species
- Whether coupling agents must be used with specific wood species
- Whether physical and mechanical wood-plastic interactions are similar with different wood species, and how this affects WPC properties
- Whether it is possible to predict properties of WPCs made from different species

Wood species have an important influence on the properties of wood-thermoplastic composites (Stark, 1997), predominantly because wood structure controls the flow direction of the thermoplastic movement in cell lumens. The location where the wood material is collected from the log is another factor that results in different levels of plastic interlocking. Finally, the surface topography of the solid phase affects physical interactions between wood and thermoplastics; however, this aspect has not been addressed in the scientific literature.

WPCs can be made from many wood species, and mainly are formed by introducing wood flour from softwoods and hardwoods in a continuous extrusion process. Nowadays, there is tremendous interest in understanding how wood particles and the surrounding plastic matrix behave at both the macroscopic and microscopic levels. This mechanical interlocking is an important mechanism for adhesion that could relate to the performance of composites.

Due to the complex flow process controlling the penetration of a thermoplastic into the wood structure, it is difficult to state whether one wood species is superior to another one as a filler material, especially when some additives enhance adhesion and stress transfer between phases. Wood is a complex structure consisting of discontinuous fibers (mainly made of cellulose) embedded in an organic matrix acting as glue (lignin). The tortuous structure of wood, generated by the interconnectivity of anatomical structures called pits, creates differing degrees of fluid mobility and final interpenetration in some dynamic processes. Because the conversion of solid wood into wood flour results in a more complex filler structure with a non-uniform surface morphology than conventional fillers, it is difficult to quantify and model the mechanical contribution of a particular filler to the stiffness and strength of a natural fiber composite. Also, collapse of the hollow wood cells may impede penetration of the thermoplastic and affects the performance of a WPC. Cellular collapse occurs through *elastic buckling, plastic* *yielding, or brittle crushing*, depending on the test conditions and the nature of the cell wall material (Wolcott, 1989; Gibson and Ashby 1997).

Collapse of wood cells during extrusion may reduce the potential surface area for stress transfer between phases, affecting the mechanical properties of composites. On the other hand, undamaged wood cells can potentially be filled with thermoplastic, thereby enhancing the toughness and strength of the WPC. The structure and properties of the cell wall directly relate to cell collapse. The cell wall of any wood species can be considered an anisotropic material. The tilt angle of the cellulose fibrils with respect to the longitudinal cell axis, often called the microfibril angle (MFA), can vary considerably within a single individual tree. This is a key parameter in determining the mechanical strength and elasticity of wood (Bodig, 1982; Salmen, 2004; Wood Handbook, 1999).

Nanoindentation testing, a method of hardness testing at a very small scale applied to the study of mechanical properties of a variety of materials, may be useful in characterizing the mechanical behavior of the cell wall and other phases in a WPC. Gindl et al. (2004) and Wimmer et al. (1997) demonstrated that is possible to measure and study the structural variability of the cell wall with this method, where the MFA is the main factor.

Finally, understanding the physical interaction between filler and matrix, adhesion between them and filler damage helps us to model the effects of internal flaws, generated during extrusion, and quantify their contribution to the mechanical properties of the composite under monotonic loading. Damage may occur in one or more forms, such as the failure of the filler-matrix interface, matrix cracking or crazing, fiber breaking, and void growth. In composites, initial damage propagation may be arrested by the internal structure of the composite (Agarwal & Broutman, 1990). In critical applications, design loads should be less than those that are known to cause damage within the composite. Therefore, a good understanding of various aspects of WPC microstructure will definitely aid in the design of structures using this material.

In WPC production, the system is difficult to analyze and model. Many phenomena make modeling difficult; among them are wood particle alignment, wood cell densification due to cellular collapse, cell wall damage due to environmental conditions (temperature and pressure), and the presence of small voids distributed mainly in the thermoplastic phase (Facca, 2006). In this scenario, it is necessary to adapt actual models for better prediction of WPCs properties.

PROJECT OBJECTIVES

WPCs properties not only depend on specific adhesion and processing conditions, but are also are related to the nature and thermomechanical behavior of wood particles in an extrusion or injection molding process. Therefore, we explore how wood particles behave during processing and how this affects the performance of natural fiber composites in order to develop new, customized composites based on wood species properties. We also established quantitative correlations between mechanical properties, microstructure and phase properties in WPCs produced with different wood species. Then, the specific objectives of this research are to:

1. Quantify the contribution of anatomical features of wood that could relate to the physical interaction (interlocking) between a molten thermoplastic and the wood cell structure.

2. Evaluate the contribution of anatomical features of different wood species affecting the interrelation wood fiber-matrix and mechanical behavior of wood plastic composites.
3. Relate the morphological properties of wood particles and matrix with the mechanical behavior of WPCs.
4. Develop methodologies to quantify phase properties and define new adapted prediction models based on microstructure and nanoproperties characterization.

Figure 1.1 and 1.2 show an overview of the analysis at different scales next to the responses and results associated to each stage and chapter.

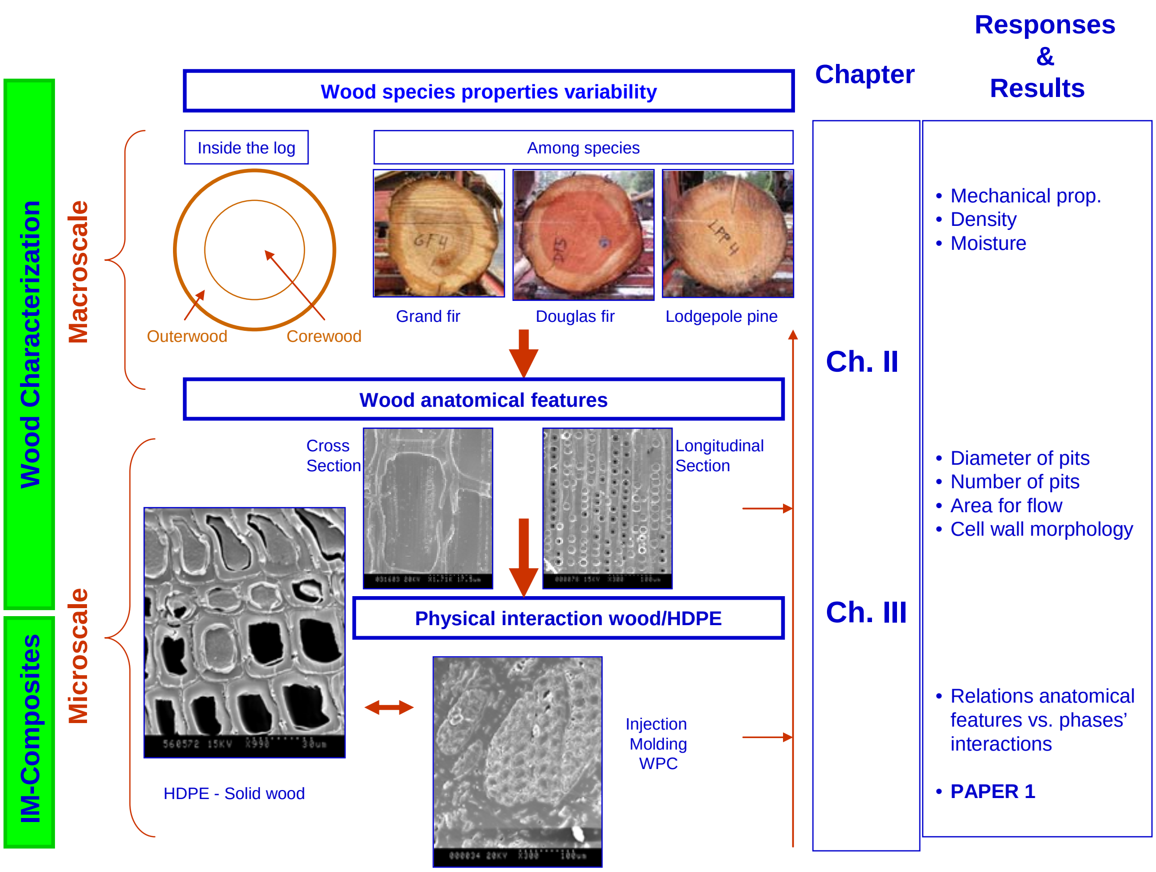

Figure 1.1: Wood characterization of wood species and Injection Molding (IM) composites made of different wood species. Responses and results.

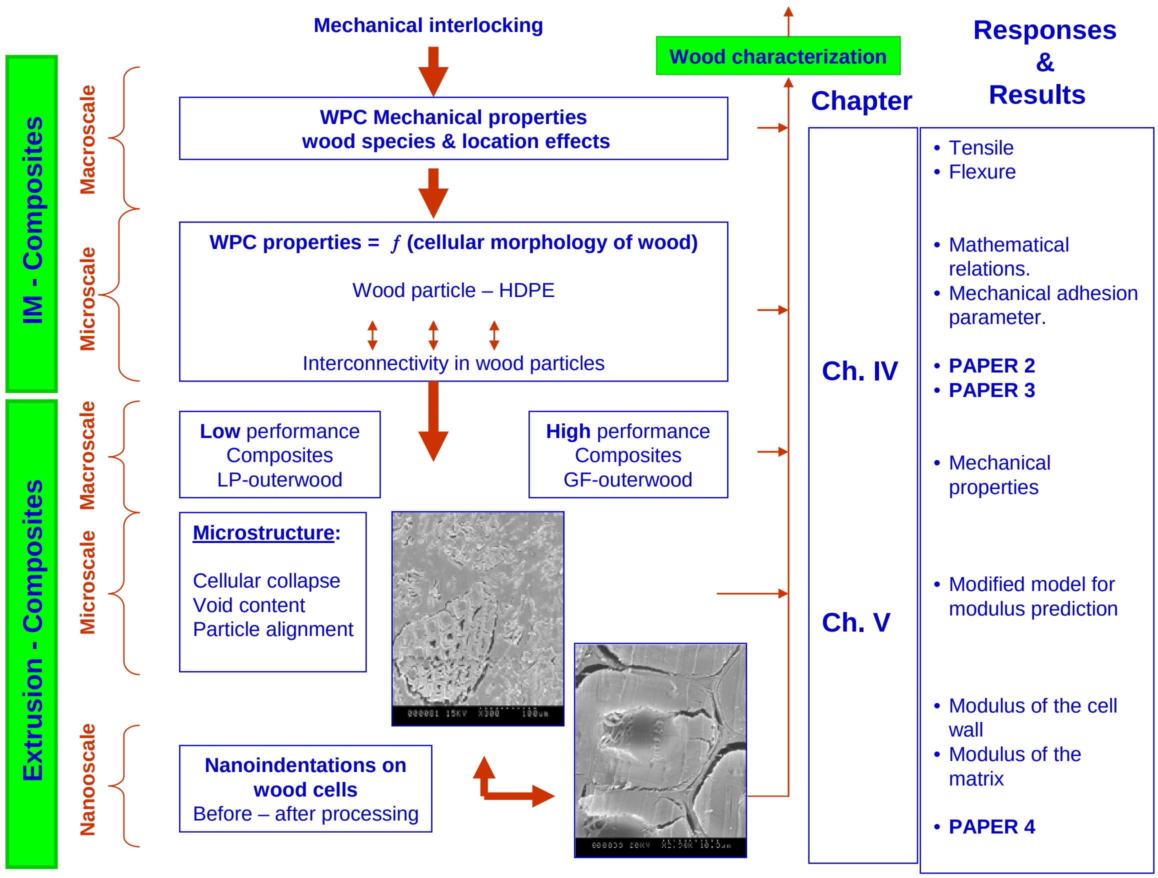

Figure 1.2: Injection Molding (IM) composites and Extrusion composites made of different wood species. Responses and results.

REFERENCES

Agarwal B., Broutman L. Analysis and performance of fiber composites. John Wiley & Sons Inc. 1990.

Bodig J., Jayne B.A. Mechanics of wood and wood composites. Van Nostrand Reinhold Inc., 1982 p 317.

Dalvag H., Klason C., Stromvall H.-E. 1985. The Efficiency of Cellulosic Fillers in Common Thermoplastics. Part II. Filling with Processing Aids and Coupling Agents. International Journal of Polymeric Materials, Vol. 11, pp. 9-38.

Facca, A. 2006. Predicting the tensile modulus and strength of single and hybrid natural fibre reinforced thermoplastic composites. Ph.D thesis dissertation, Graduate Department of Chemical Engineering and Applied Chemistry University of Toronto, Canada.

Gibson L., Ashby M. Cellular solids: structure and properties. 2nd edition.,1997. Cambridge university press.

Gindl W., Gupta H.S. 2002. Cell-wall hardness and Young's modulus of melamine-modified spruce wood by nanoindentation. Composite part A, 33 pp. 1141-1145.

Harper D. 2003. A thermodynamic, spectroscopic, and mechanical characterization of the wood-polypropylene Interphase. Thesis dissertation, Wood Material and Engineering Laboratory, Washington State University, Pullman WA.

Horst J., Salienko N., Spoormaker J. 1998. Fibre-matrix debonding stress analysis for short fibre-reinforced materials with matrix plasticity, finite element modeling and experimental verification.

Hull D., Clyne T.W. An introduction to composites materials. Cambridge solid state science series, 1996 p 27.

Matuana L. M., Balatinecz J. J., Park C. B., 1998. Effect of surface properties on the adhesion between PVC and wood veneer laminates. Polym. Engineering and Sci. 38(5) 765.

Salmen, L. 2004. Micromechanical understanding of the cell wall structure. C.R. Biologies 327, 873-880.

Sirvio J., Karenlampi P., 1998. Pits as natural irregularities in softwood fibers. Wood and fiber science, 30 (1), pp. 27-39.

Smith M., Dai H., Ramani K., 2002. Wood-thermoplastic adhesive – method of characterization and results. International Journal of Adhesion and Adhesives,22 pp 197-204.

Stark N. (1997). Effect of Species and Particle Size on Properties of Wood-Flour-Filled Polypropylene Composites. Intertech conferences, Functional fillers for thermoplastics and thermosets.

Stark N., Rowlands R. (2003). Effects of wood fiber characteristics on mechanical properties of wood/polypropylene composites. Wood fiber and science, 35 (2): 167-174.

Wimmer R., Lucas B.N., Tsui T.Y., Oliver W.C. WC. Longitudinal hardness and Young's modulus of spruce tracheid secondary walls using nanoindentation technique .Wood Sci. Technol. 1997; 31: 131.

Wolcott, M.P. 1989. Modeling viscoelastic cellular materials for the pressing of wood composites. PhD Dissertation. VPI&SU, Blacksburg, VA.

Wolcott M. P. Mechanical interlocking in wood-plastic composites: southern yellow pine vs Douglas-fir filler. Internal report, Wood material and engineering laboratory, Pullman, WA. 2003.

Wood handbook. Wood as an engineering material. General technical report FPL-GTR 113. Forest product laboratory, 1999.

CHAPTER 2
MORPHOLOGY OF WOOD SPECIES AFFECTING WOOD-PLASTIC INTERACTION. PART 1: MECHANICAL INTERLOCKING

ABSTRACT

The main objective of this research is to quantify the anatomical features that could relate to the interaction between a molten thermoplastic and the wood cell structure. Using a vacuum bagging process and scanning electron microscopy (SEM), we studied the mechanical interlocking mechanism between wood species from small diameter logs and high density polyethylene (HDPE) without coupling agents or additives. Both the vacuum process and the pressure at high temperatures increased flow of the HDPE, mainly through the radial face (tangential direction) in small softwood samples. This flow generated a 3D interpenetration of the thermoplastic into the cellular wood structure. As a result, a contact interfacial area of HDPE-cell wall appears. According to SEM analysis, the presence of open pits and their size and distribution on the cell wall create a potential path for the transverse movement of HDPE. The collapse of cell walls under pressure during the vacuum bagging experiment was identified as a competing phenomenon, preventing the free flow of the molten thermoplastic. Empirical models based on the main effects and interactions were constructed to estimate the wood-thermoplastic interaction. Both penetration and interface area are significantly affected by the presence of earlywood or latewood. The wood species grand fir (*Abies grandis*) presented the highest interfacial area, indicating potential for stress transfer in a composite. The interaction within tree location of the wood sample and the wood species is also an important factor to consider. The vacuum bagging cycle used here, combined

with the morphology analysis with SEM, provided a good comparison of the physical interaction of a thermoplastic with different wood species.

INTRODUCTION

There is a tremendous interest in finding new applications for small logs from dry, moist and cold forests in the Inland Northwest region, as well as their sawmill wastes. These forests contain small diameter trees of less than 12 inches diameter (Russell 2002). One of the most challenging uses for these small logs and sawmills wastes is the production of wood plastic composites (WPC); for this, it is relevant to understand the physical, chemical and mechanical relations between wood and matrix when wood species are utilized as a filler material. There are a variety of available wood species in the Inland region that are potentially useful in producing WPC, but before starting massive production it is necessary to understand how wood particles and surrounding plastic matrix behave at macroscopic and microscopic levels. This is referred to as mechanical interlocking, and is an important mechanism for adhesion. Because wood is very hydrophilic and plastic for many WPC are very hydrophobic, achieving a strong bond between these two materials can be challenging. Chemical means such as coupling agents have been used with success to improve the interfacial bond between the wood particles and plastic, thereby increasing certain mechanical properties (Dalvag et al. 1985, Matuana et al. 1998, Harper 2003). At this point, and due to the complex mobility process of a thermoplastic into the wood, it is difficult to state if one wood species is superior to another as a filler material.

Wood is a complex structure consisting of discontinuous fibers that are primarily composed of cellulose embedded in an organic matrix of lignin. The tortuous structure of wood is generated by the interconnectivity of anatomical structures called pits, resulting in different levels of fluid mobility and final interpenetration in some dynamic processes.

Small openings in the cell wall called pits are created where the secondary wall has not formed. These structures are normally matched in pairs between adjacent cells, allowing liquids to pass freely from one cell to the next. However, because of their small size, they can be easily plugged by deposits in the heartwood of some wood species, making the cell wall almost impermeable to liquids and therefore difficult to treat (Milton 1995).

From the mechanical point of view, other authors (Sirvio and Karenlampi 1998) have suggested that the appearance of pits as stress-enhancing irregularities in fiber structure should be considered in fiber network theories predicting composites properties, as well as in the measurement of the mechanical properties of fibers. They found that relative pit size and pit density was greatest in the vicinity of fiber tips, and the strength of the fiber was lowest there.

In an experiment to quantify the interaction of wood with a thermoplastic adhesive (Smith et al. 2002), they found that the thermoplastic adhesive (a blend of isotactic polypropylene and ethylene-propylene copolymer) can penetrate the vascular tissue of oak (*Quercus*) for more than 150 μm through openings 15 μm across. They conclude that the amount of mechanical interlocking of the thermoplastic adhesive and the wood surface is dependent on the processing details of the adhesive joint, the porosity of the wood surface, viscosity of the molten adhesive, applied pressure and the processing duration. The resulting adhesive-adherend interaction is referred to the mechanical theory of adhesion, and applies to rough and porous surfaces. Surface roughness of interest may range in scale from hundreds of microns to nanometers. The increase in surface area, possibly by a very high factor, also raises the surface energy when expressed per unit nominal area.

Rough surfaces, when stressed, may be able to redistribute the stress so as to increase energy dissipation during failure of the joint (Packham 2003). The strengthening of an interface resulting from increasing roughness may change the mechanism of fracture from a less to a more energetic mode. With increasing interfacial roughness between two incompatible polymers, the mechanism may change from chain pull-out to crazing or other forms of plastic deformation (Packham 2003). For moderately rough surfaces, an increase in surface area may lead to a proportionate increase in adhesion, as long as the roughness does not reduce contact between the surfaces (Gen and Lai 1995).

On the other hand, a diffusion process operates during the interaction of a solid with a viscous fluid. If we consider wood a porous medium characterized by an absolute permeability K, then the fluid flow through the wood can be described by Darcy's law (Gibson and Ashby 1997):

$$u = -\frac{K}{\mu}\frac{dp}{dx} \qquad \text{Eq. 2.1}$$

where u is the velocity of the fluid, μ is its dynamic viscosity and dp/dx is the pressure gradient. The units of K are m^2, and those for the dynamic viscosity are Ns/m^2. For a permeable material like wood, with pores of diameter d (for longitudinal flow those porous are lumens, and for transverse flow pits can be considered as those pores), the permeability factor becomes:

$$K = A\, d^2 (1 - \rho/\rho_s)^{3/2} \qquad \text{Eq. 2.2}$$

where A is a general constant usually equal to 0.4, and ρ and ρ_s are the density of wood and the density of the solid cell wall material respectively. Therefore, the longitudinal and transverse flow in wood is directly dependent on the diameter of pores**.**

The cellular structure of wood may change through a local densification process (plastic deformation of the cell wall) and is affected by pressure, temperature, and time. One of the major factors influencing the mechanical and physical behavior of densified wood is the amount and type of cellular collapse. Cellular collapse occurs by either elastic buckling, plastic yielding, or brittle crushing, depending on the test conditions and the nature of the cell wall material (Wolcott 1989).

The already described competing processes of fluid diffusion and cellular collapse, occurring during processing WPCs, must be considered in understanding the behavior of the two phases of the system. In this research, we designed a method to quantify anatomical features that could relate to the interaction between a molten thermoplastic and the wood cell structure.

MATERIALS AND METHOD

Materials and samples. Logs of small diameter (< 30 cm) from three species including lodgepole pine (*Pinus contorta Dougl*), grand fir (*Abies grandis*) and Douglas-fir (*Pseudotsuga menziesii*) were used. Five logs per wood species were used for this experiment. Two sets of samples were cut, one to evaluate the wood-thermoplastic interaction and the other to study the morphology of the wood; the same small samples were used for both experiments, allowing a better correlation in the final statistical analysis. Because previous experiments showed that the mobility of melt HDPE through the tangential face (radial flow) is practically zero, only the tangential flow of HDPE was measured. Figure 2.1 shows a detail of dried wood samples with small sections, 5x5 mm and 150 mm length, obtained from 2x2 inch sections located close to the pitch (inner section or corewood) and close to the bark (outer section or outerwood), used in an experiment to relate the melt thermoplastic mobility inside the cellular structure of wood through the radial face. Pellets of HDPE, supplied by Equistar (LB 0100-00) melt flow index (MFI) = 0.3 g/10 min, were used to carry out the experiment for diffusion of molten thermoplastic in wood.

Vacuum bagging. A device was designed to support a bed of pellets of HDPE, over which wood samples were placed, allowing only the interaction of the radial face with melt HDPE (see Figure 2.1.b and Figure 2.2). The other three faces were coated and sealed with epoxy resin to avoid contact with molten thermoplastic. Using a vacuum bag, samples were set in and autoclaved, and a designed vacuum-pressure cycle was applied to allow the diffusion of HDPE into the wood (See Figure 2.2). The maximum pressure and temperature were 620 kPa and 200 °C, respectively (see Figure 2.3).

Morphology analysis, SEM. A Hitachi S-570 scanning electron microscope was used (voltage 20 kV, work distance 20 mm). Sections of 0.5x0.5x2.0 cm were obtained from the same small samples shown in Figure 2.1.

Analysis of anatomical features: To expose the radial face for a further microscopic characterization, a razor blade and a frozen shock with liquid nitrogen were used to fracture wood samples. Then the diameter of pits and their distribution on the cross field and next to it, were measured. Anatomical features such as cell wall thickness and lumen diameter were evaluated for latewood or earlywood. For each wood species, 30 areas of interest (AOI=220x350 μm^2) were used to quantify anatomical features.

Interpenetration of HDPE: After the vacuum-pressure cycle, small 5-mm cubes were cut from the base of the 5x5x150 mm sample, allowing us to study the interpenetration of HDPE into the wood structure. A transverse face of the small cube was cut with a diamond knife mounted in an ultramicrotome Leica and coated with gold (150 Angstrom thickness). Scanning analysis was performed using a SEM, with magnification up to 300X. The images were digitally recorded and stored.

Image processing. The software Image-pro was used to quantify anatomical features and the wood-plastic interaction at the interphase. To quantify the interfacial interaction of the solid phase with the thermoplastic, random areas of interest (AOI=220x350 μm^2) were used, either for earlywood and latewood (Figure 2.4). In the study of penetration, a total of 60 AOI's per wood species were used (30 to study corewood and 30 for outerwood). The response variables evaluated for each combination (wood specie - location into the log - earlywood/latewood) were determined as:

$$AP = \frac{\sum_{1}^{5} P_i}{5} \qquad IFA_{AOI} = \frac{\sum_{1}^{n} IFA_i}{n} \qquad \text{Eq. 2.3}$$

AP : the average penetration of thermoplastic into wood cells (μm).

P_i : the maximum penetration measured for each AOI (μm), with five measurements per AOI.

IFA_{AOI} : the average interfacial area per AOI (μm^2).

IFA_i : the perimeter of the lumen (π x lumen diameter) for those cells filled with thermoplastic, multiplied by one micrometer depth (μm^2).

Main effects and empirical models. In a parallel experiment, wood plastic composites made of wood flour obtained from lodgepole pine logs (LPP) and grand fir (GF), showed very significant differences in terms of tensile and flexure strength-modulus. Based on that experiment, these two wood species were selected to apply a 2^3 factorial design (Montgomery et al., 2006) to determine mean effects and principal interactions between wood anatomical features and interpenetration of HDPE into wood samples. To compare anatomical features, analysis of variance was utilized (ANOVA, 95% of confidence) combined with the Tukey test to infer about differences between mean values. Similar analysis was used to compare response variables (Penetration and interfacial area). Table 2.1 presents the selected settings for a 2^3 factorial design and codes of design of experiment (DOE) for the study of wood morphology and interpenetration of HDPE. Three replicates were used for this factorial design, one as the mean and the others based on the 95% interval of confidence for each response variable. A particular DOE was applied for the following of responses or dependent variables: Penetration and Interfacial Area. The independent variables that are affecting these responses were: wood species (LPP and GF), type of wood (earlywood and latewood), and location (corewood or outerwood). Finally, according to the t-test (confidence level= 95%), only significant factors and interactions were considered for regression models.

Non-linear regression was used to obtain empirical models to describe the physical interaction between phases, particularly for penetration and interfacial area where in this case the cell wall thickness and lumen diameter were considered as independent variables.

RESULTS AND DISCUSSION

Anatomical features of wood species from samples located close to the bark (outerwood) and pith (corewood) were determined with SEM analysis of the radial face. Cross sections of those samples were used to evaluate the interpenetration of thermoplastic into the wood structure. The vacuum bagging process was used to melt the thermoplastic and then produce flow tangential to the annual rings. The vacuum–pressure cycle guaranteed a uniform normal pressure over wood samples. The potential pit area for flow was determined based on the diameter and number of pits per AOI, and varies among wood species and according to location in the log. The interaction between HDPE and wood is described in terms of the averaged maximum penetration and the interfacial area. A 2^3 factorial design was applied to quantify the main factors and interactions between variables associated with the wood anatomy that may affect interconnectivity or mechanical interlocking. To simplify the analysis of this complex process, only two wood species were analyzed (GF and LPP). Earlywood and latewood differed significantly in the penetration of HDPE, the interfacial area of the wood-thermoplastic and in the cell wall thickness. On the other hand, the diameter and number of pits and the potential area for flow was a main factor in their position (close to the cross field or in the cross field).

The empirical models presented here describe the interrelationships between anatomical features and wood-HDPE interconnectivity with a good level of confidence. These models may be used to analyze the ability of particular wood species to present cellular collapse in a process involving flow of a thermoplastic, pressure, temperature and time.

Anatomical features. Table 2.2 presents the average characteristics and variability of anatomical features of the three wood species analyzed. Pits close to the cross field present similar characteristics for all wood species; primarily bordered and open pits (See Figure 2.5). In the cross field, the following types and distributions of pits were found:

Douglas-fir:	Piceoid pits on the cross field, with a narrow and often slightly extended aperture.
Lodgepole pine:	Pinoid pits on the cross field. The smaller type of earlywood cross field pit found in softwood.
Grand fir:	Taxodioid pits on the cross field with a large, avoid to circular, included aperture that is wider than the lateral space on either side between the aperture and the border (Panshin and Zeew 1975).

Figure 2.6 presents a comparison for open pit diameter on and in the cross field. In terms of diameter of open pits and based on the ANOVA and Tukey test, grand fir presented a significant difference for this variable measured close to the pith and near the bark (p-value= 0.0019). The other wood species did not present significant differences in terms of the location from which samples were obtained. Similar differences between corewood and outerwood sections occurred in grand fir, specifically in the distribution and number of pits on AOI's taken close to the cross field and in the cross field (p-value=0.0000004). According the Tukey test, in the analysis of the diameter and number of pits per AOI in earlywood showed a higher potential area for transverse flow in Douglas-fir corewood. This wood species and location had the lowest cell wall thickness, which could cause collapse of wood cells under pressure. The second potential area for transverse flow was for the outer section of Grand fir. The worst potential condition for transverse flow occurred in Lodgepole pine corewood and outerwood, which differed significantly of the rest wood species according the Tukey test..

Figure 2.7 shows the average cell wall thickness (p-value=0.00000003) and lumen diameter of earlywood for each wood species and location. According the ANOVA, there are significant differences for these two anatomical features when wood species are compared. Cell wall thickness and lumen diameter play fundamental roles in the probable collapse of wood cells under pressure and temperature, especially in earlywood. A further discussion is presented in the empirical models section. According to the individual analysis of each AOI for latewood, there is no significant evidence of plastic cell collapse, mainly due to the thicker walls that these cells presented for all wood species. Earlywood cells tend to have a higher cell wall thickness in the outer section for all wood species. The exception was for Lodgepole pine, which did not present significant differences for corewood and outerwood, according the Tukey test.

Maximum penetration and interfacial area. Penetration is higher in some species in which the thermoplastic can freely move into the wood. This occurs with higher interconnectivity between cells. Collapse or buckling in particular areas, shown in a few AOI's, impedes the free flow of the viscous phase into the solid during the vacuum-pressure cycle. This phenomenon takes place under special circumstances related to cell wall structure (S1, S2, S3, and middle lamella layers) and natural flaws (pits) on the cell wall. When this occurs, the maximum penetration does not scale with the maximum interfacial area between phases. As Figure 2.8 shows, for each wood species there is a particular probability of the thermoplastic taking a specific path into the wood's cellular structure.

We will discuss two sources of this percolation, or spreading of the fluid phase through a disordered medium (wood) which involves some random elements. In one source of percolation, the randomness is ascribed to the fluid: the fluid particles dictate their own paths through the porous medium (diffusion process). In the other source, the randomness is ascribed to the medium: the medium dictates the path of the particles. The percolation process must be considered for further application, such as wood plastic composites made of softwood. Another source of percolation related to the results of this study is the potential for cell collapse that some wood species could present.

The anatomical element allowing interpenetration of HDPE was the open pit. Bordered pit membranes generate a barrier for melt flow of the thermoplastic, especially when the torus of the bordered pit is aspirated (see figure 2.9b). Figure 2.9a shows a clear evidence of this interconnectivity, which is useful for transverse flow and mechanical interlocking between wood particles and thermoplastic.

For all wood species, penetration was higher in earlywood than latewood, but no significant differences were found. In general, grand fir presented a high penetration in outerwood even in corewood. In terms of location and kind of wood (earlywood or latewood), the wood species Douglas-fir had the lowest penetration (see figure 2.10).

With respect to the interfacial area for earlywood, both responses (corewood-outerwood) for grand fir had the highest value. A similar trend was observed for latewood, but with a wide variability in response. Figure 2.11 shows the average interfacial area expressed in μm^2, determined based on AOI's from different wood species and locations. The measured interfacial area could be related with the probability of the melt HDPE taking a particular path through the interconnected wood cells (percolation process). The diameter and number of pits, as well as their distribution, also generate a potential for the flow of the thermoplastic. In general, Lodgepole pine presented a weak interfacial area.

Empirical models and main effects. Tables 2.3 and 2.4 show results of the factorial analysis with three replications applied to study the physical interaction between the solid and molten phase. The type of wood (earlywood or latewood), wood species (grand fir or lodgepole pine) and the interaction between them have significant effects on the penetration of thermoplastic into the wood structure. With respect to the interfacial area, the type of wood, location of the sample and the interaction type of the wood have the largest effect on this response variable. On the other hand, cell wall thickness is mainly a response of the kind of wood (early or late), location (corewood or outerwood) and wood species. The potential area for transverse flow increases by performing measurements using AOI's close to the cross field where open pits are abundant. Measurements of potential area for flowing on grand fir also increased this response variable. From studies of wood anatomy, it is well-known that pitting in the cross field present just a few void structures of small diameter connecting cells oriented parallel and perpendicular to the grain direction. As for pitting in the cross field, a larger effect on the number of pits per AOI is produced when wood species is considered as a factor. Grand fir has a higher amount of pits per AOI than lodgepole pine. The general regression model for predicting responses (Y) of factors under group I and group II was:

$$Y = \beta_0 + \beta_1 a + \beta_2 b + \beta_3 c + \beta_4 ab + \beta_5 ac + \beta_6 bc + \beta_7 abc + \varepsilon \qquad \text{Eq. 2.4}$$

where the intercept β_0 is the grand average for all observations. The coefficients β_1 to β_7 are one half of the estimate effect for each factor and interaction. The estimated coefficient is one half because regression coefficients measure the effect of a unit change in each factor on the mean of Y, and the effect estimated is based on a two-unit change from -1 to +1. The error is expressed as ε. The factors a, b and c are the correspondent factors for each experiment (table 2.1); the cross product between factors represents the interaction between them. This regression model can be used to obtain predictions from the 2^3 factorial experiments analyzed here. According to the t-test (*hypothesis* H_o*:* $\beta i=0$ *vs.* H_1*:* $\beta i\neq 0$*, confidence level=95%*), some factors and interactions are not significant. Then some terms were removed and the final equations of the models for the relevant responses become:

Response variable	*Regression model from factorial analysis*	*Non-significant factors and interactions (95%confidence)*
Penetration (P)	P(μm) = 74 – 14.1 b – 3.6 c + 13.8 ac	a, ab, bc, abc
Interfacial Area (A)	A (μm^2) = 1284 + 133.5 a – 367.5 b + 169.5 ac	c, ab, bc, abc

The penetration model, type of wood, wood species and interaction contribute significantly to the maximum penetration of the molten thermoplastic into the lumens. The interaction location-type of wood created non-significant results for responses like the interfacial area for wood species studied here. The potential area for transverse flow was significantly affected by the location (in or close to the cross field), the wood species (grand fir or lodgepole pine) and their interactions.

Non-linear regression models. Polynomials models were used to predict particular responses of the wood-thermoplastic interaction because they gave better correlations, they have moderate flexibility of shapes and they are computationally easy to use. Besides these advantages, these models were able to describe phenomena such as the potential collapse of cell walls for particular wood species, reducing the average value for response variables like the maximum penetration and interfacial area. Cell wall thickness and lumen diameter were analyzed because their relationship could explain certain effects (collapse, for example) that impact the potential contact surface between phases of the composite system at the interface. Another mechanism affecting the interpenetration of HDPE (already described in the factor analysis) is the potential area for transverse flow and interconnectivity between wood cells by pits. A specific analysis was made for earlywood and two wood species: grand fir and lodgepole pine. The regression equation and coefficient of determination were calculated for each case.

Figures 2.12 and 2.13 show the surface responses and non-linear regression models for penetration in lodgepole pine and grand fir. As mentioned earlier, wood from the outer location was selected for this analysis due to the extreme mechanical properties obtained in a parallel experience making wood plastic composites with these species.

In the analysis of AOI's associated with low penetration for a specific relation cell wall thickness/lumen diameter, we observed that this unusual decrease could be related to the collapse of cell walls in some cases, as SEM analysis shows on Figure 2.12. On the other hand, the wood species grand fir presented a uniform penetration of thermoplastic through the cell structure with less evidence of collapse that could impede a higher penetration, as SEM pictures show in Figure 2.13. In terms of interfacial area, the regression models had a lower coefficient of determination compared with those for penetration in both wood species. As the cell wall thickness of grand fir increases, the interfacial area increases. This is probably due to the proportional enhancement of strength of wood cells associated with the change in geometry and mechanical properties of the cell wall. This could allow a higher state of hydrostatic pressure (applied during the vacuum bagging experiment) without significant deformations on the cell wall that can reduce the mobility and penetration of HDPE. An opposite trend was observed for lodgepole pine; this trend could be connected with the phenomenon of collapse that this wood species presented in a few samples (See Figure 2.14).

CONCLUSIONS

Conducting a morphology analysis of the interaction between a viscous phase and a cellular solid with a vacuum bagging cycle helped to elucidate the complex environment for flow of the liquid phase governed by several anatomical features present in wood species. Regression models presented here are representative of the significant effect of anatomical features in the interfacial area and penetration of molten HDPE into the cell wood structure. Results showed a high correlation between the potential area for transverse flow and the interaction between HDPE and wood species. There was also higher potential area for transverse flow as the interfacial area increased between phases. This potential area was determined based on the diameter and number of pits in or close to the cross field. The collapse of cells in specific wood species was identified as a probable mechanism impeding mobility of the thermoplastic and thus the interpenetration and interfacial area. Further research may examine how this phenomenon could affect processing of different wood species in which a particular thermomechanical condition could impact the performance of the final composite system through mechanical interlocking.

REFERENCES

1. Dalvag H., Klason C., Stromvall H.-E. (1985). The Efficiency of Cellulosic Fillers in Common Thermoplastics. Part II. Filling with Processing Aids and Coupling Agents. International Journal of Polymeric Materials, Vol. 11, pp. 9-38.

2. Gent AN, Lai SM. (1995). Interfacial bonding, energy dissipation and strength. Rubber Chem Technol; 68:13.

3. Gibson L.J., Ashby M.F. Cellular solids: structure and properties. Second edition, Cambridge solid state science series, Cambridge University press, 1997.

4. Harper D. A thermodynamic, spectroscopic, and mechanical characterization of the wood-polypropylene Interphase. Thesis dissertation, Wood Material and Engineering Laboratory, Washington State University, Pullman WA. 2003.

5. Jane F. W., The structure of wood. 2nd edition, A. & C. Black, 1970.

6. Matuana L. M., Balatinecz J. J., Park C. B. (1998). Effect of surface properties on the adhesion between PVC and wood veneer laminates. Polym. Engineering and Sci. 38(5) 765.

7. Milton T. The Preservation of Wood.A Self Study Manual for Wood Treaters. Minnesota extension service, University of Minnesota College of Natural Resources, 1995.

8. Montgomery D., Runger G., Hubele N. 2006. Engineering Statistics. John Wiley & Sons, 3rd edition.

9. Packham D.E. (2003). Surface energy, surface topography and adhesion. International Journal of Adhesion & Adhesives 23, 437–448.

10. Panshin A.J., .Zeeuw C. Textbook of wood technology. Structure identification properties and uses of the commercial woods of the United States and Canada, 4th edition, Mc Graw-Hill book company, 1975.

11. Russell T.G. Historical landscapes and forests structures. Small diameter timber: Resource management, manufacturing and market. Symposium proceedings, Spokane, WA – USA, February 2002.

12. Sirvio J., Karenlampi P. (1998). Pits as natural irregularities in softwood fibers. Wood and fiber science, 30 (1), pp. 27-39.

13. Smith M., Dai H., Ramani K. (2002). Wood-thermoplastic adhesive – method of characterization and results. International Journal of Adhesion and Adhesives, 22 pp 197-204.

14. Wolcott, M.P. (1989). Modeling viscoelastic cellular materials for the pressing of wood composites. PhD Dissertation. VPI&SU, Blacksburg, VA.

Table 2.1: Coded design of experiment (DOE) in standard order for 2^3 factorial (*).

Group I

Run	Treat. combinations	Design Factors Inner-Outer	Early-Late	GF - LPP
1	1	(-) Inner	(-) Earlywwod	(-) GF
2	a	(+) outer	(-) Earlywwod	(-) GF
3	b	(-) Inner	(+) Latewood	(-) GF
4	ab	(+) outer	(+) Latewood	(-) GF
5	c	(-) Inner	(-) Earlywwod	(+) LPP
6	ac	(+) outer	(-) Earlywwod	(+) LPP
7	bc	(-) Inner	(+) Latewood	(+) LPP
8	abc	(+) outer	(+) Latewood	(+) LPP

Group II

Run	Treat. combinations	Design Factors Inner-Outer	Close CF - in the CF	GF - LPP
1	1	(-) Inner	(-) Close Cross field	(-) GF
2	a	(+) outer	(-) Close Cross field	(-) GF
3	b	(-) Inner	(+) in Cross field	(-) GF
4	ab	(+) outer	(+) in Cross field	(-) GF
5	c	(-) Inner	(-) Close Cross field	(+) LPP
6	ac	(+) outer	(-) Close Cross field	(+) LPP
7	bc	(-) Inner	(+) in Cross field	(+) LPP
8	abc	(+) outer	(+) in Cross field	(+) LPP

* (-) Low and (+) high level variables; (1) The low level factor; a, b, and c the main effects; ab, ac and bc two factors interaction; abc three factors interaction. GF is grand fir and LPP is lodgepole pine. Inner is corewood and outer is outerwood.

Table 2.2: Mean Anatomical features of softwoods: lodgepole pine, Douglas-fir and grand fir.

Wood species	Lodgepole pine		Grand fir		Douglas-fir	
Anatomical feature	Corewood	Outerwood	Corewood	Outerwood	Corewood	Outerwood
t*, earlywood (μm)	2.76	3.19	2.69	3.41	2.72	2.90
	(0.66)	(0.81)	(0.73)	(1.17)	(0.83)	(0.96)
t, latewood (μm)	4.48	4.34	4.84	5.46	5.00	5.56
	(0.98)	(0.81)	(1.01)	(1.07)	(1.79)	(1.68)
Diameter open pit/AOI	4.79	5.23	4.26	5.49	4.66	4.78
close cross field (μm)	(0.39)	(0.57)	(0.37)	(0.41)	(0.32)	(0.36)
Diameter pit/AOI in	1.89	2.43	3.38	3.79	3.11	2.56
cross field (μm)	(0.58)	(0.79)	(0.35)	(0.38)	(0.36)	(0.47)

* t is cell wall thickness. ( ) is the standard deviation.

Table 2.3: Calculated effects and interactions for penetration, interfacial area and cell wall thickness responses from a 2^3 factorial design.

Factors	Effect	Estimated Penetration and standard error (μm)	Estimated Interfacial area and standard error (μm^2)
	Average main effect	74 ± 8.5	1284 ± 37.5
a	Type of wood (early-late), t	-28 ± 3.5	267 ± 15.3
b	Location (core-outer), l	0.7 ± 3.5	-735 ± 15.3
c	Wood species (GF-LPP), s	-7.3 ± 3.5	-138 ± 15.3
ab	t x l	2.8 ± 3.5	48 ± 15.3
ac	t x s	27.6 ± 3.5	339 ± 15.3
bc	l x s	4.9 ± 3.5	142 ± 15.3
abc	t x l x s	-0.2 ± 3.5	-134 ± 15.3

Table 2.4: Calculated effects and interactions for potential flow area, diameter of pits and number of pits from a 2^3 factorial design.

Factors	Effect	Estimated Potential flow area and standard error (μm^2)
	Average main effect	133 ± 31.6
a	Location (core-outer), l	23 ± 12.1
b	Cross field (in-close), f	-82 ± 12.9
c	Wood species (GF-LPP), s	-57 ± 12.9
ab	l x f	12 ± 12.9
ac	l x s	-9 ± 12.9
bc	f x s	-49 ± 12.9
abc	l x f x s	-24 ± 12.9

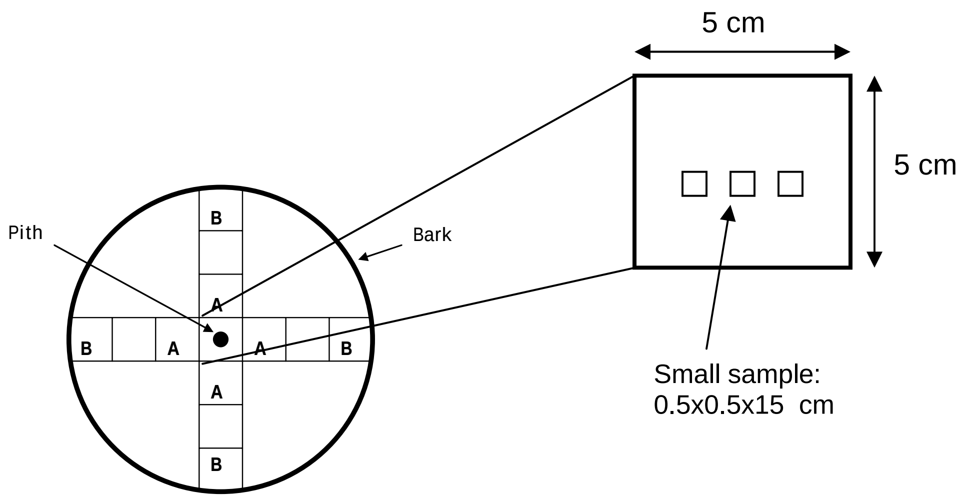

Figure 2.1: Location of base 5x5 cm sections (A-B) and small samples for the penetration study.

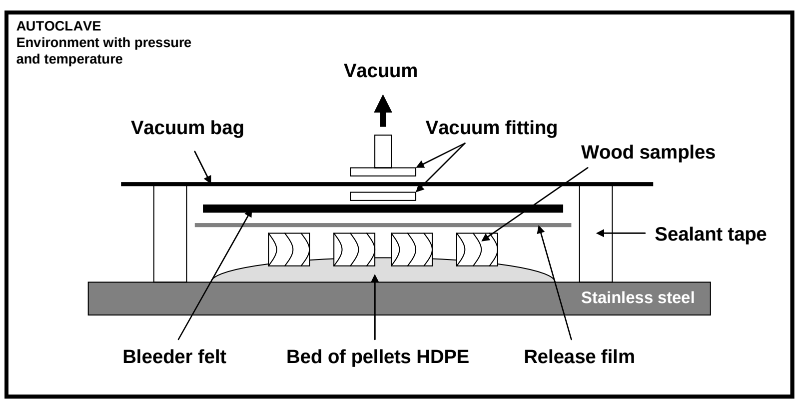

Figure 2.2: Set of the vacuum bagging experiment.

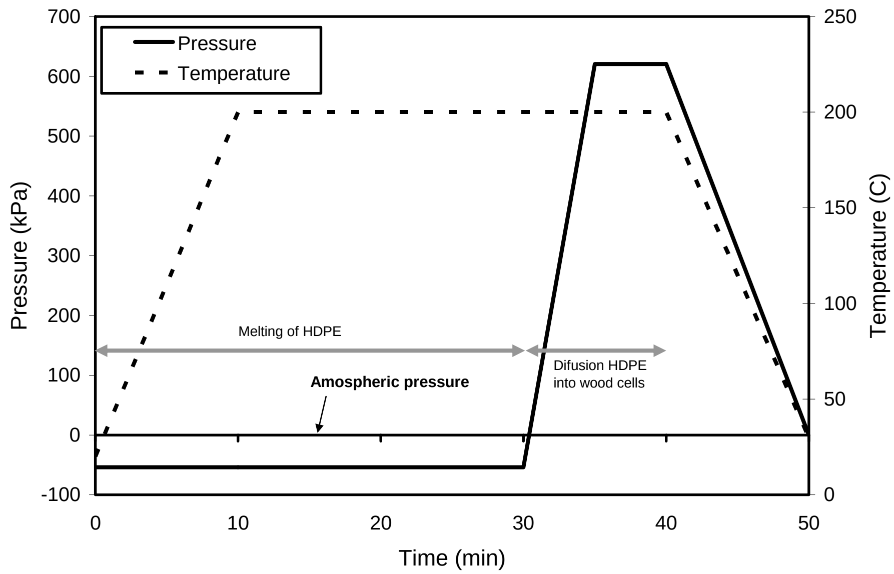

Figure 2.3: Pressure-temperature cycle for the vacuum bagging experiment.

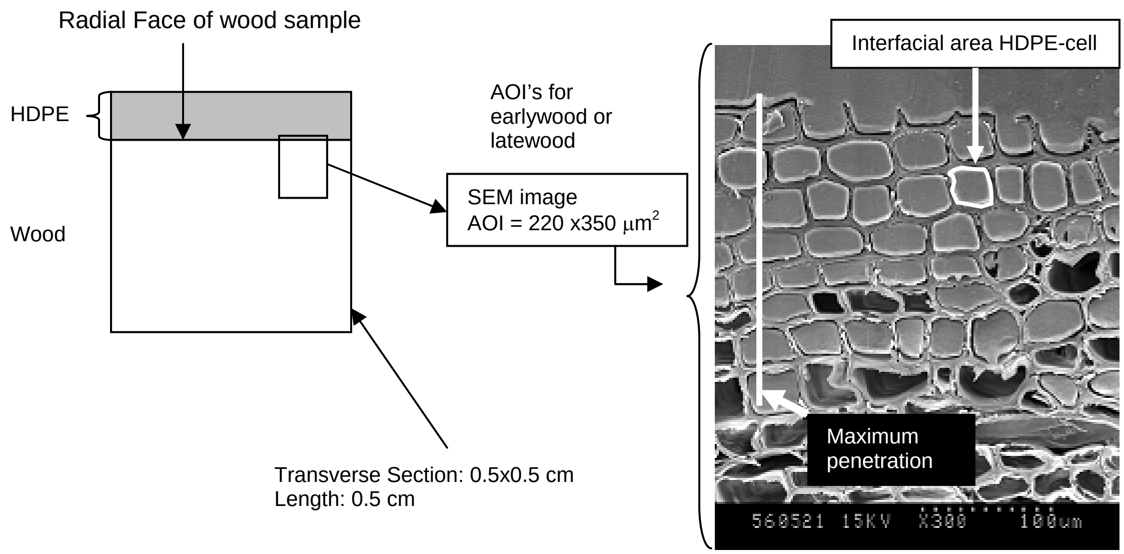

Figure 2.4: Areas of interest (AOI) used to evaluate the HDPE-wood interaction.

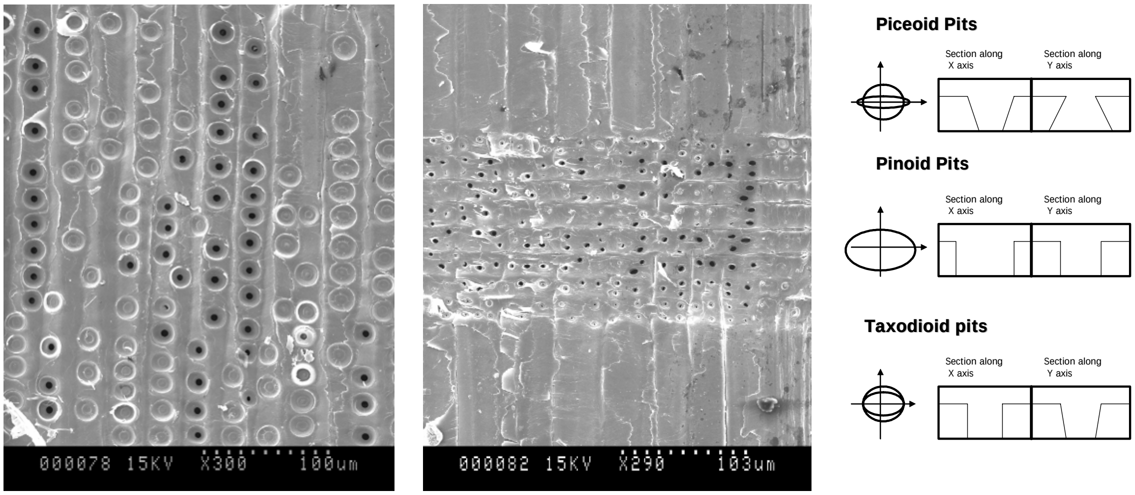

a) b) c)

Figure 2.5: Open pits close to the cross field (a), piceoid pits on the cross field (b) and a scheme showing the geometry of pits through the cell wall (c) (Jane 1970).

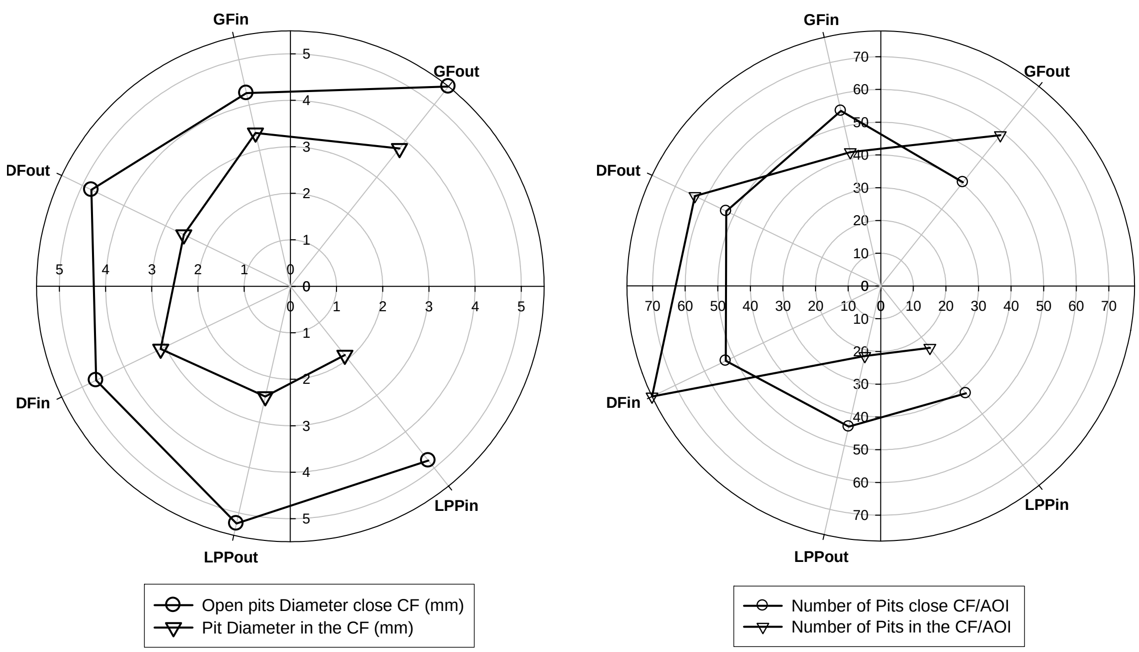

a) b)

Figure 2.6: Diameter (a) and number of pits (b) close and in the cross field (CF). Notation example: GFout is grand fir outerwood and GFin is grand fir corewood.
LPP and DF are lodgepole pine and Douglas-fir respectively.

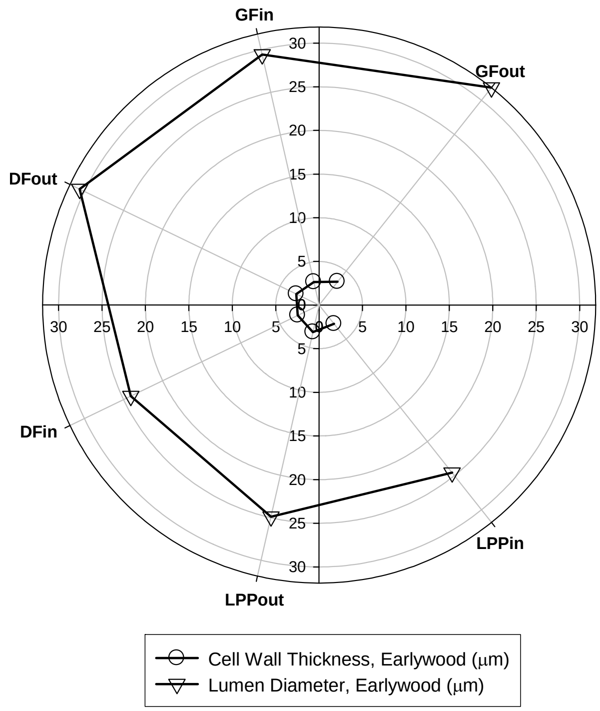

Figure 2.7: Earlywood; cell wall thickness and lumen diameter.

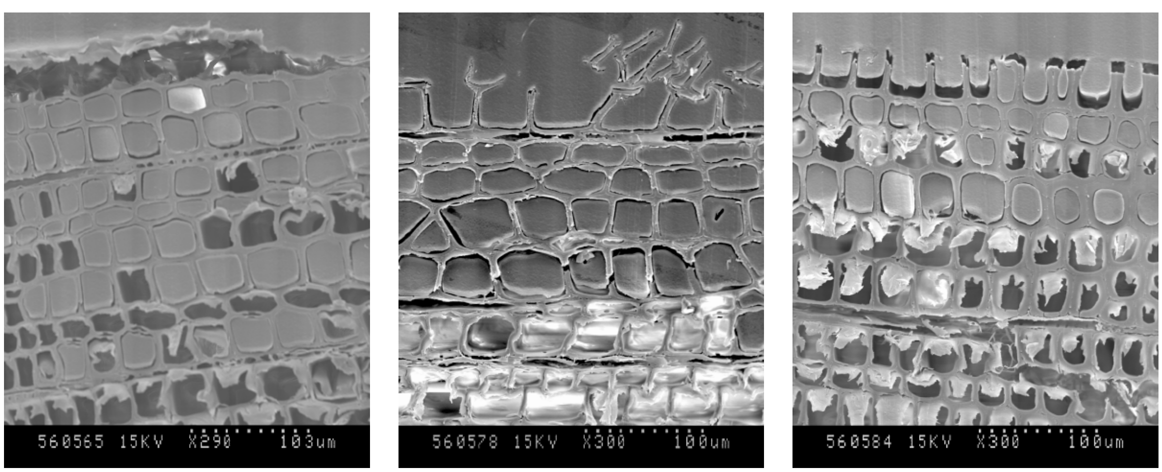

Lodgepole pine, outer section | Grand fir, outer section | Douglas-fir, outer section

Figure 2.8: Comparison between higher penetration versus interfacial area for earlywood.

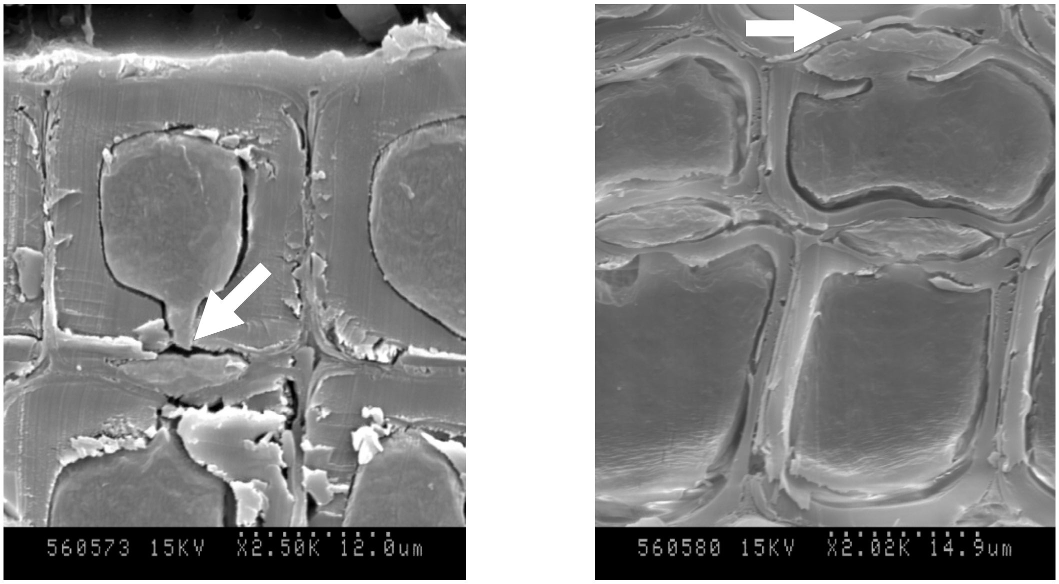

a) b)

Figure 2.9: Interconnectivity between wood cells with the thermoplastic passing through (a). Aspirated torus impeding the flow of HDPE to an adjacent cell lumen (b).

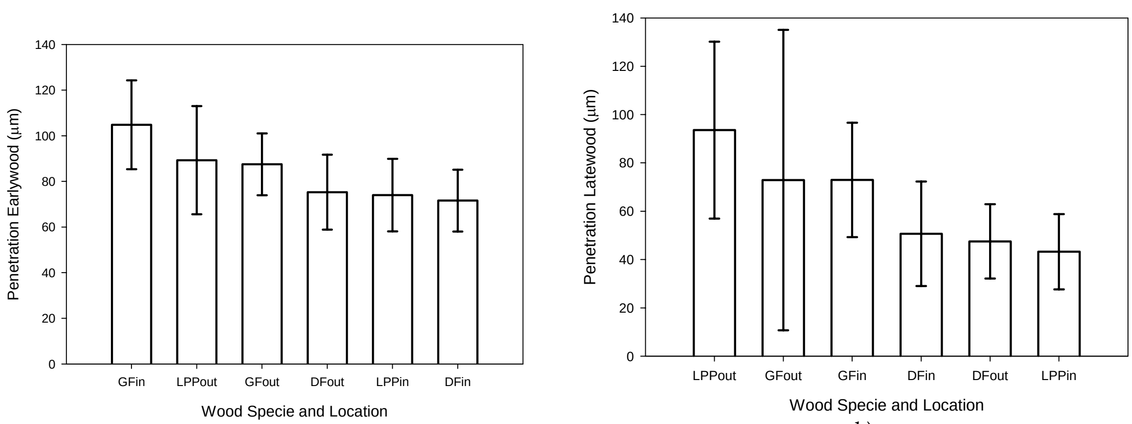

a) b)

Figure 2.10: 95% interval of confidence for penetration of HDPE into earlywood (a) and latewood (b).

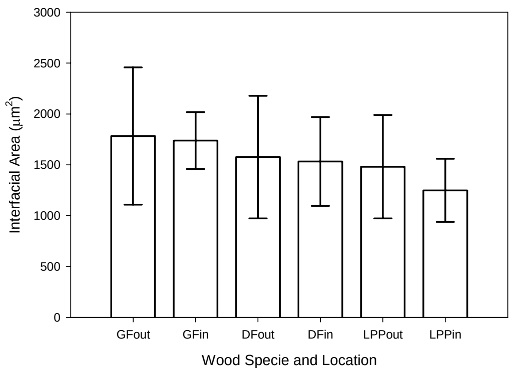

a)

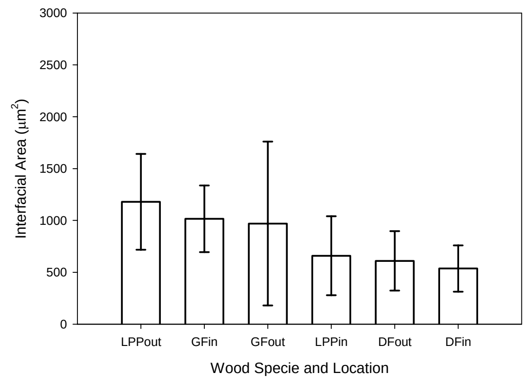

b)

Figure 2.11: Interfacial area in earlywood (a) and latewood (b).

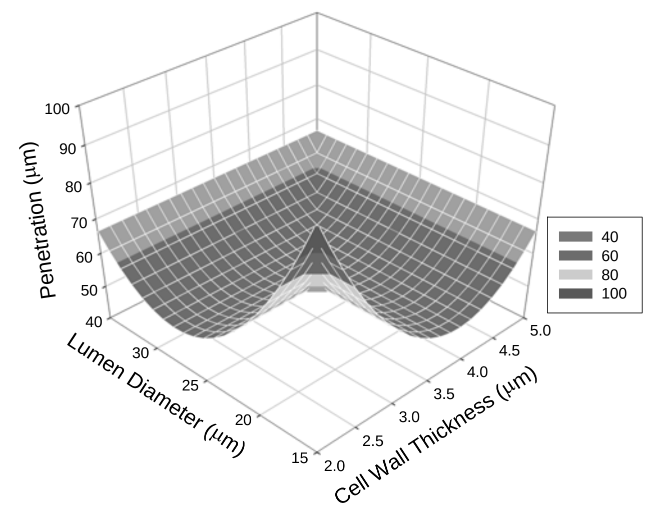

$$P = 219 - 277\ t + 36\ t^2 + 27\ d - 0.5\ d^2$$
$$r = 0.60$$

a)

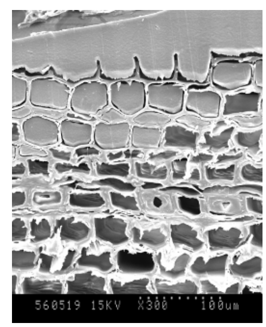

b)

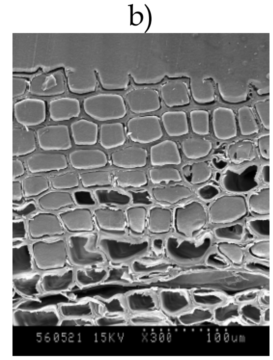

c)

Figure 2.12: Surface response and regression model for penetration (P) in wood of lodgepole pine from outerwood (a). d is lumen diameter and t is cell wall thickness, both in µm. A characteristic morphology of collapsed wood cells impeding penetration (b) and an AOI with high penetration (c).

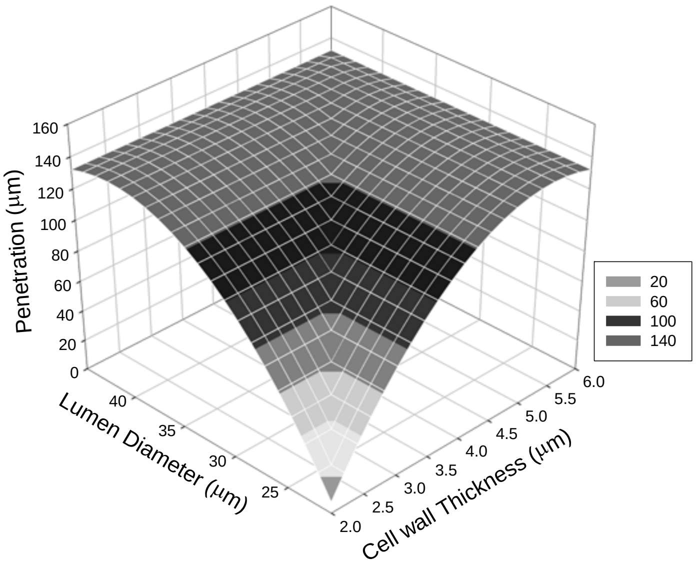

$P = -277.8 + 72\,t - 6.7\,t^2 + 10.7\,d - 0.13\,d^2$

$r = 0.75$

a)

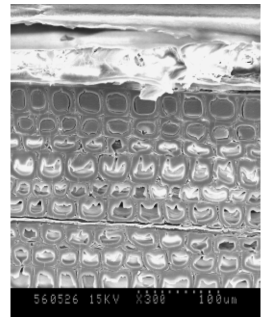

b)

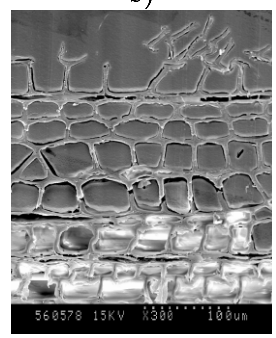

c)

Figure 2.13: Surface response and regression model for penetration (P) in wood of grand fir from outerwood (a). d is lumen diameter and t is cell wall thickness, both in µm. A characteristic morphology of undamaged wood cells and low penetration (b) and an AOI with high penetration, cells without collapse (c).

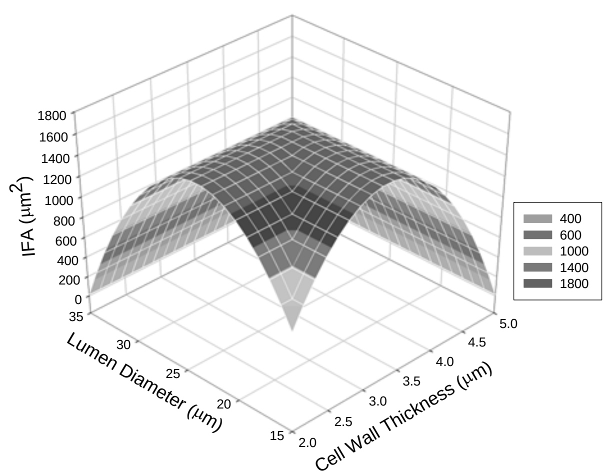

a)

<u>Grand fir, outerwood</u>

$A = -17395 + 4891\,t + 568\,t^2 + 616d - 9.7\,d^2$

$r = 0.49$

<u>Lodgepole pine, outerwood</u>

$A = -5644 - 1269\,t + 93t^2 + 798d - 14.9\,d^2$

$r = 0.60$

b)

Figure 2.14: Response surface for interfacial area (A) lodgepole pine-HDPE (a). Regressions models for interfacial area, grand fir and lodgepole pine (b). d is lumen diameter and t is cell wall thickness, both in µm.

CHAPTER 3
MORPHOLOGY OF WOOD SPECIES AFFECTING WOOD-THERMOPLASTIC INTERACTION
PART II: MICROSTRUCTURE AND MECHANICAL ADHESION

ABSTRACT

In the first part of this research, factors associated with the morphology of wood species were found to significantly affect the penetration of HDPE (high density polyethylene) and the potential interfacial contact area of the cell wall-thermoplastic. The main objective of the research presented here is to relate anatomical features of wood species that affect the interactions between polymeric phases and performance of wood plastic composites (WPC). These interactions are related to the probable interlocking volume and surface area for stress transfer in a WPC. Composites were produced from different wood species and analyzed using SEM (scanning electron microscopy). Results showed that wood species with high interfacial areas may increase mechanical interlocking, reflected in the viscous constant of the Maxwell model. A complicating factor is that the relation of cell wall thickness-lumen diameter and the interconnectivity between wood cells in a wood, affect the potential for cell collapse. When wood cells collapse, the penetration of the thermoplastic into the wood structure is almost always ceased. The collapse of wood cells during extrusion-injection molding processes reduced the potential surface for stress transfer between phases affecting the mechanical properties of composites. Undamaged wood cells may potentially be filled with HDPE thermoplastic enhancing modulus and increase the strength of WPC.

INTRODUCTION

The study of wood plastic composites is an emerging area in materials science. Wood as a natural filler is low-cost material with low density and high specific properties, and is also biodegradable and non-abrasive. Stark (1997) studied whether the wood species influences the mechanical properties of WPCs and investigated the micro-structural interactions between the wood and HDPE. According to Wolcott, SEM micrographs of southern yellow pine (*Pinus spp*.) composites revealed that the thermoplastic penetrates the pits around the periphery of the wood particles. In contrast, micrographs of a Douglas-fir composite (*Pseudotsuga menziesii*) did not reveal such penetration.

Pore penetration and roughness may seriously affect the extent of contact between the matrix and filler phases in a composite (Packman, 2003). Surface roughness may range in scale from hundreds of microns to nanometers. Packman found that increasing the surface area between phases increases the measured surface energy per unit nominal area. Also, surface area and contact between phases may interact to redistribute stress and thus increase energy dissipation between a filler and matrix during the failure of composites.

To examine the effects of different wood species, composites were made using wood flour from ponderosa pine, loblolly pine, maple and oak as filler for polypropylene at 20, 30, 40, 50, and 60% by weight (Stark, 1997). Results showed that with increasing wood flour content, the flexural and tensile modulus, density, heat deflection temperature, and notched impact energy increased, while the flexural and tensile strength, tensile elongation, mold shrinkage, melt flow index, and un-notched impact energy decreased. Hardwoods exhibited slightly higher heat deflection, as well as tensile and flexural properties than softwoods.

Creep, the deformation over time of a material under stress, is one characteristic correlated to interface adhesion in composites. Increasing the amount of filler in a composite enhances creep resistance. Some researchers have used a creep test to describe strain behavior and interfacial interactions (Nunez et al., 2004, Houshyar et al., 2005, Acha et al., 2007). Houshyar et al. used a four-parameter viscoelastic model to quantify the viscoelastic behavior of polypropylene fibers reinforced composites. They found high agreement between creep model predictions and experiment results from high interfacial bonding between the fiber and matrix. They also studied the morphology of the composites using optical and scanning electron microscopy. SEM photographs displayed a thin layer of matrix on the reinforcement, which was attributed to good impregnation and wetting of the fibers to the matrix, enhancing the adhesion between phases. According to Acha et al. (2007), creep deformation could be directly related to interfacial properties, and this effect is enhanced when compatibilizers like maleated polypropylene are used.

Due to the production parameters of composites, they commonly contain large numbers of inhomogeneities such as cracks, voids, matrix pockets, and fiber bundle misalignments. These features cause an appreciable scatter in strength which is higher than for conventional materials. In the design process for composites, one must use statistical tools to adjust for this variability in properties (Omena-Pina et al. 2004). The Weibull distribution is one of the most widely used statistical tools for materials such as composites. Omena-Pina et al. found that the Weibull modulus was useful for describing the flaw population of bi-directional carbon fiber reinforced carbon composites.

It is possible that in the complex interactions between wood particles and thermoplastics in WPC, the mechanical interlocking between the natural filler and thermoplastics are significantly affected by the anatomical features of wood species. The goal of this research is to establish relationships between the anatomical features of wood, and microstructure, mechanical adhesion and performance of softwood WPCs.

MATERIALS AND METHOD

Five solid wood sections, measuring 5x5 cm^2 in cross section, were obtained from the inner area (close to the pith or corewood) and outer area (close to the bark or outerwood) of logs obtained locally for the following species: lodgepole pine (*pinus contorta Dougl*), grand fir (*abies grandis)* and Douglas-fir (*psudotsuga menziesii*). This material was subsequently reduced to wood flour using a Bliss hammer mill, dried to a nominal moisture content of 2% and screened to obtain a 60-mesh fraction for composites manufacture. Pellets of HDPE (LB 0100-00, melt flow index MFI= 0.3 g/10min), were used for the extrusion trial and for the injection molding.

Extrusion and injection. A Leistritz ZSE 18 HP, 18 mm twin screw extruder was used for compounding. Wood flour-HDPE composites of 40% wood by weight were made without additives. The screw speed, barrel temperature and melt pressure at the die were 70 rpm, 180 °C and 3450 to 3800 kPa respectively. A round orifice die was used in the extruder to produce the composite for the subsequent pelletization. The produced pellets were used to feed the Sumitomo SE 50D injection molder. Injection molding trials for each combination wood species-location were run, while processing conditions were held such that mold filling occurred in 2 seconds with a cooling time about 25 seconds. During plasticization, the screw speed was set at 200 rpm and rear-to-front (hopper to nozzle) temperature profile was regulated to 185 °C. The filling pressure and mold temperature were 1100 kg/s and 70 °C respectively. The mold allowed one tensile bar and one flexure bar per cycle for mechanical testing, according ASTM D638 and ASTM D790. Type I tensile specimens and 12x3x127 mm flexure bars were produced.

Macroscopic features of wood species. The latewood and earlywood proportion of representative wood samples was quantified by analyzing thirty square sections from the 5x5 cm^2 sections for each combination of wood species and location. The cross-section of the square sections were scanned with a HP Scanjet ADF scanner. The digitalized images were analyzed using Image-pro software. To determine the latewood proportion on each image (area based), the bi-level mask (sensitivity= 4) was used to manually select the intensity range of latewood. Once selected, the latewood proportion (l_w) was determined based on fraction of the total scanned area (25 cm^2). The earlywood proportion (e_w) was then calculated as:

$$e_w = 1 - l_w$$

Phase morphology. Five flexure samples were selected from injection molding composites made with flour representing the combination of wood species and locations. Small 6.0x2.8 mm^2 cross areas were sectioned, which represents half of the cross section of a flexure injection sample. The sample surface was polished with a diamond knife mounted in a Leica ultramicrotome; then, assuming symmetric morphology, both sides of the midline on this cross section (Figure 3.1) have similar microstructure. Four areas of interest (AOIs) of 770x880 μm^2 were obtained using a Hitachi S-570 scanning electron microscope (SEM) with a magnification of up to 120x, voltage 20 kV and work distance 20 mm. A total of 20 AOIs per combination wood species-location were analyzed. SEM pictures were digitalized and then processed. These pictures were used to analyze the morphology of wood particles embedded in the HDPE matrix. Cell collapse and interpenetration of HDPE into the filler was observed. The SEM analysis allowed an important feature to be found and measured: *the void content*. This is the percentage of void area per AOI, and was measured using image analysis through a Pruning filter with a threshold number of 53.

Viscoelastic parameters and mechanical adhesion in WPC. Small specimens (2.8 x 12 x 60 mm^3) were cut from the injection molded flexure specimens and used for a creep test in a Rheometrics RSA II dynamic mechanic analyzer. Creep tests were conducted with a three-point flexure system using 7850 mN static load in an environment at 60 °C. A total test time of 10-min at constant load was used for all cases. A four-element Maxwell–Voigt Kelvin model (Throne 1988), shown in Figure 3.2, was used to fit to the data for determining the viscoelastic parameters for WPCs. The four parameter model qualitatively accounts for the observed response of WPC under constant load; it includes instantaneous elastic strain, retarded elastic strain and viscous flow. This model results from the combination of the Maxwell and Voigt elements. For the four parameter model, the total deformation is:

$$\varepsilon_T = \varepsilon_M + \varepsilon_V \qquad \text{Eq. 3.1}$$

where ε_M and ε_V are the strain of the Maxwell and Voigt elements respectively (Throne, 1998). The governing differential equations for these elements are

Maxwell: $$\dot{\sigma} + \left(\frac{E}{\eta}\right)\sigma = E\,\dot{\varepsilon}_M \qquad \text{Eq. 3.2}$$

Voigt: $$\dot{\varepsilon} + \left(\frac{E}{\eta}\right)\dot{\varepsilon}_v = \frac{\sigma}{\eta} \qquad \text{Eq. 3.3}$$

where $\dot{\sigma}$ and $\dot{\varepsilon}$ are the first time derivatives of stress and strain; respectively. Subscript $_M$ and $_V$ denote the Maxwell and Voigt, respectively), σ is the applied constant stress, and E and η are the elastic and viscous constants for the spring and dashpot for each model. By combining equation 3.2 and 3.3, the final model provides responses to constant stress, strain rate and instantaneous fixed strain; then the response of the 4-parameter model is:

$$\varepsilon = \left[\frac{\sigma_o}{E_1} + \frac{\sigma_o t}{\eta_1}\right] + \frac{\sigma_o}{E_2}\left(1 - e^{-\left(\frac{E_2 t}{\eta_2}\right)}\right) \qquad \text{Eq. 3.4}$$

where, σ_o is the applied stress (5,630 kPa), t is time, t_o is the initial time, ε is the strain, E_1 and η_1 are the elastic and viscous constants of the spring and dashpot in series; E_2 and η_2 are the elastic and viscous constants of the spring and dashpot in parallel. The constants for the 4-parameter model were determined from the time-strain curve as Figure 3.2 shows, thus:

$$E_1 = \frac{\sigma_o}{\varepsilon_o} \quad \text{and} \quad \eta_1 = \frac{\sigma_o}{m} \qquad \text{Eq. 3.5}$$

where m is the slope of the viscous flow on the curve strain-time (see figure 3.2b). E_2 and η_2 were determined using the tool solver on an Excel spreadsheet. Through a response surface analysis, a correlation was made between microscopic flow and interactions between the solid phase and the thermoplastic.

Analogy model parameters to mechanical interlocking. The analogy presented by Rosen (1982) can be used to explain the mechanical interlocking mechanism between filler and the thermoplastic, thus:

Dashpot 1: represents the slippage between phases. This interfacial movement is responsible for unrecoverable viscous flow in the composite. The value of η_1 governs the equilibrium flow of the composite.

Spring 1: represents the initial elastic strain of the composite. The magnitude of this component is represented by the constant, E_1.

Dashpot 2: represents the recoverable time-dependent strain resulting from the molecular motion of both phases during deformation.

Spring 2: represents the restorative force brought about by disruption of the chains and wood particles oriented by a stress to their most original random or highest entropy configuration.

Flaw probability and wood species. When wood cells collapse during processing, results an empty lumen that cause increase in void content of WPCs. In this study, the void content (in percentage based on the total AOI area) was determined for a large numbers of AOIs for each case. We observed that the stress at which WPCs made of different wood species fail, usually depends on the presence of flaws (voids) that may occur randomly across the transverse section of a WPC. When many voids are expected across the transverse section of the composites, variability in strength should also be expected (Hull 1996). Statistical tools were used to explain the variability in properties of WPCs that may influence the future design of these materials. When a stress σ is applied, the parameter "n" defines the number of voids (of arbitrary size) per unit of area sufficient to cause failure under stress. Then, the Weibull distribution can be used to analyze the failure mechanisms on WPCs studied here (Bodig 1982). The probability of any given element failing depends on n and on the probability of rupture or failure (P_f). Then, the equation to predict the probability of failure of WPCs made of different wood species, assuming that all samples tested have practically the same volume (V), becomes (Askeland, 2004):

$$P_f(V) = 1 - \exp\left[-V_C\,(\sigma/b)^w\right] \qquad \text{Eq. 3.6}$$

which is a two-parameter (b, w) Weibull distribution. σ is the stress level at which the probability of failure is calculated; σ_o is the minimum possible ultimate stress for which the survival probability, P_s, is $\cong 0.37$ or 37%; assuming brittle failure during the tensile test, b takes a characteristic value which is the strength corresponding to the 63rd percentile of the cumulative density function of σ. V_C represents the void content into each WPC under longitudinal tensile stress. Taking the logarithm twice on Equation 3.6 we get:

$$\ln\left[\ln(1/P_s)\right] = w\,(\ln\sigma - \ln b) - \ln V_C \qquad \text{Eq. 3.7}$$

A plot, in this form, of the data for P_s as a function of σ should give a straight line with a gradient of w (Hull, 1996). Lastly, the Weibull modulus was estimated using the tensile data by fitting the data to Equation 3.7. Tensile strength values were arranged in an increasing order (for each WPC) assigning a numerical rank to each specimen, with the specimen having the lowest tensile strength assigned the value of 1. The total number of specimens is n_T. The probability of failure P_f is then the numerical rank divided by (n_T + 1). Then $\ln[\ln(1/P_s)]$ versus σ was plotted and using simple linear regression analysis, the Weibull modulus was determined for each WPC.

RESULTS AND DISCUSSION

Different wood species were used to make WPC's of 40% wood content. Usually, the production of these composites involves higher ratios of natural fibers; but it was found in previous experiments that a lower percentage of wood facilitates the morphological study of the wood-thermoplastic interaction through SEM image analysis. Interrelationships between the wood species' anatomical characteristics and the mechanical properties of the final composite can be established. Anatomical features, determined in the first part of this research, explain the phase morphology and mechanical properties of experimental composites. We found that void content is a significant factor affecting the performance of WPCs and the probability of failure under stress, and results from interactions between the anatomical features and the behavior of wood species during processing. Results showed that collapse of wood cells during extrusion impedes the free flow of the thermoplastic into the lumens and contributes to the void content measured with SEM on transverse sections of WPCs made of the three wood species.

Latewood-earlywood proportion and mechanical properties. Figure 3.3 shows the latewood proportion for all wood species and locations, obtained from cross sections of the solid wood sections used to produce wood flour. According to these measurements, the earlywood volume is estimated at over 70% of the total volume of the wood species analyzed here. The method used can detect differences among wood species in terms of this macro-anatomical feature. There was a higher average earlywood proportion in lodgepole pine (corewood) and grand fir (outerwood), at 79% and 77% respectively. A lower earlywood proportion was determined for Douglas-fir (corewood) and lodgepole pine (outerwood), at 72% and 73% respectively. The earlywood proportion was used as an input to determine the relative interface area parameter in the first part of this research to construct empirical models for predicting mechanical properties.

Figure 3.4 shows the effect of wood species and location on the flexure and tensile strength. There is not a unique combination wood species-location with higher mechanical properties, but significant differences were found in some cases in terms of modulus of elasticity (MOE) and modulus of rupture (MOR). In general, composites made of grand fir presented significantly higher MOE-MOR compared to the other wood species. Grand fir from outerwood performed better in the mechanical tests applied in this study. Initially, this can be explained in terms of the physical interaction of wood-HDPE parameters determined in the first part of this research. Grand fir from outerwood presented a high interfacial area parameter (Gacitua and Wolcott 2007) and lower potential for cell collapse under a vacuum-pressure treatment at 200 °C. The opposite extreme occurred for lodgepole pine composites. Again, considering the interaction parameter interfacial area, lodgepole pine from outerwood was the species with the lowest interfacial area, especially when earlywood was measured (being that the volume of earlywood was significantly higher than the latewood volume, in all cases). This interaction depends on anatomical features for this species (diameter and number of pits, cell wall thickness) that may impede the interlocking during cell collapse. This could explain the reduced mechanical properties determined for this composite.

Douglas-fir presented an intermediate level of mechanical properties compared with the other wood species. Douglas-fir composites from outerwood had a lower MOE-MOR, for both flexure and tensile, than corewood. The area under the entire stress-strain diagram on Figures 3.4a and 3.4b provides a measure of the composite's ability to absorb energy up to the point of fracture; this is called the modulus of toughness. The greater the total area under a stress-strain diagram, the tougher the composite. According to this definition, the design of a tough WPC for a specific application and better performance would depend on the correct choice of the wood species to produce wood flour and finally the composite. Grand fir (outerwood) presented the higher modulus of toughness for flexure and tensile tests.

In terms of strength and modulus, the expected differences among species for the composites would become more significant as the weight fraction of wood flour increases. An increase in the weight fraction of the natural filler would increase the affect of the anatomical features of wood on phase interactions and mechanical properties.

Viscoelastic properties. Viscoelastic constants of the 4-parameter model can be used in an analogy to describe the interactions, at microscale, between phases of the composite under constant stress. One of these mechanisms is mechanical interlocking, due to the interpenetration of the molten thermoplastic into the wood cell structure during the extrusion and injection molding processes. It was discussed that the interpenetration was affected by the cell collapse. Cell collapse does not contribute for a good stress transfer in a composite and could also affect the magnitude of the viscoelastic parameters.

Table 3.1 presents values of the 4-parameter viscoelastic constants. A higher resistance to strain was determined for grand fir composite outerwood and a lower resistance for lodgepole pine outerwood composites. Comparable results were presented by other researchers in terms of the parameter related to interfacial interactions, the viscous constant, η_1. Betiana et al. reported a η_1 value of 9.91×10^{12} Pa·s for composites made of 30% jute fabrics (by weight), polypropylene (PP) without additives and determined at room temperature. Nunez et al. calculated a η_1 parameter equal to 1.92×10^{13} Pa·s for wood flour composites (*Eucalyptus saligna*), PP, copolymer maleic anhydride and PP and also determined at 20 °C. Values reported here for η_1 vary between 2.28×10^{12} to 6.15×10^{12} Pa·s, depending on the wood species.

A higher interfacial area, already determined using a vacuum-bagging experiment and SEM analysis, could enhance mechanical interlocking between phases and ultimately affect the slips between phases responsible for flowing between the matrix and the natural filler. There was a significant difference for composites fabricated with different softwoods in terms of the equilibrium flow under a constant flexure stress.

As Table 3.1 presents, the decrease in magnitude for each viscoelastic constant is consistent with mechanical properties of composites from different combinations wood-location. Of particular interest is the constant that could be related with slippage between phases, η_1. An increasing elongational viscosity of the Maxwell Dashpot, η_1, results in a decreasing in the slope of the viscous flow portion of the strain-time curve. As shown in Figure 3.5a, the ranking of η_1 and the associated interface interaction was consistent to the descending ranking obtained for mechanical properties like tensile, flexure and modulus of toughness. Figure 3.5b shows the comparison between predicted strain at a certain time and the experimental strain.

SEM morphology analysis. The selection of specific AOIs in a symmetric cross section of wood composites allowed a very precise micro-description of filler and thermoplastic phase. Through this analysis it was possible to identify and quantify the number and area of voids as their probable source associated to processing conditions and wood morphology. Figure 3.6 shows the average void content determined from AOIs of wood composites fabricated of different wood species. Figure 3.7 shows a characteristic result for the image analysis process designed to measure the void content. In general, the decreasing order of void content on composites made of wood flour particles was:

Grand fir < Douglas-fir < Lodgepole pine

In all cases the void content was lower than 2.5%. According to Agarwal and Broutman, a good composite should have less than 1% of voids, whereas a poorly made composite has up to a 5% void content. Voids are formed between the fiber and matrix which can cause a pull-out effect. A higher mechanical interlocking can increase the interfacial frictional sliding. This process can absorb significant quantities of energy and can affect the modulus and toughness of the WPC. Another void source observed was due to cell collapse and the small spaces in the lumen after plastic deformation during extrusion. A poor interpenetration of the molten thermoplastic into lumens generates conditions for a free buckling of the cell wall during extrusion. WPCs made of grand fir and Douglas-fir have an average void content lower than 1%. In composite science, higher void contents usually mean lower fatigue resistance, greater susceptibility to water penetration and weathering, and increasing variation or scatter in strength properties (Agarwal and Broutman, 1990, Askeland and Phule, 2004).

Prediction of failure under tensile stress. This study found an important number of inhomogeneities, or voids, in experimental WPCs. This feature may reduce the mechanical properties because voids do not transmit stresses and can cause stress concentration. Statistical tools such as the Weibull distribution were used to ensure reliability of the data, to address variability in properties of WPCs, and to avoid premature failures. Table 3.2 presents the estimated Weibull modulus using Equation 3.7; then tensile strength is analyzed from the point of view of Weibull modulus related to the void distribution. The analysis of Table 3.2 suggests that the tensile strength of composites prepared using Douglas-fir (outerwood) presented the higher "w "value (≈ 9.5), indicating a more uniform distribution of flaws (voids) into the composite. The larger the slope or m value, the more uniform the composite. This statement is supported by the lower variability of tensile strength for composites made of Douglas-fir (outer area) shown in Figure 3.4d. The characteristic strength for composites prepared using lodgepole pine (corewood) was also higher (24.24 MPa), suggesting that a smaller average void size area (13.5 μm^2) may not lead to fracture easily. The Weibull parameter for the void area distribution for this composite was on the upper level, which represents a more uniform flaw distribution. Data on survival probability (log scale) and tensile strength resulted in a straight line when plotted. The slope of this line provides a measure of the variability (i.e. the Weibull modulus). Figure 3.8 shows an example of the probability of survival of WPCs prepared with material from the outerwood of different wood species. For composites of Douglas-fir (outerwood), the regression line is almost vertical (high w value); this means that there is a small variation in the tensile strength. On the other hand, composites made of grand fir (outerwood) presented a high tensile strength but a high variability (w = 4.8). Good reliability in design could be obtained for WPC with a high w value. The WPCs studied here have the same family of flaws or defects, mainly voids (due to cell collapse and subsequent empty cells), resulting in a Weibull modulus between 1 to 10; this means there is significant effect of the selected wood species in the strength and reliability of WPCs. Weibull plots confirm that tensile strength increases as the void content reduces (figure 3.6).

Macroscopic features of wood species affecting mechanical properties. In Part 1 of this research, it was demonstrated that anatomical features such as open pits, as well as their number and distribution, are directly related to the potential flow area of molted HDPE into the wood cell structure, causing mechanical interlocking and eventually enhancing properties including modulus, toughness and strength. Wood species presenting a high interfacial area have the potential for better mechanical interlocking reflected on the viscous constant of the Maxwell model (Dashpot 1). Figure 3.9 shows a response surface plot of the tensile modulus of elasticity versus η_1 and the relative interfacial area (A_R). The relative interfacial area for each wood species-location, was determined as:

$$A_R = A_{EW}\, e_w + A_{LW}\, l_w \qquad \text{Eq. 3.8}$$

where A_{EW} and A_{LW} are the mean interfacial area for latewood and earlywood, respectively. These areas of interaction were determined with a vacuum bagging experiment (Gacitua and Wolcott, 2007). The relative interfacial area is a representative parameter of wood used as raw material to produce wood flour and the composite. This relative parameter was used for correlations, considering different responses of earlywood and latewood in a specific wood-thermoplastic interaction process. Macroscopic features (earlywood-latewood) for all wood species-locations, IFA and mechanical properties, were considered in a multiple regression analysis.

Based on the polynomial regression analysis for factors η_1 - relative IFA and the response variable, MOE in tensile and flexure, good correlation coefficients were obtained in both cases ($r > 0.96$). As Figure 3.9 shows, an increase of the relative IFA presents a positive correlation to the viscous constant, and both combined tend to increase significantly the elastic parameter of the wood plastic composite. Also, the η_1 variation had a direct impact on tensile elastic properties. In general, as relative IFA and η_1 increase, the elasticity parameter of WPCs take higher values, also affecting strength.

CONCLUSIONS

Anatomical features may explain the phase morphology and mechanical properties of WPCs made without additives. An interphase factor affecting the mechanical properties and toughness of WPC is the slippage between phases determined using a viscoelastic model and its parameters as an analogy. The higher the viscous flow parameter (η_1), the lower is the deformation of the WPC under constant stress. The increase of the η_1 constant (phase friction slip) is facilitated by a higher interpenetration and interface area between wood particles and HDPE. Composites made of grand fir outerwood produced a higher η_1 value, which agrees with mechanical properties and toughness of experimental WPC. Another associated factor contributing to the final strength and variability of WPCs is the void content. A poor interpenetration of the molted thermoplastic into the cell lumens generates conditions for the free buckling of cell walls during extrusion, which finally results in an important source of void generation. According to the Weibull distribution analysis for void content, there is a significant effect of the selected wood species in the strength and reliability of the final wood composite. High correlation coefficients were determined for multiple regression models used to predict mechanical properties of experimental WPCs based on the slippage between phases and the interfacial area determined in previous experiments.

REFERENCES

1. Agarwal B.D., Broutman L.J. Analysis and performance of fiber composites. John Wiley & Sons, Inc., 1990.

2. Askeland D.R., Phule P.P. Essentials of materials science and engineering. Thomson Canada Limited, 2004.

3. Acha B., Reboredo M., Marcovich N. (2007). Creep and dynamic mechanical behavior of PP-jute composites: Effect of the interfacial adhesión. Composites part A 38: 1507-1516.

4. Bodig J., Jayne B.A. Mechanics of wood and wood composites. Van Nostrand Reinhold Inc., 1982.

5. Gacitua W., Wolcott M.P. Morphology of wood species affecting wood-plastic interaction. part 1: mechanical interlocking. Submitted to Holzforschung in August 2007.

6. Hull D., Clyne T.W. An introduction to composites materials. Cambridge solid state science series, 1996.

7. Houshyar S., Shanks R.A, Hodzic A. (2005). Tensile creep behaviour of polypropylene fibre reinforced polypropylene composites. Polymer Testing 24:257–264.

8. Nunez A., Marcovich N., Aranguren M. (2004). Analysis of the creep behavior of polypropylene-woodflour composites. Polymers engineering and science, vol. 44 (8): 1594-1603.

9. Omena-Pina S.R.; Pardini L.C.; Pionino-Neto F. (2004). Weibull modulus of bi-directional carbon fibre reinforced carbon composites. Centro Tecnico Aeroespacial Instituto de Aeronautica e Espaco. Divisao de Materiais – AMR 12228-904- Sao Jose dos Campos - SP- Brazil.

10. Packman D.E. (2003) Surface energy, surface topography and adhesion. International journal of adhesion & adhesives, 23 p 437-448.

11. Rosen S.L. Fundamentals principles of polymeric materials, section 18.3. John Wiley & Sons, 1982.

12. Stark N. (1997). Effect of Species and Particle Size on Properties of Wood-Flour-Filled Polypropylene Composites. Intertech conferences, Functional fillers for thermoplastics and thermosets.

13. Stark N., Rowlands R. (2003). Effects of wood fiber characteristics on mechanical properties of wood/polypropylene composites. Wood fiber and science, 35 (2): 167-174.

14. Throne J.L. Creep and stress relaxation, section 7. Engineering plastics, Vol. 2 engineered materials handbook, ASM International, 1988.

Table 3.1: Viscoelastic constant for the 4-parameter model used on composites with different wood species.

Wood species – location	Dashpot 1, η_1 Pa·s x 10^{12}	Spring 1, E_1 Pa x 10^6	Dashpot 2, η_2 Pa·s x 10^{11}	Spring 2, E_2 Pa x 10^6
Grand fir, outerwood	6.1484	15.07	1.3933	33.28
Douglas-fir, corewood	4.4807	14.31	1.2107	30.39
Grand fir, corewood	4.1849	14.03	1.2475	30.15
Lodgepole pine, corewood	3.4064	14.06	1.0837	27.00
Douglas-fir, outerwood	3.1718	14.14	1.0936	27.13
Lodgepole pine, outerwood	2.2814	11.96	1.0898	23.40

Table 3.2: Weibull modulus and Weibull parameter for tensile strength and void content, respectively.

Composite	Weibull modulus Tensile strength		Composite	Weibull parameter Void content	
	w and correlation coefficient	Average tensile strength (MPa)		w	Average void area (μm^2)
Grand fir, corewood	1.1126 (r=0.88)	23.93	Lodgepole pine, corewood	1.1646	13.50
Lodgepole pine, corewood	3.555 (r=0.89)	24.24	Grand fir, outerwood	1.1591	14.68
Douglas-fir, corewood	3.7651 (r=0.92)	23.07	Douglas-fir, outerwood	1.1686	14.75
Grand fir, outerwood	4.8389 (r=0.93)	23.54	Lodgepole pine, outerwood	1.1204	15.20
Lodgepole pine, outerwood	5.3787 (r=0.99)	22.57	Grand fir, corewood	1.0868	15.76
Douglas-fir, outerwood	9.4794 (r=0.99)	22.44	Douglas-fir, corewood	1.0499	15.81

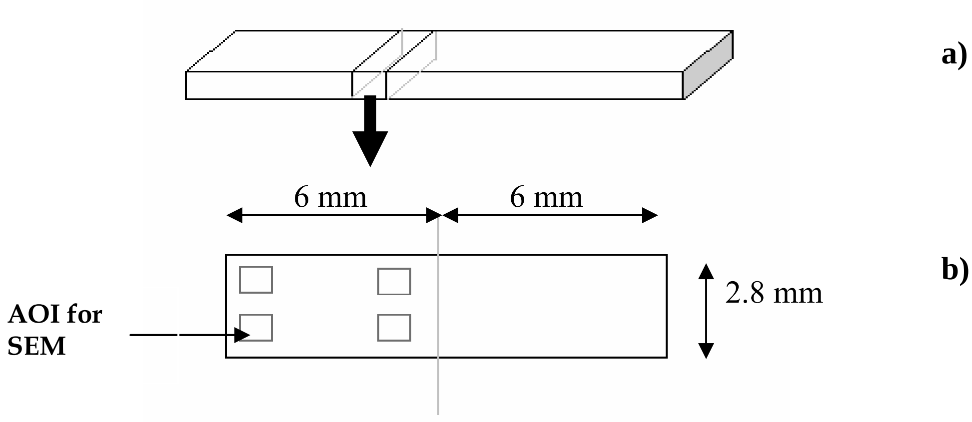

Figure 3.1: Flexure injection sample (a) and AOIs on the cross section (b) for SEM analysis and void content determination.

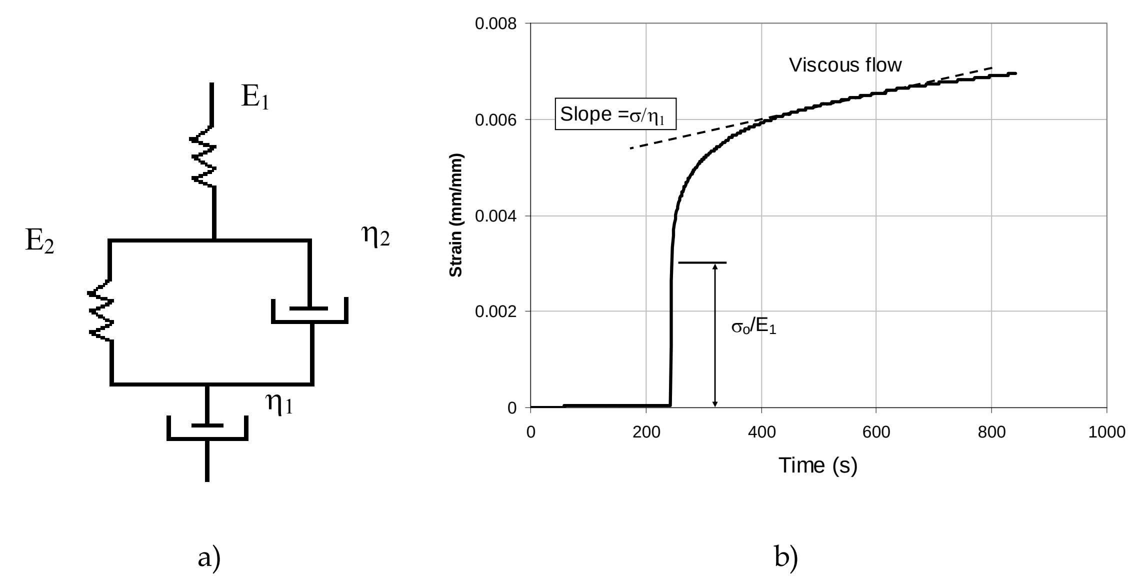

Figure 3.2: Four-parameter model with Maxwell elements and Voigt element in series (a). Response of the 4-parameter model to a constant applied stress (b).

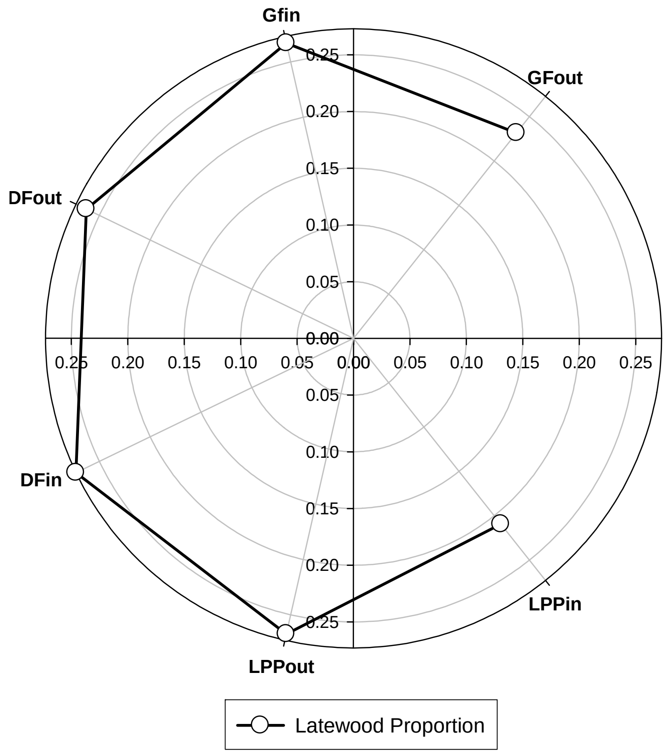

Figure 3.3: Latewood proportion for different wood species and locations into a log (DF: Douglas-fir, GF: grand fir, LPP: lodgepole pine and “in-out” are corewood and outerwood).

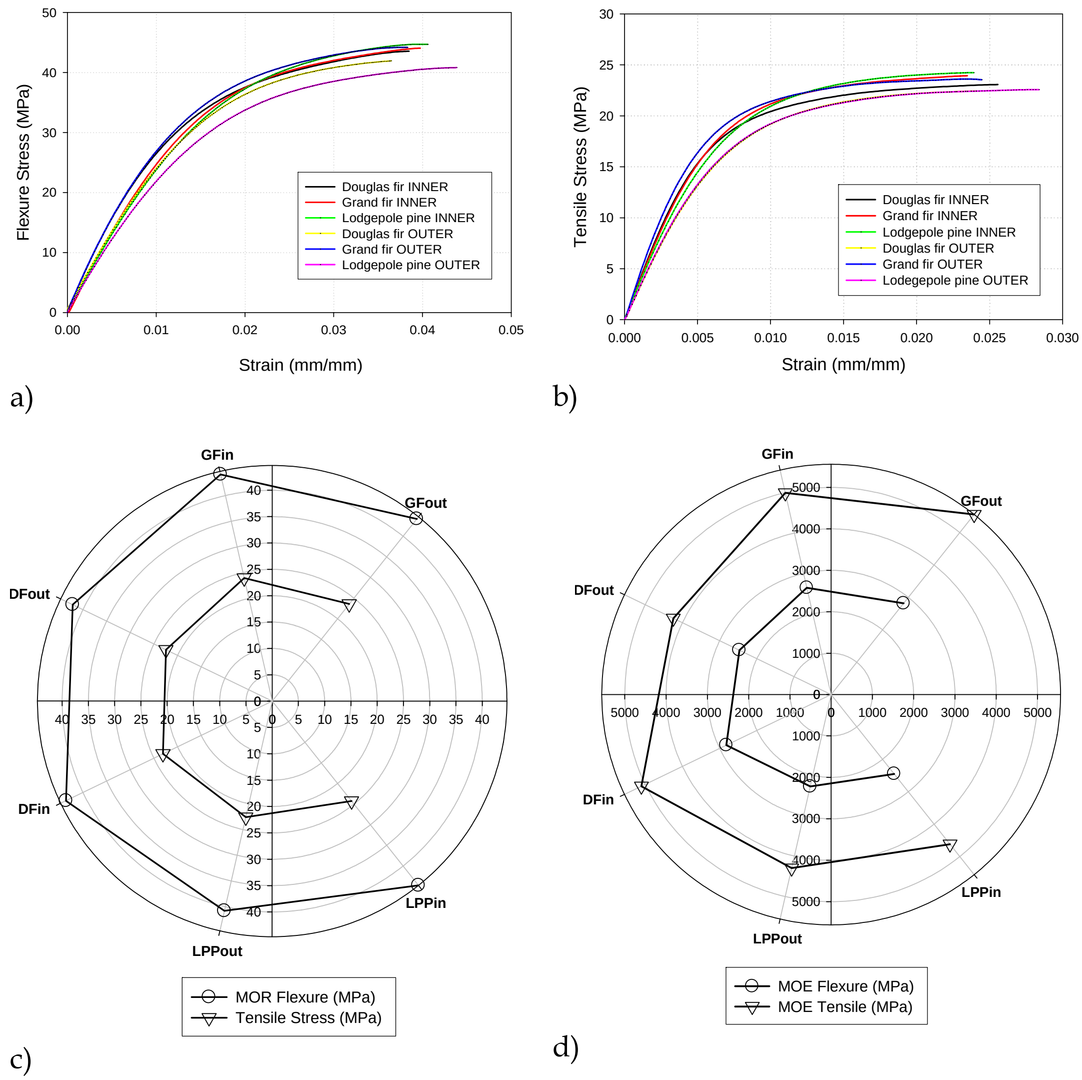

Figure 3.4: Wood-HDPE composites in flexure and tension: Stress-strain curves (a, b); MOR and tensile stress (c) and MOE (d). Notation: out and outer is outerwood; in and inner is corewood; DF: Douglas-fir, GF: grand fir, LPP: lodgepole pine.

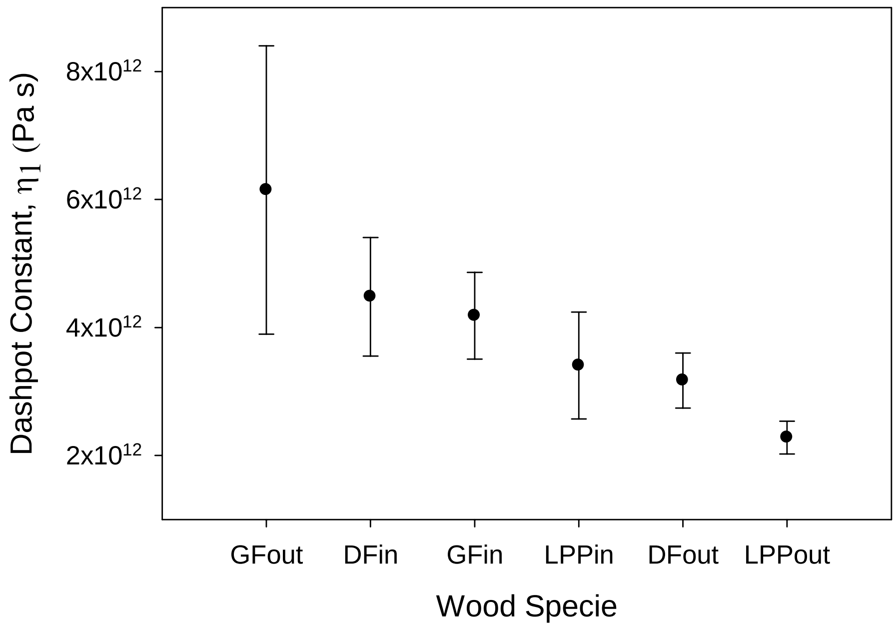

a)

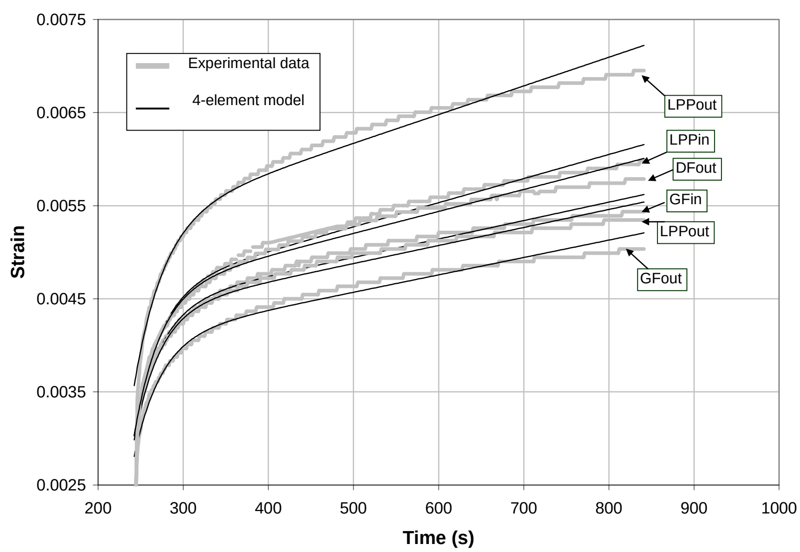

b)

Figure 3.5: 95% interval of confidence for the calculated elongational viscosities for experimental WPCs (a). DF: Douglas-fir, GF: grand fir, LPP: lodgepole pine. Corewood (in) and outerwood (out). Creep response of experimental WPCs made with injection molding. Comparison experimental vs. 4-element model (b).

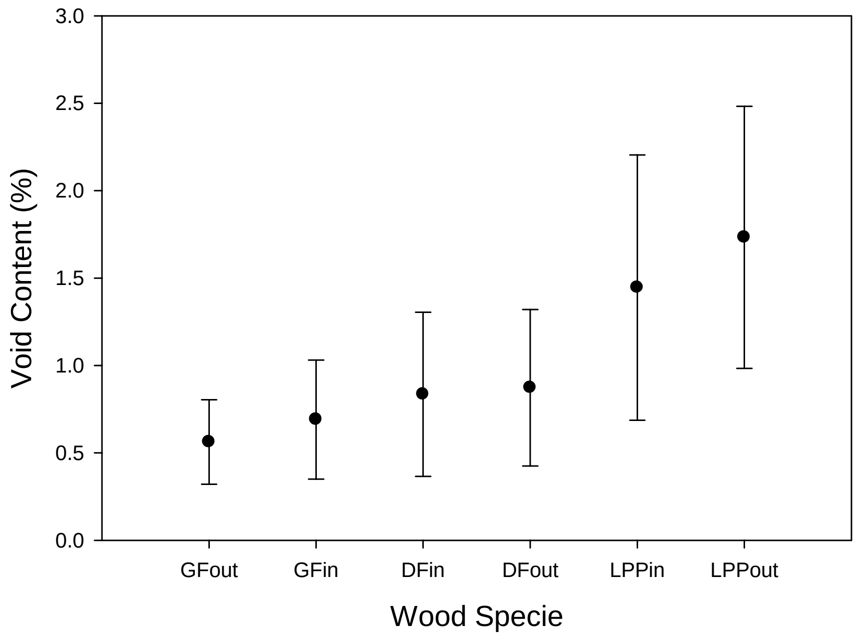

Figure 3.6: The 95% interval of confidence for mean void content of WPC with different wood species. DF: Douglas-fir, GF: grand fir, LPP: lodgepole pine corewood (in) and outerwood (out).

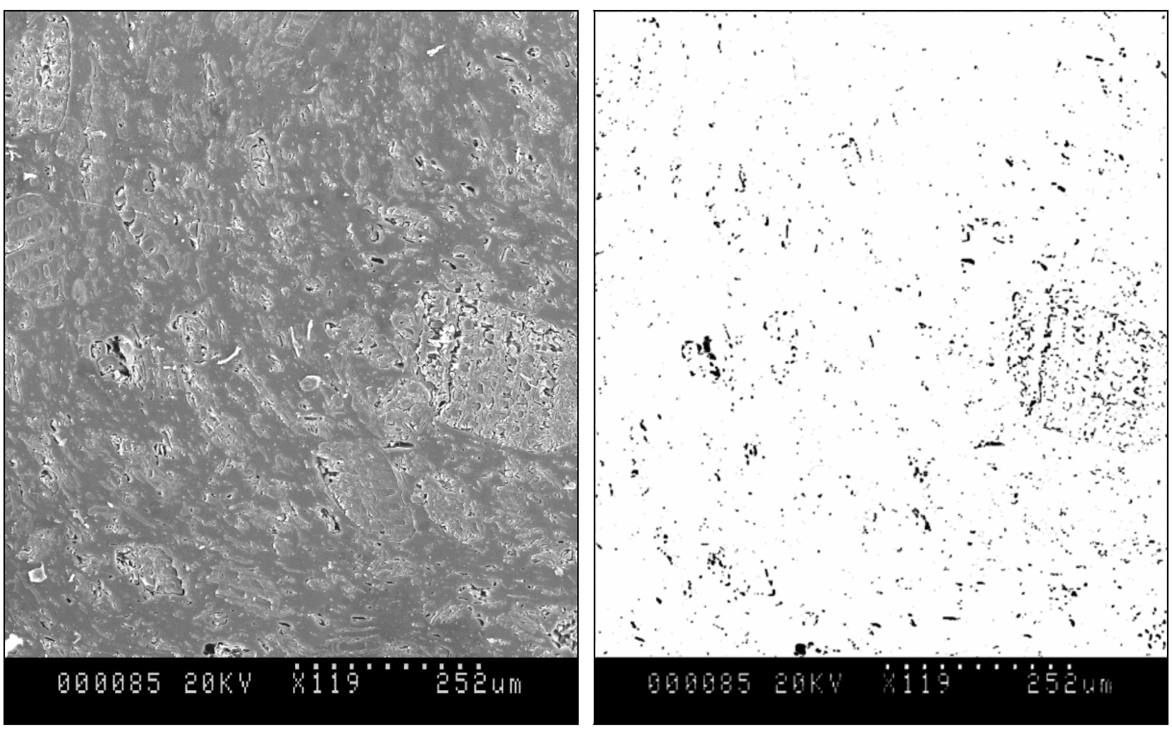

Figure 3.7: An example of a SEM picture and subsequent image treatment to determine void content. Composite made with Lodgepole pine wood flour (outerwood).

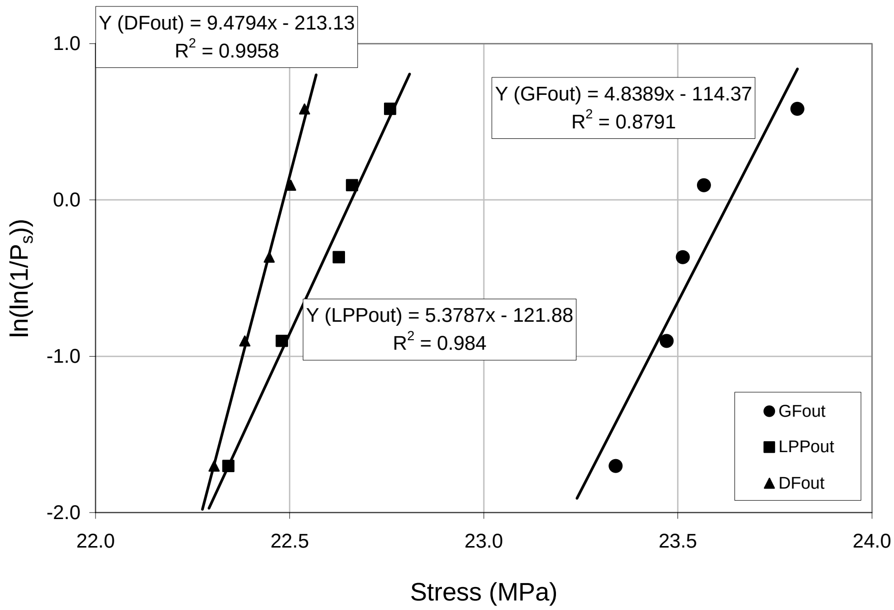

Figure 3.8: Survival probability of composites under tensile stress. WPC produced of three wood species from outerwood.

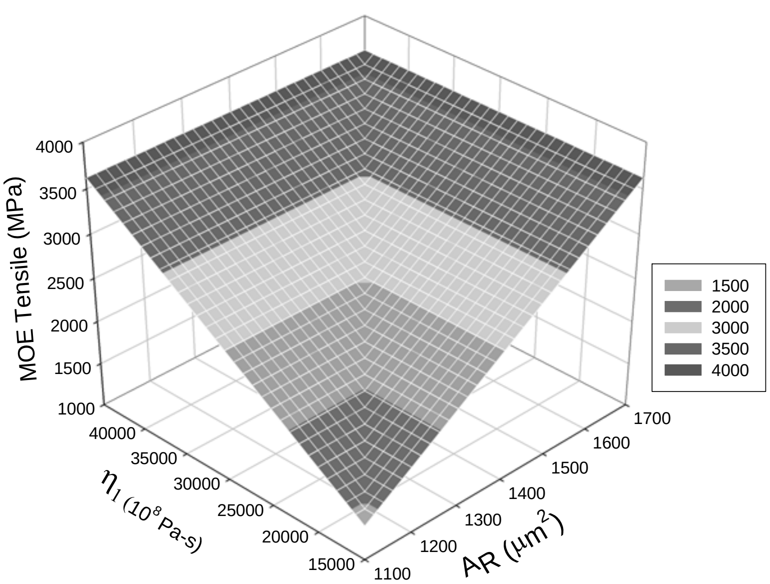

MOE = 725 + 0.547 A_R + 0.0035 η_1

r = 0.96

Figure 3.9: Response surface and polynomial regression models for tensile-MOE (MPa) as function of the relative interface area (A_R) and viscous constant η_1.

CHAPTER 4
DAMAGE OF THE CELL WALL DURING EXTRUSION AND INJECTION MOLDING OF WOOD PLASTIC COMPOSITES

ABSTRACT

Until now, no clear quantitative correlation between structural properties and internal damage measurements has been established for wood plastic composites (WPCs). To study material damage in wood cells during any transformation process, one must consider the molecular architecture of natural cellulosic fibers, which may eventually impact the overall mechanical behavior of wood fibers. In particular wood species, anatomical features and mechanical properties of the cell wall may determine the potential for stress transfer in hybrid materials. In this study, we quantified wood cell damage in terms of the stiffness reduction of the S2 layer for the cell wall by measuring Young's modulus with nanoindentations of the cell wall before and after processing. We then propose and validate a modified rule of mixture based on a damage parameter affected by the latewood proportion and cell wall properties.

INTRODUCTION

Until now, no clear quantitative correlation between structural properties and internal damage measurements has yet been established for wood plastic composites (WPCs). During WPC production, the preferred method for manufacturing is extrusion and injection molding, where temperatures of about 200 °C and high pressures are normally used (Wolcott and Englund, 1999). By using this method, composites of 40% to 70% (by weight) of wood, used as fibers or wood flour, can be produced with additives to improve the processability and performance of the final composite.

Wood cell architecture may suffer significant changes due to loading, heating conditions and physical-chemical environments during WPC production. Extreme processing conditions may induce structural damage of wood flour particles, evidenced as buckling, cellular collapse and eventually fracture in cell walls, and consequently a poor reinforcement of the thermoplastic phase. To study material damage in wood cells during any transformation process, it is necessary to consider that natural cellulosic fibers have an individual molecular architecture that may eventually impact the overall mechanical behavior of wood fibers. Fiber walls are largely composed of a multitude of filaments wound helically with respect to the fiber axis (Mark, 1967); these are called microfibrils. The principal constituent of microfibrils is cellulose. Inside the primary wall of wood cells is the secondary wall, composed of a thin outer layer (S1), broad central layer (S2), and thin inner layer (S3). The S2 layer represents the major component of the cell wall, and its microfibrils are more longitudinally directed, explaining its relevance in terms of the mechanical properties of the cell wall and of wood (Mark, 1967; Reiterert et al., 1999; Salmen, 2004). This cell ultrastructure of the natural filler for WPCs may be altered in processing, resulting in plastic flow and eventually fracture at the microfibril or nanoscale level.

In related literature, damage to composites is referred to as failure of the fiber-matrix interface, matrix cracking or crazing, fiber breaking and void growth (Agarwal and Broutman, 1990). However, more research needs to be conducted on damage caused to materials during the production of composites. Geimer, et al (1985) studied damage in wood composites and found no microscopic internal damage during the flaking process to produce flakeboards; but, the flakes did suffer internal damage during hot pressing resulting in lower mechanical properties, and evidenced in buckling, shearing and bending failure, most frequently in earlywood. More research needs to be done to quantify the actual damage in WPC, particularly in the filler material. In our research, we quantified wood cell damage in terms of the stiffness reduction of the S2 layer for the cell wall by measuring Young's modulus with nanoindentations on the cell wall before and after processing.

MATERIALS AND METHODS

For particular wood species, anatomical features and mechanical properties of the cell wall may determine the potential for stress transfer of hybrid materials like WPC. Since wood is an anisotropic material, in normal stemwood cells the secondary cell wall layer S2 dominates the mechanical properties of about 80% of the cell wall due to its thickness (Fengel, 1973). In this study, we determined nanomechanical and localized properties (mainly of the S2 layer and middle lamella) before processing solid wood samples**.** We also established the potential decrease in mechanical properties for wood and proposed a modified rule for mixture. This includes an additional factor that takes into account the reduction in axial stiffness for the cellular material caused by microstructural damage of the cell wall during milling, extrusion and injection processes.

Materials. Two wood species, Grand fir (GF) and Lodgepole pine (LP) from outerwood of 12 inches log diameter were used to produce wood flour and composites with high density polyethylene (Equistar LB 0100-00) as the matrix. Ponderosa pine and polypropylene (PP) were then used to validate the proposed model, adding a damage factor in the rule of mixture to predict the axial stiffness of the WPC. In this last particular composite, a lubricant, Strucktol TPW113, was added to the formulation.

Nanoindentation on solid wood. A Triboscope Hysitron Nanomechanical test instrument equipped with a force transducer for nanoindentation was used to quantify the mechanical properties of the cell wall. Indentations were performed in earlywood and latewood cells, and also in the middle lamella of solid wood samples. A Berkovich-type triangular pyramid indenter was used in a loading cycle with 300 μN nominal force. The loading cycle and resultant load displacement plot are presented in Figure 4.1. In an individual indentation experiment, the peak load (P_{max}), the depth at peak load (h) and the initial unloading stiffness (S), which is the slope of the unloading curve, were obtained. The geometry of the indenter and h, the contact area (A) was also calculated. Then, the reduced modulus (E_r) is determined according the equation:

$$E_r = \frac{\sqrt{\pi}}{2}\frac{S}{\sqrt{A}} \qquad \text{Eq. 4.1}$$

The main idea is that even for materials which exhibit plastic deformation during loading, the initial unloading is elastic. Thus, the initial slope of the unloading curve is directly related to the elastic modulus (Sneddon, 1948; Sneddon 1951). When E_r is a resultant of the elastic deformation of the indenter and the sample, then the reduced elastic modulus is:

$$E_r = \left[\frac{1-\nu_s^{\ 2}}{E_s} + \frac{1-\nu_i^{\ 2}}{E_i} \right]^{-1} \qquad \text{Eq. 4.2}$$

where the sub-indexes *s* and *i* represent the sample (*cell wall*, *S2 layer*) and indenter respectively and ν is Poisson's ratio. The indenter modulus, E_i, is constant and equal to 1240 GPa, with a Poisson's ratio equal to 0.07. A Poisson's ratio of 0.34 and 0.33 is assumed for Grand fir and Lodgepole pine respectively (Wood Handbook, 1999). For HDPE, a Poisson's ratio of 0.3 was assumed. For each wood species, 5 mm cubes were embedded in an epoxy resin by exchange with acetone acting as a solvent for the epoxy resin. This embedding process gives support to the cellular structure during cutting with a diamond knife, which was used to get a smooth surface for indentations. Nanoindentations on the cell wall, S2 layer, and the middle lamella were performed for latewood and earlywood cells.

Extrusion and injection: damage to the cell wall after processing. Wood flour-HDPE composites were made in an 18 mm twin screw extruder followed by injection molding, with 40% wood by weight). Then, to validate a proposed prediction model, composites made of PP and Ponderosa pine wood flour were produced with inclusion of 4% of lubricant using a series of wood/PP proportion. These composites were produced with a 0%, 20%, 30% and 40% weight fraction, using extrusion and injection as before. The screw speed, barrel temperature and melt pressure at the die were 70 rpm, 180 °C and 500 to 550 psi, respectively. Then tensile specimens according to ASTM D638 were obtained in an injection molding Sumitomo SE 50D. A morphology analysis on cross sections of tensile samples was conducted using a Hitachi S-570 scanning electron microscope (SEM).

In this research, we use tensile tests to examine the effect of the reduction in stiffness of the cell wall due to the wood size reduction and extrusion-injection processes on the performance of WPCs evaluated. The same methodology described to characterize solid wood was used on tensile samples. The axial modulus of random undamaged and buckled wood cells on cross sections of WPC samples was determined using nanoindentations. The three phases presented in cross sections of tensile samples without any loading history were characterized; thus, the bulk matrix (HDPE), the transcrystalline layer (TCL) and the cell wall (undamaged and collapsed) were considered. This three-phase evaluation is necessary for considering extra terms on modeling the axial modulus of experimental composites.

Modified rule of mixture and processing damage parameter. A semi-empirical model to predict the axial modulus of experimental composites was developed based on the wood cell damage due to the processing and the well known Rule of Mixture (ROM). The damage parameter was experimentally determined based on nanoindentation measurements in the cell wall, which allowed the calculation of Young's modulus of the cellular filler before and after processing. For the simple rule of mixture (constant strain), the Young's modulus in the 1-Direction, E_1 (Agarwal et al. 1990, Hull 1996, Voyiadjis 2005), is:

$$E_1 = E_1{}^f V^f + E^m V^m \qquad \text{Eq. 4.3}$$

where E_1^f is the Young modulus of the cellular material in the 1-Direction while E^m is the Young's modulus of the matrix. This original model assumes that fibers are aligned throughout the composite, a perfect bonding between main composite's phases where no slippage can occur at the interface and the strains experienced by the fiber, matrix and composite are equal. For all composites with well bonded reinforcements, Young's modulus in the 1-Direction will always be less than the value predicted by the Rule of Mixtures (Facca, 2006). None of the available models to predict stiffness of composites consider adjustment factors associated to the produced damage of the filler material. The damage parameter for wood cells takes into account reduction in modulus, moisture content and latewood-earlywood proportion of the species used. Because tensile tests and nanoindentations on the bulk polymer and TCL showed no significant differences in terms of this modulus for the thermoplastic, damage during this phase was not considered. The volume fraction V_f for experimental composites was estimated using the equation:

$$V_f = \frac{W_f \rho_c}{\rho_f} \qquad \text{Eq. 4.4}$$

where W_f is the weight fraction of wood, ρ_c is the density of the composite and ρ_f is the density of the fiber or wood. The density of the composite was 1.00 g/cm^3, and the density of the wood varied according to the species, moisture content and earlywood-latewood proportions, and whether corewood and outerwood was analyzed. Density is usually expressed as specific gravity, SG_1, which is a function of humidity (Bowyer et al., 1990); thus:

$$SG_1 = \frac{SG_2}{1 - SG_2(0.01MC_1MC_2)} \qquad \text{Eq. 4.5}$$

where SG_2 is the specific gravity at the moisture content MC_2. The last expression allows predictions of specific gravity when the change in moisture content is known. This physical change occurs during the drying of wood flour to target moisture of about 2%. Finally, the filler volume fraction was calculated. An adjustment of mechanical properties of wood as function of humidity was performed according the relation (Bowyer et al., 1990):

$$P = P_{12}\left[\frac{P_{12}}{P_g}\right]^{\left(\frac{12-M}{\mathrm{Mp}-12}\right)} \qquad \text{Eq. 4.6}$$

where P_{12} is a particular mechanical property at 12% moisture content, P_g is the property at green condition, Mp is a constant equal to 21 for softwoods, and P is the mechanical property at the M% moisture content. M was about 2% in wood used to make the experimental composites examined here.

After these corrections, the *Damage parameter* was introduced. As we stated, the damage parameter depends on the earlywood-latewood proportion. According to nanoindentations measurements, the axial modulus of cell walls from latewood is significant higher than that of earlywood. The reduction in the modulus of the cell wall due to the thermo-mechanical effect during the extrusion-injection process was lower for latewood cells.

Thus, we designed an experiment to quantify the latewood and earlywood proportion of representative wood samples. Thirty 5x5 cm^2 sections were cut for each wood species and scanned in a HP Scanjet ADF scanner. Digitalized images were analyzed using Image-pro software. To determine the ratio of area of latewood/area of earlywood in each image, a bi-level mask with a sensitivity of 4 was used to manually select the intensity range of latewood, determining the latewood proportion $l_{w.}$ The earlywood proportion, e_w, was calculated as:

$$e_w = 1 - l_w \qquad \text{Eq. 4.7}$$

The damage of the cell walls due to the processing conditions, E_D, was first estimated as:

$$D = \frac{E_b - E_a}{E_b} \qquad \text{Eq. 4.8}$$

where, E_b and E_a are the axial modulus or Young's modulus of the cell wall measured before and after processing. Nanoindentations were used to quantify E_b and E_a, and D was determined either for earlywood (D_E) of latewood (D_L). The resulting damage parameter D^f is:

$$D^f = e_w\,(1 - D_E) + l_w\,(1 - D_L) \qquad \text{Eq. 4. 9}$$

Finally, the Modified Rule of Mixture (MROM) to take filler mechanical damage into account is:

$$E_1 = D^f E_1^{\,f} V^f + E^m (1 - V^f) \qquad \text{Eq. 4.10}$$

The potentially reduced Young's modulus of the filler material due to extreme pressure and temperature conditions during processing of WPCs may allow more realistic predictions compared with well-known models like the simple rule of mixture, the Halpin-Tsai equation, Shear-lag's theory, Nair's model and Cox's model, which were well described by Facca (2006). The modified rule of mixtures presented here was validated in an additional experiment using a different polymeric matrix and wood species. With a similar process (extrusion-injection), PP-ponderosa pine wood flour composites were also manufactured.

RESULTS

***Micro-properties of wood components and wood species effect*.** The two wood species analyzed in terms of nanomechanical properties of the cell wall (S2 layer) do not present significant differences in elastic modulus, even when comparing earlywood and latewood separately. For both wood species, the elastic modulus of the cell wall is significantly higher than the modulus for earlywood. When comparing the elastic modulus of the middle lamella, it can be stated that there are no significant differences between species. Nevertheless, the middle lamella Young's modulus for Grand fir was slightly higher than Lodgepole pine (Figure 4.2).

The elastic modulus of the cell wall is consistent with values reported by other authors in species such as Norway spruce and Red spruce (Gindl and Gupta, 2002; Gindl et al., 2004; Wimmer, 1997). The elastic modulus of the cell wall for latewood was about 17 GPa and 14 GPa for earlywood in both wood species. The average modulus for the middle lamella in Grand fir was approximately 11.5 GPa, slightly higher than the elastic modulus for the middle lamella of Lodgepole pine samples, which was about 9 GPa. Measurements performed on the middle lamella showed high variability. This may have been due to the non-uniform structure for this part of the cell wood structure, which is made basically made of lignin. According to Salmen (2004), lignin in the middle lamella of softwoods is more branched than the lignin in the secondary wall, particularly in spruce wood fibers. Thus, the elastic properties of lignin may be therefore difficult to assess.

The nanomechanical properties of the cell wall for the wood species studied here are mainly affected by the microfibril angle (MFA) between the direction of the helical windings of the cellulose microfibrils in the secondary cell wall of fibers and tracheids and the long axis of the cell (Barnett and Bonham, 2004). The variability of the MFA is a response of the tree to environmental stress. Thus, the larger the MFA the lower the Young's modulus of the secondary wall. Therefore, the wood species and growth process of the tree may significantly affect the stiffness value of the cellular structure, shown by the nanomechanical characterization. However, properties of the middle lamella, mostly comprised of amorphous polymers, do not play a fundamental role on properties in the longitudinal direction of fibers (Salmen, 2004). Mark (1967) notes that for normal fibers in tension, failure should never initiate in the middle lamella. The middle lamella, which had low elastic modulus compared with the secondary wall, will not be subjected to high stress; since the microfibrils on both sides of the lamella have the same molecular conformation, no interlaminar shear stresses of significance are likely to be induced in the middle lamella during tensile loading.

More important is the role of mechanical properties of the middle lamella on transverse fiber-wood properties (Salmen, 2004). The differences in the modulus of the middle lamella between Grand fir and Lodgepole pine may partially explain the response of wood particles during extrusion-injection in terms of the final cellular collapse that we saw in experimental WPC after processing (Figure 4.3b). Cellular collapse was more evident in Lodgepole pine cells, which usually have a lower modulus in the middle lamella.

Additional factors may affect collapse. Geometrical features (cell wall thickness and lumen diameter) and interconnectivity between cells (through open pits) facilitate the melt flow of the HDPE and may play a role in the response of wood under compression perpendicular to fibers in the barrel. In the next section, we explain how mechanical properties of the natural filler change after processing and how this can affect the performance of WPCs.

Nanomechanical properties of phase's composite. Changes in mechanical properties of the cell wall during processing, particularly the potential damage to wood cells, may be expressed as a reduction in stiffness of the cell wall after severe impact loads during milling and also as cellular collapse due to hydrostatic loading conditions during extrusion-injection. Thermal degradation of wood may be considered as a contributing factor to the overall reduction in mechanical properties of the cell wall.

In initial experiments using a vacuum bagging process and scanning electron microscopy (SEM), we quantified the mechanical interlocking between wood species from small diameter logs and HDPE without coupling agents or additives. As a response the interaction between solid wood and HDPE, the collapse of cells for specific wood species may be identified as probable mechanisms impeding higher mobility in the thermoplastic and enhancement of interpenetration and interfacial area between phases. This directly affects the stress transfer mechanism for these composites. The stress transfer mechanism also affects the effective strength and stiffness of the used filler material. This experiment quantified the individual properties of each phase of the composite and produced direct measurements that may be used in prediction models for better estimations of design properties of WPCs.

First, it is necessary to point out the significant damage that can affect wood particles during size reduction and thermomechanical processes such as in hammer milling and extrusion-injection molding. Figure 4.3a shows the abrupt separation or fracture of wood cells after being processed in a hammer mill. This picture shows the non-uniform morphology of wood flour particles and also an irregular surface which will interact with the molten thermoplastic in the extrusion. Figure 4.3b shows a characteristic cross section of an experimental composite evidencing cellular collapse and, in some cases, cell wall fracture. Results presented earlier suggest that cumulative damage of the cellular material can affect the performance of WPCs.

It was also necessary to quantify properties of the thermoplastic phase after processing and before mechanical testing. There was a slight increase in the modulus of the TCL compared with the bulk HDPE. With nanoindentations, a Young's modulus of 1.07 GPa and 1.32 GPa were determined for the bulk thermoplastic and TCL, respectively (Figure 4.4). No significant differences were found, and this may be due to the high variability of the TCL modulus. The longitudinal modulus calculated based on nanoindentations is consistent with mechanical testing results obtained according to ASTM D638. Using this standard, the tensile modulus of the unreinforced HDPE was 1.014 GPa. Klein et al. (1995) found similar differences between TCL-bulk when quantifying mechanical properties of TCL in aramid fibers reinforced nylon 66 microcomposites. By isolating the TCL by microtoming and then using DMA (dynamic mechanical analysis) these researchers found that the viscoelastic energy damping of this layer is smaller, while the elastic modulus is higher compared with that of the crystallized matrix. They also stated that the magnitude of energy damping by the TCL can be used in a rule of mixture expression to calculate energy damping of the composite. This difference in magnitude of modulus of the TCL for HDPE may explain differences in predictions of the axial stiffness for composites analyzed here. Nevertheless, we are assuming that there is not a significant effect of the TCL properties on differences predicted with the experimental modulus, at least in formulations studied here.

The effect of transcrystallinity on mechanical properties depends on its thickness and thereby on the wood flour volume fraction. Although the effect of these variables is beyond the scope of this research, we consider this to be a very important issue that should be addressed. Quan, et al. (2005) also agree that the anisotropy of the TCL significantly influences the performance of fiber/polymer interfaces, and hence properties of the composite. Mechanical properties of the TCL can be attributed to the preferred crystallite orientation relative to the wood flour particles, thereby conferring on the matrix in the wood particle direction higher strength and rigidity.

The methodology presented here, based on nanoindentations, is a reliable research tool for TCL investigations, particularly because TCL has not yet been fully understood, nor has its effect on properties of composites like WPCs (Klein et al., 1995; Nuriel et al. 1999; Quan et al. 2005).

Modified rule of mixture and damage parameter. According to Equation 4.10, prediction of the longitudinal stiffness for experimental WPCs depends on latewood and earlywood proportions, and on the associated structural damage of the cell wall. The latewood proportion varies between wood species, and latewood cells have higher thickness and longitudinal stiffness. These characteristics lead to a different damage state of the cellular filler after extrusion. Despite the fact that the latewood proportion in Lodgepole pine outerwood is higher than in Grand fir, there are no significant differences between them (see Figure 4.5). The data in Figure 4.5 was used to estimate the earlywood proportion, following Equation 4.7.

As Figure 4.6 shows, there was a significant decrease in the axial modulus of the cell wall for both wood species when we compared to their properties before and after processing. There was a reduction in the modulus (Equation 4.6) of about 40% and 70% for latewood and earlywood cells respectively. This significantly affects the damage parameter estimation (see Equation 4.9). Table 4.1 presents estimated averaged values for the damage parameter for wood species used in our experiments. It shows a generalized damage parameter related to extrusion-injection processes that can be used for further predictions using Equation 4.10. Thus, $D^f = 0.35$ may represent a good approximation in predicting the longitudinal modulus of composites made with identical processes. This approximation considers an average condition in terms of latewood/earlywood proportion and the associated damage of softwoods utilized in this study. Results for this prediction are presented in the next section.

MROM, validation. Figure 4.7 shows predictions of the longitudinal modulus for WPCs made of PP and Ponderosa pine using different weight fractions of the natural filler. Predictions with the rule of mixture and modified rule of mixture are compared to the experimental determination of the modulus in the 1-Direction. The new materials used to validate the proposed model, based on the damage of the cell wall in processing, were subjected to identical extrusion and injection molding as before. The tensile modulus, predicted with ROM and MROM, increases linearly with an increase in wood flour content. The proposed MROM predicts very precisely the tensile modulus of the PP-Ponderosa pine composites (figure 4.7). A damage parameter, $D^f = 0.35$ represents the impact of the particular manufacturing process used here for decreasing the properties of wood flour particles.

The methodology presented here using nanoindentations on the cell wall, allowed us to gain a very reliable determination of the decrease in properties of the cell wall toward on effective tensile modulus. This can be utilized in feeding models and for improving estimations in the WPC design process.

A different approach discussed by Facca (2006) considered the introduction of fitting factor χ in order to account for the imperfect straining of fibers in composites made of hardwood. In his work, he multiplied the χ parameter by the fiber modulus, obtaining the named effective fiber modulus, which took into account the influence of fiber length, imperfections in fiber alignment and adhesion. He used a secant method algorithm to determine the best fit value of χ, which minimizes the sum of squared errors between the ROM and the experimental data. The calculated best fit χ value for HDPE-hardwood composites varied from 0.300 to 0.301, included in the ROM, and showed excellent predictions of the longitudinal modulus for those WPCs. Values reported for the χ factor are close to the D^f parameter determined here.

However, our analysis differs from that of other authors in terms of the definition and determination for the mechanism behind the modification D^f parameter. The D^f

parameter represents the cumulative damage of the filler material expressed as reduction of the stiffness due to processing (mechanical and thermal conditions), determined experimentally using nanoindentations.

As wood content increases, the estimation error also increases in predictions using MROM. For composites made of 40% of wood flour (% weight), the prediction error was 50% and 35% for HDPE-LP and HDPE-GF wood composites respectively. Under similar conditions, the predicted error for PP-ponderosa pine composites was 5%, which represents a very good estimation of the tensile modulus in the 1-Direction (Table 4.2). The reduced error for estimations in HDPE-GF composites compared to HDPE-LP composites may be explained by the better adhesion (interlocking) found in a previous experiment for composites made of GF (Gacitua and Wolcott, 2007). Similarly, the addition of lubricant in the PP-ponderosa pine formulation may significantly enhance the mobility of the molten PP in the barrel, increasing the penetration and interface area between the thermoplastic and solid phase; therefore, improvements in interlocking adhesion may accomplish one of the requirements for applying the rule of mixture, which is perfect adhesion.

CONCLUSIONS

In this research, we successfully quantified the damage of wood particles to two wood species during processing and its impact on the performance of WPCs. We demonstrated this using a methodology based on nanoscale measurements of properties of the cellular filler before and after extrusion-injection processes. There was a reduction in Young's modulus of the cell wall due to processing from 40% to 70%. In general, the elastic modulus of the S2 layer was higher in latewood cells. These cells experienced lower collapse and damage than earlywood cells. Potential contributing factors to the cellular collapse of wood cells during processing may be the anatomical features of particular wood species, properties of the secondary and middle lamella and operation conditions (temperature-pressure-additives).

This research resulted in a modified rule of mixture. In the new model for predicting the modulus in the 1-Direction, it was assumed that the TCL and bulk matrix had similar mechanical properties because no significant differences were detected between them. The new model also introduced a modification or damage factor affecting the filler properties. The damage factor, which is a material parameter, was determined experimentally using nanoindentations. This factor represents the cumulative damage in wood cells due to processing, and is expressed as a reduction in modulus in the 1-Direction. This proposed model also proved to be very precise in predicting the longitudinal modulus for different formulations using other materials.

REFERENCES

1. Agarwal B.D., Broutman L.J. Analysis and performance of fiber composites. John Wiley & Sons, Inc. 1990, p 59.

2. Bowyer J., Rubin S., Haygreen J. Forest products and wood science, an introduction. Iowa State University Press 2003.

3. Barnett J.R., Bonham V.A. Cellulose microfibril angle in the cell wall of wood fibres. Biol. Rev. 2004; 79: 461–472.

4. Facca A. G. Predicting the tensile modulus and strength of single and hybrid natural fibre Reinforced thermoplastic composites. Dissertation Doctor of Philosophy, 2006. Department of Chemical Engineering and Applied Chemistry University of Toronto.

5. Fengel D., Stoll M. Uber die Verandenburg des Zellquerschnitts, der Dicke der Zellwand und der Wandschichten von Fichtenholz-Tracheiden Innerhalb eines Jahrrings. Holzforschung 1973; 27: 1-7.

6. Gacitua W., Wolcott M. Morphology of wood species affecting wood-plastic interaction. Part I: Mechanical interlocking. 2007; Being submitted to Holzforschung.

7. Gacitua W., Wolcott M. Morphology of wood species affecting wood-thermoplastic interaction. Part II: enhancing toughness and mechanical properties. 2007; Being submitted to Holzforschung.

8. Geimer R., Mahoney R., Loehnertz S., Meyer R. Influences of processing-induced damage on strength of flakes and flakeboards. United states Department of agriculture, Forest Service, Forest Products Laboratory. Research paper FPL 463, 1985.

9. Gindl W., Gupta H.S. Cell-wall hardness and Young's modulus of melamine-modified spruce wood by nanoindentation. Composite part A. 2002; 33: 1141-1145.

10. Gindl W., Gupta H., Schoberl T., Lichtenegger H. Fratzl P. Mechanical properties of spruce wood cell walls by nanoindentation. Appl. Phys. A 2004; 79: 2069–2073.

11. Hull D., Clyne T.W. An introduction to composites materials. Cambridge solid state science series, 1996.

12. Klein N., Marom G., Pegoretti A., Migliaresi C. Determining the role of interfacial transcrystallinity in composites materials by dynamic mechanical thermal analysis. Composites 1995; 26: 707-712.

13. Mark R.E. Cell wall mechanics of tracheids. Yale University, The McKay Press, Inc., Midland, Michigan. 1967.

14. Nuriel H., Klein N., Marom G. The effect of the transcrystalline layer on mechanical properties of composites materials in the fibre direction. Composites Science and Technology 1999; 59: 1685-1690.

15. Quan H., Li Z-M, Yang M-B, Huang R. Review: On transcrystallinity in semi-crystalline polymer composites. Composites Science and Technology 2005; 65: 999-1021.

16. Reiterert A., Lichtenegger H., Tscheggt S., Fratzl P. Experimental evidence for a mechanical function of the cellulose microfibril angle in wood cell walls. Philosophical magazine A 1999; 79(9): 2173-2184.

17. Salmen L. Micromechanical understanding of the cell-wall structure. C. R. Biologies 2004; 327: 873–880.

18. Sneddon I.N. Fourier Transforms, McGraw-Hill, New York 1951.

19. Sneddon I.N. Proc. Cambridge Philos. Soc. 44 (1948) 492.

20. Tucker C., Erwin L. Stiffness predictions for unidirectional short-fiber composites: Review and evaluation. Composites Science and Technology 1999; 59: 655-671.

21. Voyiadjis G., Kattan P. Mechanics of composite materials with Matlab. Springer-Verlag Berlin Heidelberg 2005.

22. Wimmer R., Lucas B.N., Tsui T.Y., Oliver W.C. WC. Longitudinal hardness and Young's modulus of spruce tracheid secondary walls using nanoindentation technique .Wood Sci. Technol. 1997; 31: 131.

23. Wolcott M.P., Englund K. A technological review of wood plastic composites. 33rd international particleboard/composite material symposium. Washington State University, Pullman WA, 1999.

24. Wood handbook. Wood as an engineering material. General technical report FPL-GTR 113. Forest product laboratory, 1999.

Table 4.1: Average damage parameter for experimental natural filler (outerwood). Process: Extrusion-Injection.

Filler	D_E Dimensionless	D_L Dimensionless	D^f Dimensionless
Grand fir, earlywood	0.72	---	0.350
Grand fir, latewood	---	0.43	
Lodgepole pine, earlywood	0.73	---	0.353
Lodgepole pine, latewood	---	0.42	

Table 4.2: Comparison predicted-experimental values for composites made of 40% of wood flour (% weight).

Composite	E_1 (GPa) Experimental	E_1 (GPa) Predicted	Error (%)
HDPE-LP	2.50	3.75	50
HDPE-GF	3.41	4.60	35
PP-pond. pine	3.69	3.88	5

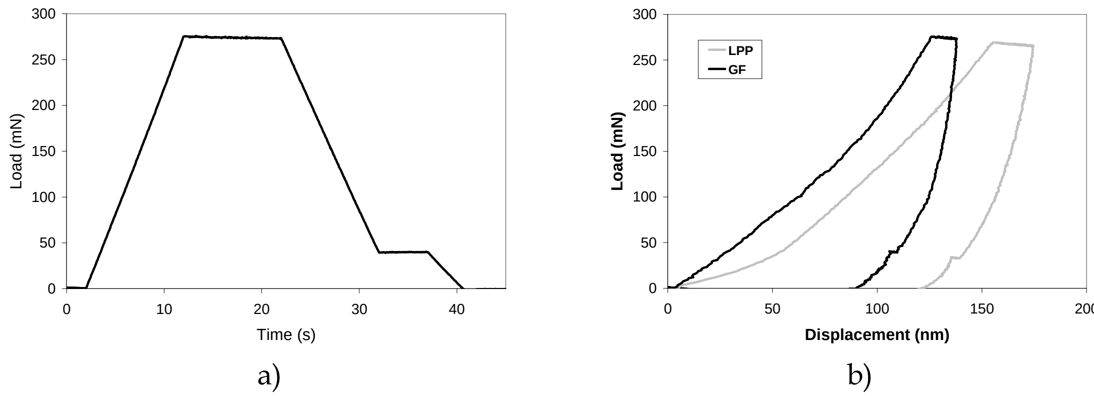

Figure 4.1: Effective loading cycle for nanoindentations (a) and the effective load-displacement plot after nanoindentations; example for indentations on grand fir (GF) and lodgepole pine (LP), outerwood.

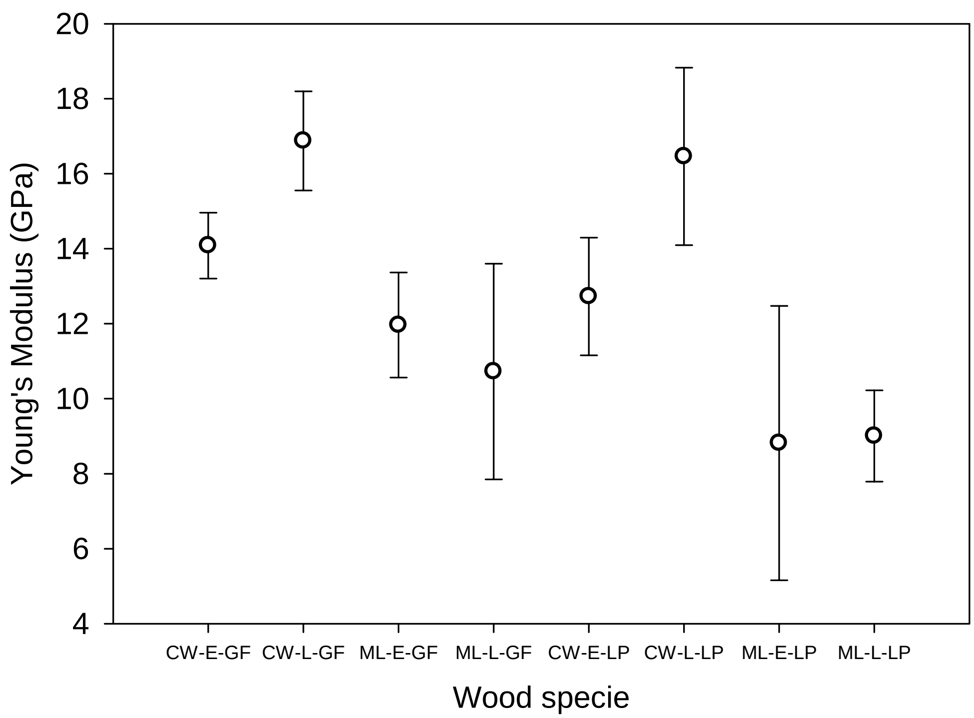

Figure 4.2: 95% interval of confidence and mean value for elastic modulus of wood species. GF and LP are grand fir and lodgepole pine, respectively; E is earlywood, L is latewood, CW is cell wall and ML is middle lamella.

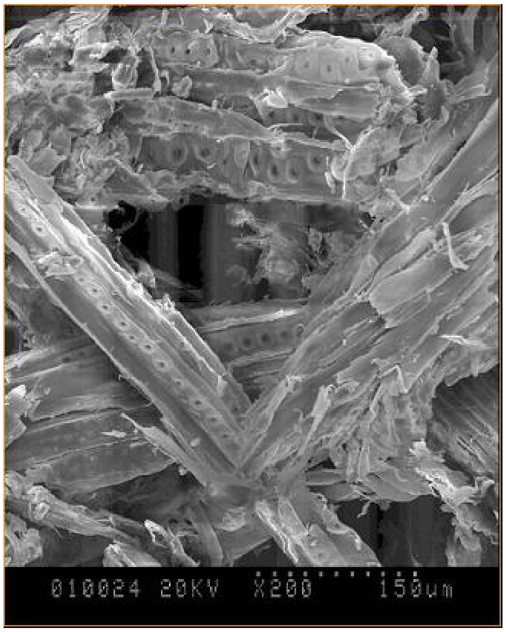

a)

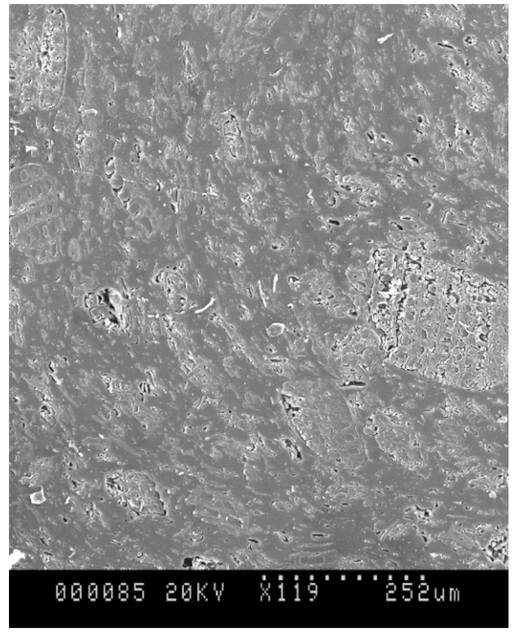

b)

Figure 4.3: SEM analysis of damage of the cellular filler during processing. a) after milling (wood flour 60 mesh), b) after extrusion-injection, 40% weight fraction for wood. Wood species is lodgepole pine, outerwood.

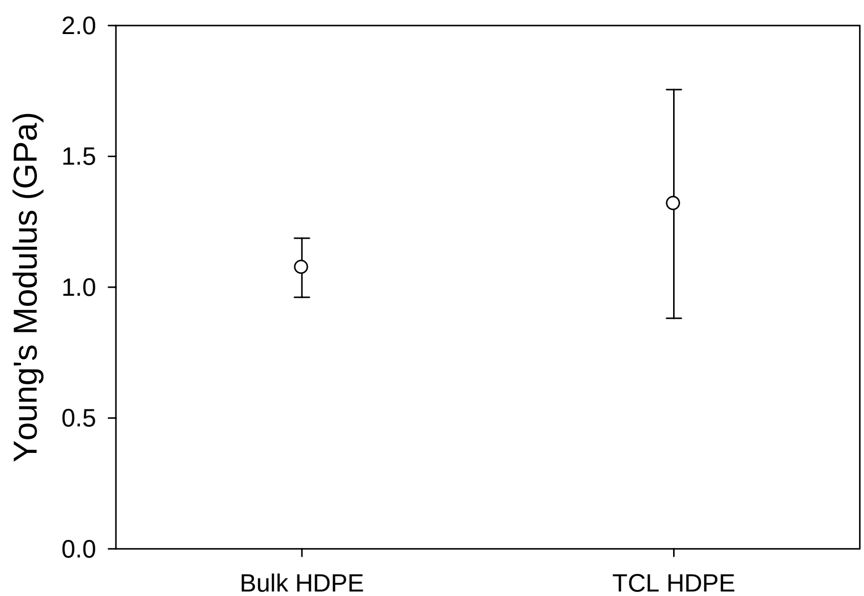

Figure 4.4: 95% interval of confidence for elastic modulus of the bulk and TCL thermoplastic phases in wood/HDPE composites measured with nanoindentations.

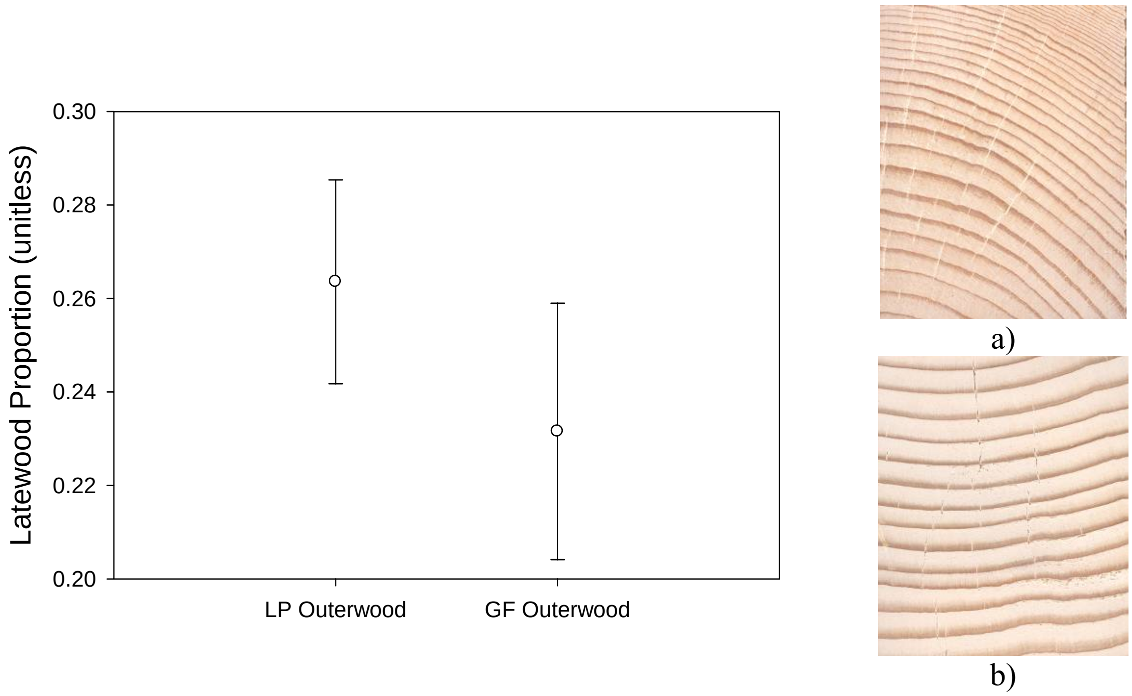

Figure 4.5: 95% interval of confidence for latewood proportion for lodgepole pine (LP) and grand fir (GF), both outerwood. Image for latewood determination in LP (a) and GF (b).

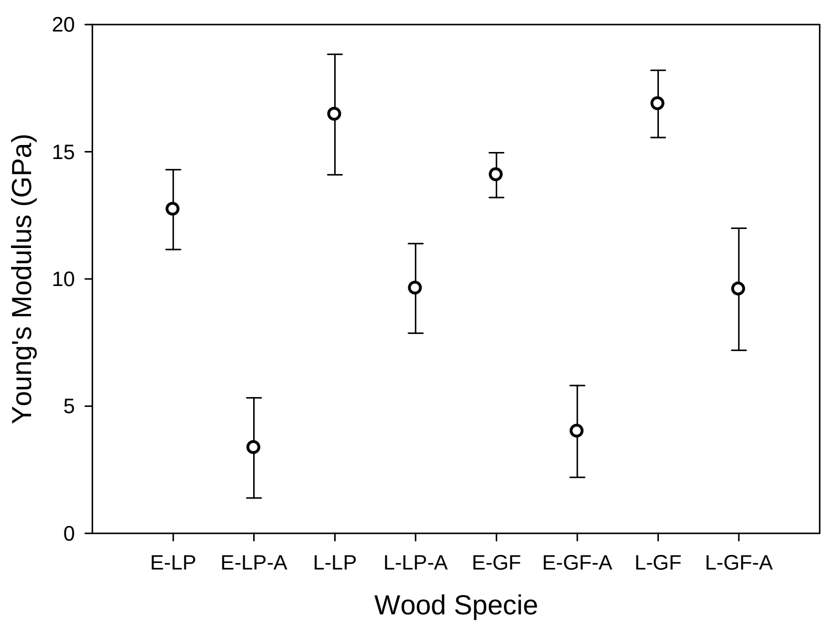

Figure 4.6: 95% interval of confidence for reduction of the elastic modulus of wood flour particles after extrusion and injection molding. GF and LP are grand fir and lodgepole pine, respectively; E is earlywood, L is latewood, and A represents the modulus measurement after processing.

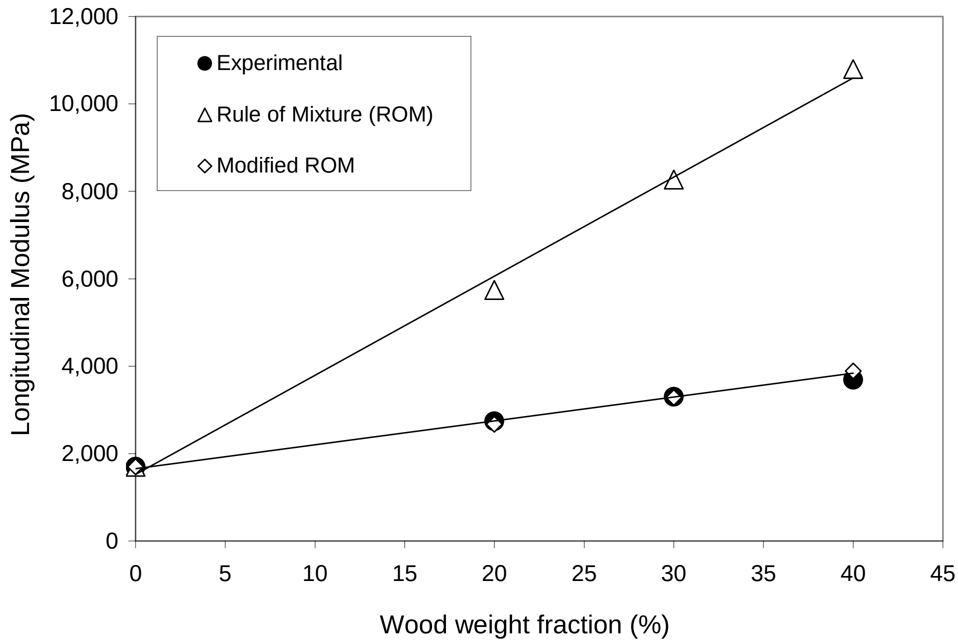

Figure 4.7 : Comparison of experimental and predicted tensile modulus based on rule of mixture and the modified rule of mixture. PP-ponderosa pine composites.

CHAPTER 5
AN ADAPTED MICROMECHANICAL MODEL FOR PREDICTING WPC PROPERTIES

ABSTRACT

This research developed a methodology to quantify the effects of wood species, type of process and WPC (wood plastic composite) formulation on mechanical and morphological properties of the experimental composites. Results show that the modulus of elasticity of grand fir wood plastic composites resulted in higher mechanical properties compared with lodgepole pine composites. Results also show that the morphological characteristics of experimental composites, such as void content and wood particle alignment, depend on the wood species and type of process utilized. This research also developed methods to obtain numerical factors that affect the fiber modulus, which accounts for particle alignment and thermo- mechanical degradation of wood during processing. With the aid of numerical factors determined experimentally, better modulus of elasticity predictions were obtained.

INTRODUCTION

After wood plastic composites (WPC) are manufactured, a decrease in stiffness and strength may be due to the presence of crack-like defects at the microscale and reduction in properties of the natural filler material. Independent of the wood species utilized to produce WPC, the produced composite contains a population of fine cracks that can cause a brittle failure in a typical tensile test. These inhomogeneities or flaws can cause changes in the macroscopic properties of the composite, and therefore its strength decreases. This process of structural deterioration resulting from creation, growth and coalescence of micro defects is called "damage" (Gross and Seelig, 2006).

Damage may occur in one or more forms, such as the failure of the filler-matrix interface, matrix cracking or crazing, fiber breaking, and void growth. In composites, initial damage may appear very early in the fatigue life, and its propagation may be arrested by the internal structure of the composite (Agarwal & Broutman, 1990). In critical applications, design loads should be less than those required to cause any damage within the composite. Therefore, a good understanding of various aspects of the WPC microstructure will aid the design of structures using this material.

Properties of a WPC depend on the properties of its phases and their distribution and physical-chemical interaction. Simple experimental methods can be used to determine WPC properties. However, one set of experimental measurements determines the properties of a fixed wood-thermoplastic system produced by a single fabrication process such as extrusion or injection molding. These types of experiments may become time-consuming and cost-prohibitive. Therefore, the use of theoretical and semi-empirical models based on microstructure of the composite can be used to predict the effects of a large number of system variables (composite formulation, processing conditions, particle size, particle alignment and filler degradation).

Mathematical models for studying some of the longitudinal properties (tensile strength and modulus of elasticity) of unidirectional composites are quite accurate in some cases (Agarwal and Broutman, 1990). One of the most popular mathematical models for predicting unidirectional properties is the rule of mixture (Agarwal and Broutman, 1990; Facca, 2006). The assumption behind this model is that fibers are parallel throughout the composite, creating perfect bonding between phases so that no slippage occurs at the interface, and so that the strain experienced by the fiber, matrix and composite are equal. Thus, the model becomes:

$$E_c = E^f V^f + E^m V^m \qquad \text{Eq. 5.1}$$

where *E* and *V* are the modulus of elasticity and volume fraction with the sub-indexes c, f and m being the composite, the fiber and the matrix, respectively.

However, in WPC production, this system of analysis and modeling is more complex. Many phenomena at some points violate the assumptions of the rule of mixture. Among them are wood particle alignment, wood cell densification due to cellular collapse, cell wall damage due to the environmental conditions (temperature and pressure) and the presence of small voids distributed mainly in the thermoplastic phase (Gacitua and Wolcott, 2007; Facca, 2006). In this scenario, it is necessary to adapt the actual model for better prediction of WPC properties. Therefore, Facca (2006) presented a model that accounts for changes in density and moisture content of wood particles during processing. He used an empirical fitting factor defined as χ in order to account for imperfect straining of the fiber. Then the modified model becomes:

$$E_c = \chi E^f V^f + E^m V^m \qquad \text{Eq. 5.2}$$

where χ is a function of the fiber length, imperfections in fiber alignment and the phase's adhesion. Thus, modification of the rule of mixture was based on the best fit value for χ. A secant method algorithm was used to determine the fit value of χ, which minimizes the sum of square errors between the rule of mixture used and the experimental data. Using this analysis, he obtained a χ value of 0.3 for the natural fiber reinforced thermoplastic made of hardwood (10% to 60% weight fraction) and HDPE in a twin-screw Brabender mixer and compression molding. Although this was an effective approach to determining experimental values, it is still unclear whether the mechanism is related to any particular process behind the correction of the natural filler modulus.

The challenge of our research was to identify, describe and quantify the main factors of wood species affecting the increase or decrease in the mechanical properties of WPC subjected to a uniaxial state of stress. Our objective was to develop methodologies to quantify the phase's properties and define new prediction models based on the characterizations of microstructures and nanoproperties.

MATERIALS AND METHODS

In a previous paper, the damage of wood cells, quantified as modulus reduction due to the extrusion and injection conditions (high pressure and temperature), was identified as a main factor affecting the performance of a WPC. This research applies these findings to a more realistic production scenario where the extrusion, considering normal formulations that include additives like coupling agents and lubricants, will be the production process for experimental WPCs made of grand fir and lodgepole pine. Thus, we are proposing a better explained empirical model based on the reduction in mechanical properties of the cell wall and particle alignment during extrusion. Experimental data was obtained in a monotonic loading condition in a simple tensile test according to ASTM D638.

Similar methods based on nanoindentations and developed previously to investigate the reduction of mechanical properties of the cell wall due to processing are used, as well as a procedure to evaluate wood particle alignment.

Materials. A polymer matrix HDPE Equistar Petrothene LB010000 was used. The wood filler materials were grand fir (GF) and lodgepole pine (LP). OP100 Honeywell Optipak 100 and Honeywell 575A MAPE were used as a lubricant and coupling agent, respectively.

Extrusion trials. These trials were performed in a Cincinnati Milacron 35 mm extruder. An extrudate with a cross section of 9 x 37 mm was produced using eight formulations, where we considered: two wood species, two filler weight fractions (50 and 65 % of wood), and coupled-uncoupled systems. For the coupled system, 2% MAPE, based on weight, was used. The amount of lubricant used for all formulations was 1% based on weight. Table 5.1 presents the formulations analyzed. To provide an overlap in the further described wood particle alignment factor on composite properties, injection molding (IM) samples were prepared for uncoupled formulations: LP 50-0, LP 65-0, GF 50-0 and GF 65-0.

Wood particle properties. Nanomechanical properties before and after extrusion were evaluated using a nanoindenter Tryboscope Hysitron equipped with a Berkovich type indenter. A loading cycle with a maximum lad of 300 μN was used. From the unloading part of the cycle, the sample modulus E_s was obtained from the equation (Gindl and Gupta, 2002; Oliver and Phar, 1992; Pharr, 1998):

$$E_r = \left[\frac{1-\nu_s^{\,2}}{E_s} + \frac{1-\nu_\iota^{\,2}}{E_\iota} \right]^{-1} \qquad \text{Eq. 5.3}$$

where, E_r is the reduced modulus determined directly from a nanoindentation, ν_i and ν_s are the Poisson's ratio for the indenter and sample, respectively. The indenter modulus E_i is equal to 1240 GPa, with a Poisson's ratio of 0.07. A Poisson's ratio of 0.34 and 0.33

was assumed for grand fir and lodgepole pine, respectively (Wood Handbook, 1999). For HDPE, a Poisson's ratio of 0.3 was assumed. As samples for nanoindentations, 5 mm cubes were used for wood and composite materials. Solid wood samples were first embedded in an epoxy resin and then cured to aid the cutting and polishing process. Earlywood and latewood cells were indented, and the modulus of elasticity was obtained using the procedure described by Oliver and Pharr (1992). Wood and composite surfaces for indentation were prepared first using a diamond knife mounted in a Leica ultramicrotome and then polished with a 12000/4000 polishing paper. Smooth samples surfaces are required for better imaging and identification of the wood and WPC microstructure. Nanoindentations on the cell wall, S2 layer were performed. As in the previous paper, the damage of the cell wall due to the extrusion conditions was evaluated according the equation:

$$D = \frac{E_b - E_a}{E_b} \qquad 5.4$$

where, E_b and E_a are the axial modulus or Young's modulus of the S2 layer before and after extrusion. For a composite in an indentation process, first an image of the cross section is obtained and, according to the geometry of wood cells (size and wall thickness), were segregated and indented, and then E_b and E_a were obtained. D was calculated for earlywood (D_E) and latewood (D_L) cells. Finally, the modulus reduction parameter D^f that applies for the extrusion process is:

$$D^f = e_w\,(1 - D_E) + l_w\,(1 - D_L) \qquad \text{Eq. 5.5}$$

The latewood proportion l_w and earlywood proportion e_w were previously determined with image processing of the transverse section of 5x5 cm^2 sections. Thus, l_w is 0.733 and

0.768 for lodgepole pine and grand fir respectively. The earlywood proportion is $e_w = 1 - l_w$. As discussed by Facca (2006), the modification of the fiber modulus of elasticity is explained by fiber alignment and fiber length. We obtained a similar modification of the modulus parameter in a previous experiment, but in the case of our experimental approach, we may postulate that:

$$\chi \cong D^f \qquad \text{with } D^f = f\,(\text{particle alignment and wood degradation})$$

To explore this hypothesis, we decomposed the D^f parameter as follows:

$$D^f = D^f_\theta D^f_D \qquad \text{Eq. 5.6}$$

where D^f_θ and D^f_D are the numerical factors associated with wood particle alignment and thermo-mechanical degradation of wood during processing. When D^f (determined with nanoindentations) and D^f_θ, are known, the proposed damage mechanisms D^f_D may be estimated numerically. The orientation angle θ of wood particles along the 1-direction of the tensile samples was determined with SEM images and analysis with Image-pro software. For this purpose, a small surface of 10x10 mm was taken from the middle section of 3 tensile samples, and from each surface, 6 SEM areas of interest were obtained for the alignment measurements (figure 5.1a). Once an average θ value was determined, the D^f_θ was obtained as:

$$D^f_\theta = \frac{E_1 - E_\theta}{E_1} \qquad \text{Eq. 5.7}$$

with,

E_1: longitudinal modulus of elasticity for particular wood species (from Wood Handbook, 1999).

E_θ: estimated modulus of elasticity in the new arbitrary axes, oriented in a θ angle from the 1-direction (Agarwal and Broutman, 1990). Thus,

$$E_\theta = \frac{E_1}{\cos^4\theta + \left(\frac{E_1}{G_{12}} - 2\mu_{12}\right)\sin^2\theta\cos^2\theta + \frac{E_1}{E_2}\sin^4\theta} \qquad \text{Eq. 5.8}$$

where E, G and μ are the modulus of elasticity, shear modulus and Poisson's ratio respectively; sub-indices 1 and 2 are the longitudinal and transverse direction properties obtained from the Wood Handbook (1999). The presented methodology was applied to injection molding and extrusion formulations.

Matrix damage characterization. A Hitachi S-570 SEM (scanning electron microscope) was utilized to characterize the microstructure on the cross section of the produced extrudates. The observed damage in the matrix consisted of voids mainly around wood flour particles. A voided matrix carries less load and is a source of crack propagation. With SEM, twelve areas of interest were symmetrically obtained from the cross section of the extrudate to quantify the percentage of void content, based on area measurements (Figure 5.1b). This process was used before and after the tensile test. For a better observation and quantification of the composite's microstructure, the cross section of the 3 x 9 mm sample was cut with an ultramicrotome. Then, the percentage of void area per AOI was measured using image analysis with Image-pro software through a Pruning filter with a threshold number of 53. Thus, the void content is determined as:

$$Vc = \frac{\text{Voids area } (\mu\text{m}^2)}{\text{Area AOI } (\mu\text{m}^2)} x100\% \qquad \text{Eq. 5.9}$$

Properties prediction model based on the fiber reduction modulus. We proposed a model that considers fiber mechanical properties reduction due to processing. The longitudinal modulus E_1 or modulus of elasticity in the fiber direction of the composite may be initially predicted with the rule of mixtures (ROM). The main assumption of the ROM formulation is that the strain in the direction of fibers is equal in the matrix and fibers. This implies that the fiber-matrix bond is perfect (Barbero, 1999). Here we adapted the traditional ROM to account for particle orientation and potential fiber degradation due to the high pressure and thermal conditions in the barrel and then in the die. Lastly, the semi-empirical model to predict E_1 in WPC produced by extrusion is:

$$E_1 = D^f E_1^f V^f + E_1^m (1 - V^f) \qquad \text{Eq. 5.10}$$

where E_1^f is the Young's modulus of the cellular material in the 1-Direction, while E_1^m is the Young's modulus of the matrix, V^f is the filler volume fraction, D^f represents the modulus of elasticity reduction to be decomposed in the D^f_θ and D^f_D values. The modulus of rupture in tension was analyzed using regression models based on the wood content, coupling agent and void content before testing.

RESULTS

Morphology of extrudates

Figure 5.2 shows a general view of the surface quality of extrudates just after extrusion of a 9 x 37 mm section. It is possible to observe the response elastic surface instability, known as *sharkskin*, for some WPC formulations. All of the coupled systems presented sharkskin, with a varied morphology of the surface. For commercial applications, this surface appearance is unacceptable. There are many reasons for this phenomenon, especially the rheology of the polymeric fluid close to the die exit corner (Miller and Rothstain, 2004).

Another useful analysis can be done using the Deborah number. The Deborah number is defined by:

$$De = \lambda / t_p \qquad \text{Eq. 5.11}$$

where λ is the relaxation time of the polymer and t_p is the characteristic process time. The characteristic process time can be defined as the ratio of the characteristic die dimension and average speed through the die. As the Deborah number becomes > 1, the polymer, HDPE in our case, does not have enough time to relax during the process, resulting in possible extrudate dimension deviations and sharkskin that we saw in coupled formulations (Osswald and Menges, 2003).

Nevertheless, there is a consensus among researchers that the mechanism of the sharkskin instability is rooted in the stress singularity that develops at the die exit. This occurs as the melt accelerates from the rest for the case of a no-slip velocity boundary condition, or from a small velocity for the case of slip boundary condition to a consistent velocity plug flow beyond the exit plane. The presence of this stress singularity can lead to a rapid tensile deformation of the polymer molecules in the extrudate near the die wall, which can, in turn, result in enormous tensile stresses (Denn, 2001).

For the particular surface morphology observed in experimental WPCs, many factors apply for discussion. For example, according Denn (2001), there are three theories to describe slip in polymer surfaces. First, the slip may be a result of the adhesive failure of the polymer chains at the solid surface. A second holds that slip is a cohesive failure resulting from disentanglements of chains in the bulk from chains absorbed at the wall.

The last is that a lubricant layer at the wall is possibly the result of stress-induced transition to a low-viscosity mesophase. In our experimental design, we did not take into account experiments that may have provided a better understanding of the observed phenomenon, but we recognize that this must be addressed in further investigations beyond the scope of the objectives studied here.

Response of fiber properties due to extrusion: Cell wall nanoindentations

Using nanoindentations, it was possible to quantify the longitudinal modulus of earlywood and latewood cells on the cross sections of experimental composites. We found a significant decrease in the modulus of elasticity of solid wood samples without any thermo-mechanical treatment (table 5.2) compared with modulus of wood cells after extrusion (Figure 5.3).

We recognize that this decrease, which is related with the defined D^f parameter, may be due to factors associated with the experiment. These factors could relate to imperfect alignment of wood particles, mechanical degradation of the cell wall due to the hydrostatic pressure conditions in the barrel, and shearing forces, where high thermal conditions may degrade the lignin bonding microfibrils in the cell wall. Despite these contributions to the overall modulus reduction due to extrusion, it was possible to quantify a D^f modification factor equal to 0.570 and 0.603 for composites made with lodgepole pine and grand fir, respectively. It is important to note that this modification factor was equal to 0.350 for composites previously fabricated with extrusion and then injection molding (Table 5.3). A double thermo-mechanical process reduces the D^f value, which may be due to the mentioned cell wall degradation. Figure 5.4 shows a characteristic surface topography of the interface cell wall-HDPE. The image shows two indentations performed on the cell wall where the permanent plastic deformation, after applying the loading cycle, is evident.

Matrix damage response due to extrusion: Void content

WPCs are not perfect materials. At the microscale, they have irregularities in their microstructure. The main imperfection that we detected is the presence of voids located inside wood particles and due to incomplete infiltration of the cellular lumen, or in the matrix mainly around wood particles. A poor infiltration of wood cells may be due to the interconnectivity among cells governed by pits and their distribution on the cell wall. As we noted in Chapter 1, another mechanism that may cause low mechanical interlocking is the relation between the mechanical properties and geometry of the cell wall, which in some cases causes cell wall collapse, and impedes free movement in the thermoplastic phase. Voids in the matrix may be related to a non-efficient wetting process of HDPE on wood particles, particularly for systems without a coupling agent.

We proposed that these defects in the composite are caused by the wood species selected for the production of the WPC, as well as by manufacturing process conditions. We did not investigate the process conditions in this scenario, because we were focusing on wood species effects. Thus, we demonstrated the strong influence of microcracks or voids on the mechanical properties of WPCs, which is discussed in further sections of this paper.

In Figure 5.5, two extreme situations in terms of void content are presented. SEM micrographs show matrix voids around a wood particle and cellular collapse (Fig. 5.5a) in a formulation with 65% of lodgepole pine wood flour. On the other hand, a coupled formulation with 65% of grand fir wood flour showed a significant reduction of voids. The better adhesion HDPE-wood (specific adhesion) may explain the observed void reduction response. The average void content, which we found for composites made through extrusion, was higher than the void content encountered for injection molding samples. For both types of manufacturing process, voids were mainly localized in the interface wood particle-matrix.

For WPC formulations with 50% wood (based weight) there is not a clear trend (Fig. 5.6a). The variable response in terms of void content may be associated with the irregular morphology of the extrudate previously discussed. The sharkskin and melt fracture could be related factors affecting the measured void content.A completely distinct situation was observed for WPCs made with 65% wood, where grand fir formulations had lower void content than those with lodgepole pine (Fig. 5.6b). We found significant differences, particularly when we used coupling agent in the formulation. The observed void content trends for formulations with 50% and 65% of wood correlate well with MOE and MOR determined through longitudinal tensile tests. The formulation with 65% grand fir wood flour and 2% coupling agent presented the lowest void content.

WPC properties

Figures 5.7 and 5.8 present the modulus of elasticity (MOE) and the tensile strength (MOR), both in the 1-direction, for experimental composites. Both responses depend on the wood content, coupling agent and wood species utilized. It is interesting to note that the general trend for MOE and MOR is inversely related to the void content trend presented in Figure 5.6, in formulations with 50% and 65% wood flour. The mechanism behind this particular trend is consistent with the damage theory; thus, as the void content decreases the MOE and MOR increase (Fig. 5.6, Fig. 5.7 and Fig. 5.8). For MOE and MOR, composites made with 65% wood content using grand fir wood flour were significantly superior to lodgepole pine composites when coupled and uncoupled systems were analyzed. A different response occurred when we visualized MOE-MOR for 50% wood formulations, where there was no significant difference between coupled and uncoupled formulations. When we used SEM to analyze WPC morphology, the coupling agent enhanced specific adhesion, particularly in WPCs with 65% wood flour. We did not see a similar microstructure for coupled systems with 50% wood; in fact, the void content of these formulations tended to increase, mainly due to the surface and instability of the extrudate (Figure 5.2).

MOE-MOR predictions based on damage parameters

Using the proposed modified rule of mixture MROM (Equation 5.10) based on fiber modulus reduction, we predicted the longitudinal modulus of elasticity of WPCs. The modified equation accounts for factors related to the extrusion process utilized, namely, the ratio of earlywood/latewood cells and modulus of elasticity degradation in the cell wall.

Figure 5.9 shows a comparison between experimental and predicted MOE using Equation 5.10. For coupled systems, the proposed equation may underestimate the experimental value. This suggests that an extra term in Equation 5.10 can be added to account for a potential effect of the transcrystalline layer (TCL), which forms on wood particles surfaces in coupled formulations. Mathematically, this would be:

$$E_1 = D^f E_1^f V^f + D^m E_1^m V^m + E_1^{TCL} V^{TCL} \qquad \text{Eq. 5.12}$$

where E_1^{TCL} and V^{TCL} are the longitudinal modulus and the volume fraction for the TCL, respectively. The challenge here is determining the mechanical properties and volume fraction of the very thin layer surrounding wood particles in a composite.

This could be a new avenue for research, and suggests that nanoindentations may be useful as an evaluation tool. On the other hand, the predicted moduli for uncoupled systems in general overestimate the experimental value. As in predictions of MOE for injection molding samples (without coupling), over-estimations were expected because there is no guarantee of perfect adhesion (one of the assumptions of the rule of mixture next to the equal strain for fiber and matrix) in uncoupled formulations. For coupled systems, the prediction error was 13% and 32% for composites made of grand fir and lodgepole pine respectively. The source of this difference might be related to results from previous experiments, where we demonstrated that grand fir presented better interaction parameters (penetration of the thermoplastic into the cellular structure of wood and the interfacial area HDPE-wood). This enhances mechanical interlocking between phases. The mechanical interlocking mechanism of adhesion might contribute to better predictions for grand fir composites.

Predictions were also more accurate when we used a multiple regression model to calculate *MOR* based on wood content in percentage (*WC*), coupling agent in percentage

(CA) and the response void content also in percentage (Vc). Then, the prediction model for MOR is:

$$MOR = 36.02 - 0.27WC + 4.59CA - 2.85Vc \qquad \text{Eq. 5.13}$$
$$R = 0.993$$

The model makes very precise predictions for both species. According to model coefficients, the coupling agent content and void content on the cross section of experimental composites are the most significant factors for MOR predictions.

Decomposition of the D^f parameter

We were able to decompose the fiber modulus modification factor according to Equation 5.6. First, we found significant differences in wood particle alignment when injection molding and extrusion processes were compared (Figure 5.10). This misalignment presented differences for the two wood species utilized in injection molding and extrusion trials (Figure 5.11). The higher shear rate in injection molding trials allowed better orientation of wood particles (Oswald and Menges, 2003).

For lodgepole pine composites made with an extrusion process, there was no difference in the particle orientation when the wood content increases; on the other hand, grand fir composites presented a slightly different angle of particles with respect to the extrusion direction. The mean particle orientation angle was 12.5° and 33° for injection molding and extrusion, respectively.

Next, we used Equation 5.8 on the filler modulus to estimate a new arbitrary direction. We estimated the D^f_θ factor using Equation 5.7. Table 5.3 presents the results of the decomposition of the general D^f parameter, which was experimentally determined using nanoindentations.

In Table 5.3, mean values of D^f_θ and D^f_D, for injection molding and extrusion are provided. Numerically, the D^f_D factor which may be related to thermo-mechanical degradation of the cell wall during processing, had a higher impact on fiber modulus reduction, particularly for injection molding samples. The double process to produce injection molding composites (extrusion, then injection) may explain these differences. On the other hand, numerically the D^f_θ factor, due to particle alignment or orientation, had a higher impact on modulus reduction of the filler phase in an extrusion process.

CONCLUSIONS

The cell wall reduction modulus of wood cells from two wood species was quantified using nanoindentations. As part of this methodology to characterize wood species effect on an extrusion process, the wood particle alignment was measured on injection molding and extrusion samples. The prediction model based on these measurements provides good approximations to experimental results regarding the modulus of elasticity for lodgepole pine and grand fir composites with coupled and uncoupled systems. Again, grand fir produced the most promising results for WPC properties (MOE-MOR).

According to these findings, WPC properties depend largely on wood particle alignment, resulting in significant differences for the two processes analyzed here, and also for probable thermo-mechanical wood degradation during processing. Thermo-mechanical degradation, associated with the numerical factor D^f_D, was lower when the extrusion process was used.

REFERENCES

1. Agarwal B.D., Broutman L.J. Analysis and performance of fiber composites. John Wiley & Sons, Inc. 1990, p 59.

2. Barbero E.J. Introduction to composite materials design.Taylor and Francis group, 1999.

3. Denn M.M. 2001. Extrusion instability and wall slip. Annual Review Fluid Mechanics, 33: 265-287.

4. Facca A. 2006. Predicting the tensile modulus and strength of single and hybrid natural fibre reinforced thermoplastic composites. Ph.D thesis dissertation, Graduate Department of Chemical Engineering and Applied Chemistry University of Toronto, Canada.

5. Gacitua W., Wolcott M. 2007. Influence of wood species on properties of wood/HDPE composites. *Chapter 2: Morphology of wood species affecting wood-thermoplastic interaction Part II: microstructure and mechanical adhesion*. PhD thesis dissertation, Civil Engineering Department Washington State University Pullman WA.

6. Gacitua W., Wolcott M. 2007. Influence of wood species on properties of wood/HDPE composites. *Chapter 3: Damage of the cell wall during extrusion and injection molding of wood plastic composites.* PhD thesis dissertation, Civil Engineering Department Washington State University Pullman WA.

7. Gindl W., Gupta H.S. 2002. Cell-wall hardness and Young's modulus of melamine-modified spruce wood by nanoindentation. Composite part A.; 33: 1141-1145.

8. Gindl W., Gupta H., Schoberl T., Lichtenegger H. Fratzl P. 2004. Mechanical properties of spruce wood cell walls by nanoindentation. Appl. Phys. A; 79: 2069–2073.

9. Miller E., Rothstain J. 2004. Control of the sharkskin instability in the extrusion of polymer melts using induced temperature gradients. Rheol. Acta 44: 160-173.

10. Oliver W.C., Pharr G.M. An improved technique for determining hardness and elastic modulus using load and displacement sensing indentation experiments. J. Mater. Res. Vol. 7, No 6, June 1992.

11. Osswald T., Menges G. 2003. Material science of polymers for engineers. Hanser, Munich.

12. Pharr G.M. Measurement of mechanical properties by ultra-low load indentation. Materials Science and Engineering A253 (1998) 151-159.

13. Pelletier C.G.N., Dekkers E.C.A., Govaert L.E., den Toonder J.M.J, Meijer H.E.H. 2007. The influence of indenter-surface misalignment on the results of instrumented indentation tests. Polymer testing 2007.

14. Wolcott M.P., Englund K. A technological review of wood plastic composites. 33rd international particleboard/composite material symposium. Washington State University, Pullman WA, 1999.

15. Wood handbook. Wood as an engineering material. General technical report FPL-GTR 113. Forest product laboratory, 1999.

Table 5.1: WPC formulation for extrusion trials.

Formulation	Description
LP 50-0	Wood species is lodgepole pine, 50 % wood, without coupling agent and 1% of lubricant.
LP 65-0	Wood species is lodgepole pine, 65 % wood, without coupling agent and 1% of lubricant.
LP 50-2	Wood species is lodgepole pine, 50 % wood, 2% coupling agent and 1% of lubricant.
LP 65-2	Wood species is lodgepole pine, 65 % wood, 2% coupling agent and 1% of lubricant.
GF 50-0	Wood species is grand fir, 50 % wood, without coupling agent and 1% of lubricant.
GF 65-0	Wood species is grand fir, 65 % wood, without coupling agent and 1% of lubricant.
GF 50-2	Wood species is grand fir, 50 % wood, 2% coupling agent and 1% of lubricant.
GF 65-2	Wood species is grand fir, 65 % wood, 2% coupling agent and 1% of lubricant.

Table 5.2: Cell wall properties (S2 layer) measured with nanoindentations before extrusion. MOE is the modulus of elasticity or Young's modulus.

Wood species	Longitudinal MOE (GPa)	
	Earlywood	Latewood
Grand fir	14.08	16.88
Lodgepole pine	12.73	16.46

Table 5.3: Modulus reduction factor decomposition

Composite/process	D^f	D^f_θ	D^f_D
Lodgepole pine/HDPE *Injection molding*	0.353	0.450	0.784
Grand fir/HDPE *Injection molding*	0.350	0.450	0.777
Mean	**0.350**	**0.450**	**0.781**
Lodgepole pine/HDPE *Extrusion*	0.570	0.850	0.670
Grand fir/HDPE *Extrusion*	0.603	0.850	0.709
Mean	**0.587**	**0.850**	**0.689**

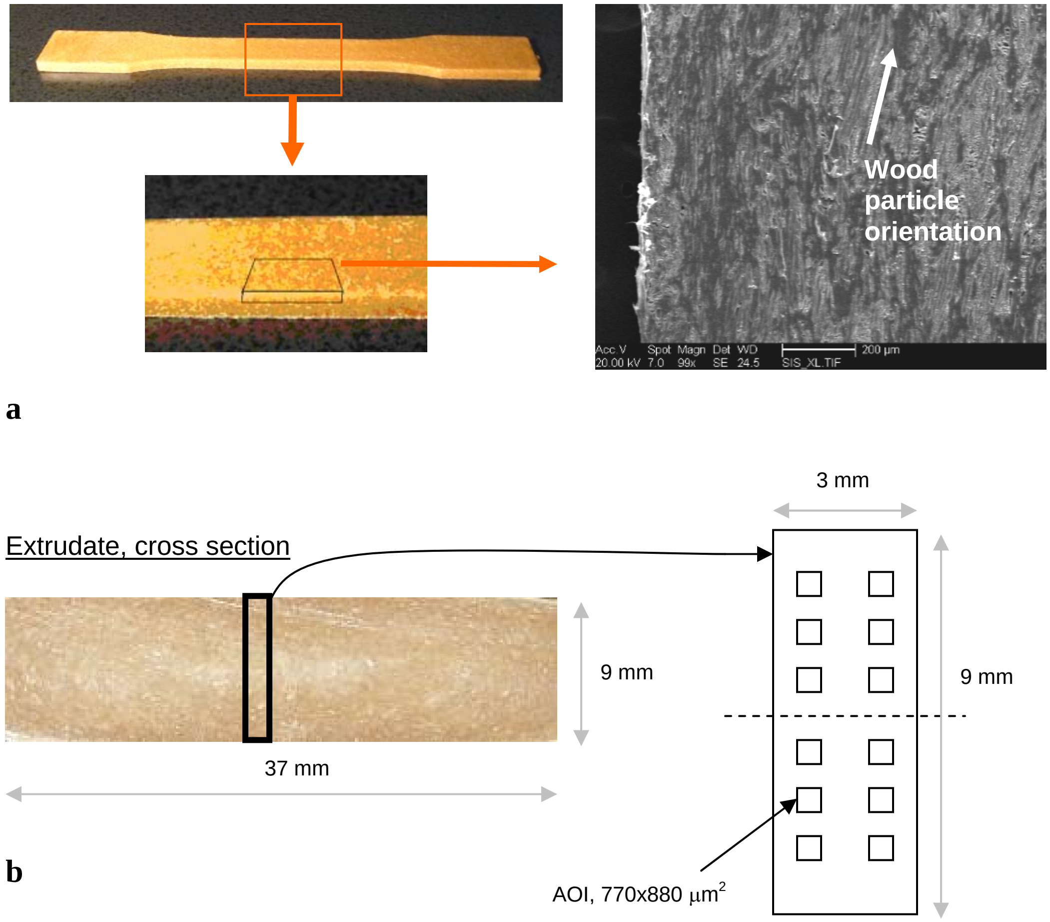

Figure 5.1: a) Sample for wood particle alignment measurements. Example for injection molding samples. b) AOIs captured with SEM from the cross section of extrudates for void content measurements.

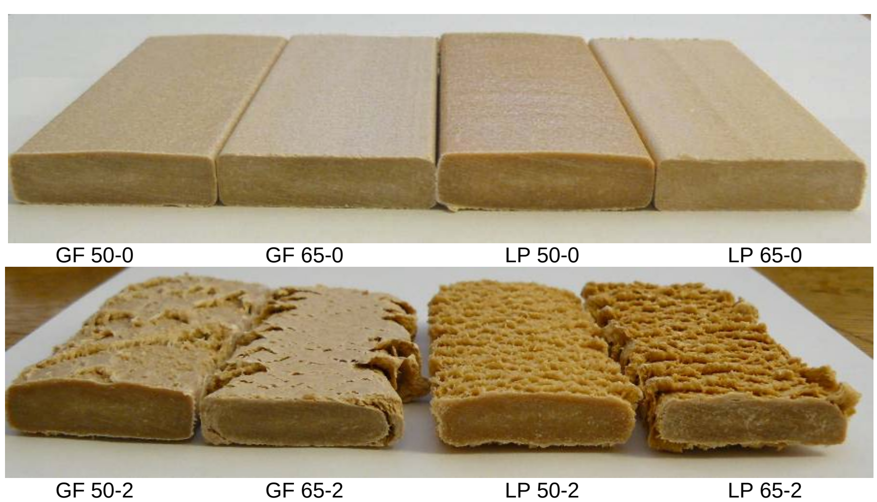

Figure 5.2: Cross section and surface characteristic of experimental WPCs.

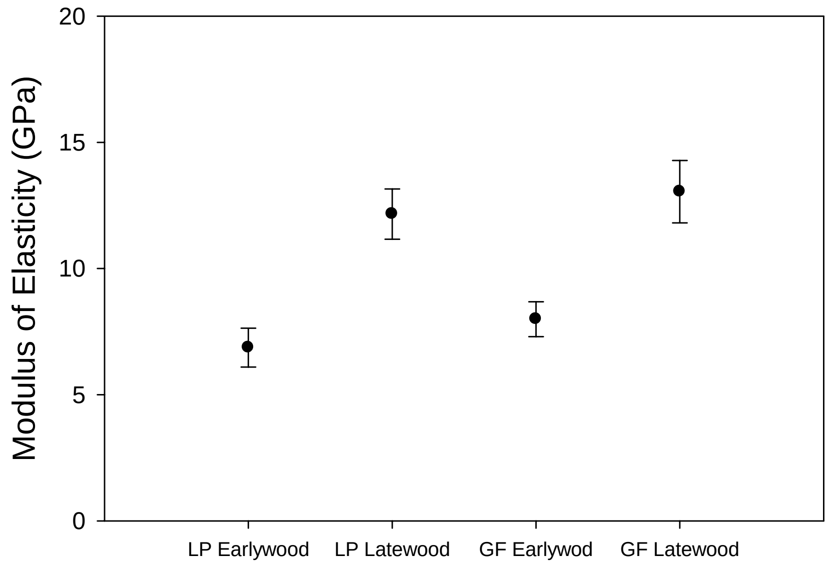

Figure 5.3: 95% interval of confidence for the reduced modulus of elasticity measured with nanoindentations on the S2 layer in experimental composites. Values represent the mean for all formulations for a particular species and type of cell (earlywood or latewood).

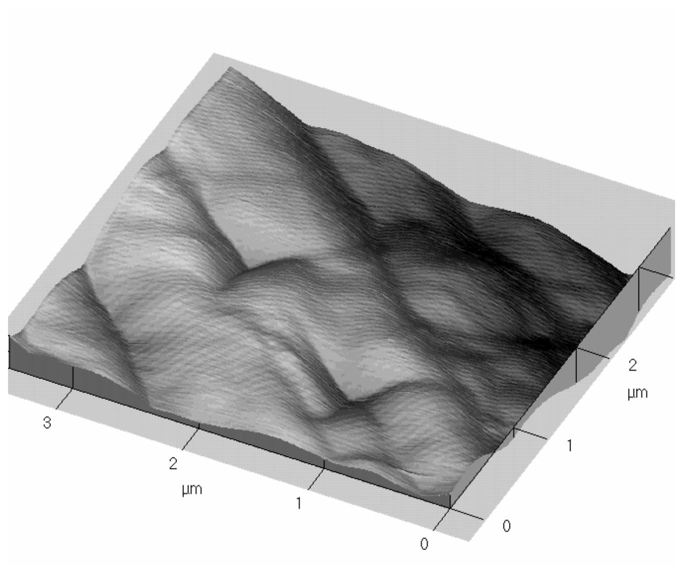

Figure 5.4: In-situ scanning probe microscope 3D image. Topography of the surface showing two indents on an earlywood cell surrounded by the thermoplastic. Grand fir composite (50% wood), without coupling, and 1% lubricant.

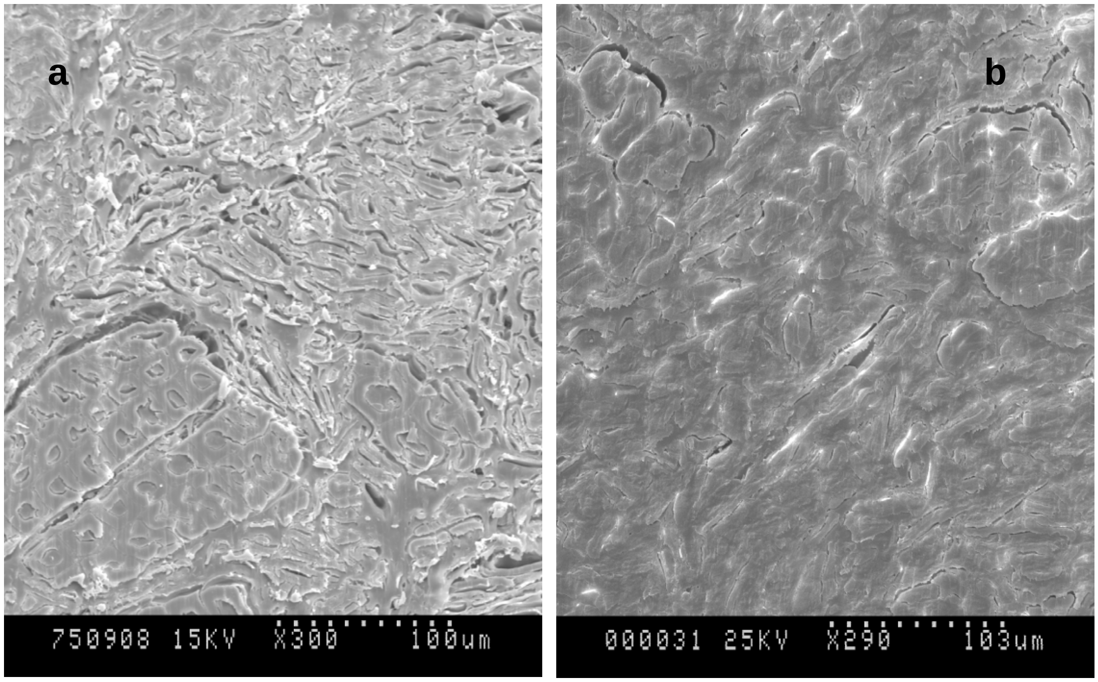

Figure 5.5: SEM images of WPC made of 65% lodgepole pine content and without coupling agent (a). WPC made of 65% grand fir content and 2% coupling agent (b).

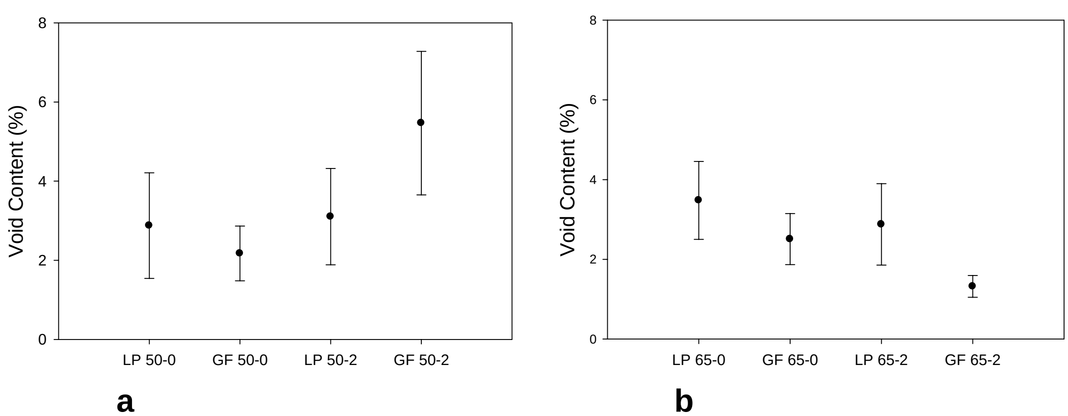

Figure 5.6: Void content of WPCs made with 50% wood, based weight (a) and 65% wood content (b). 95% interval of confidence.

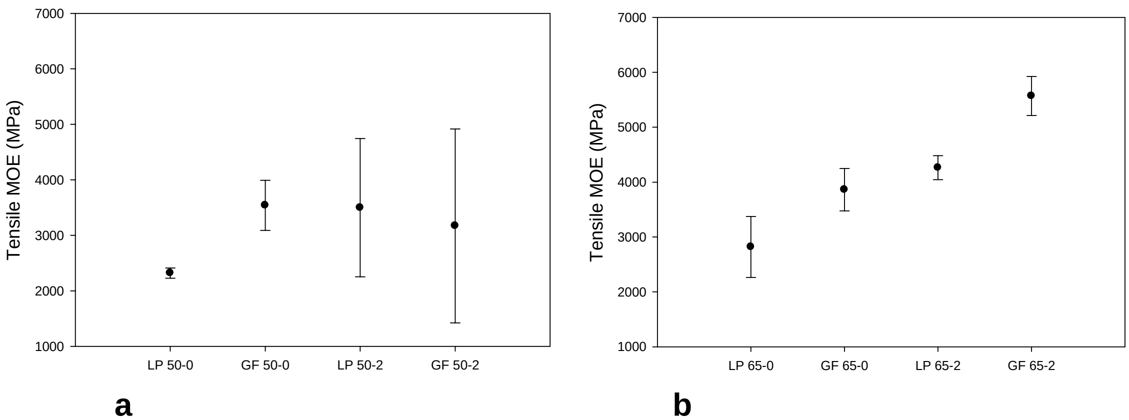

Figure 5.7: Tensile modulus of elasticity (MOE) of WPCs made of 50% wood based on weight (a) and 65% wood (b). 95% interval of confidence.

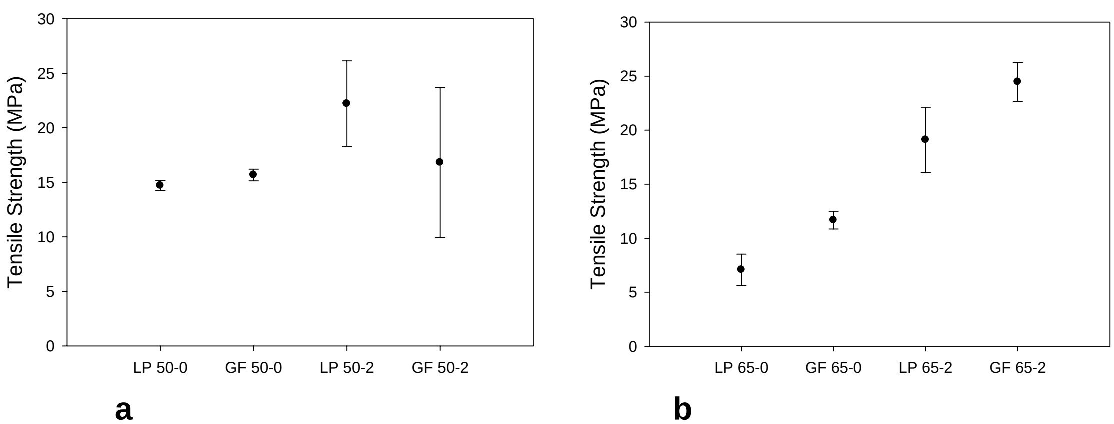

Figure 5.8: Tensile strength (MOR) of WPCs made of 50% wood based on weight (a) and 65% wood (b). 95% interval of confidence.

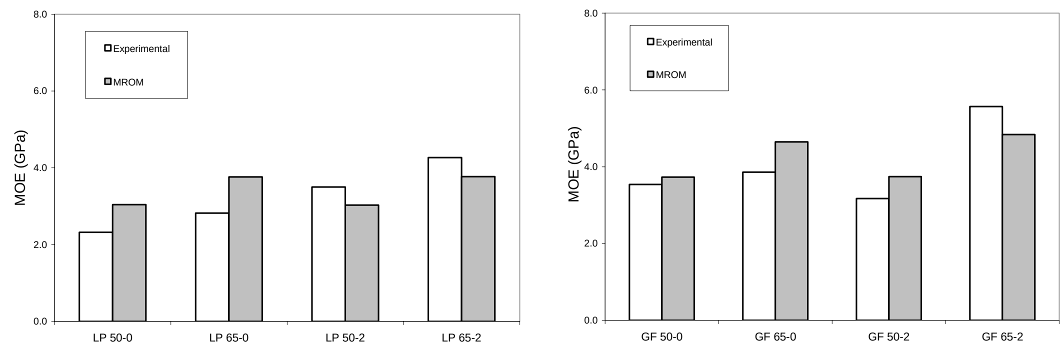

a b

Figure 5.9: Prediction of the longitudinal modulus of elasticity using the modified rule of mixture (MROM). WPCs made of lodgepole pine (a) and grand fir (b).

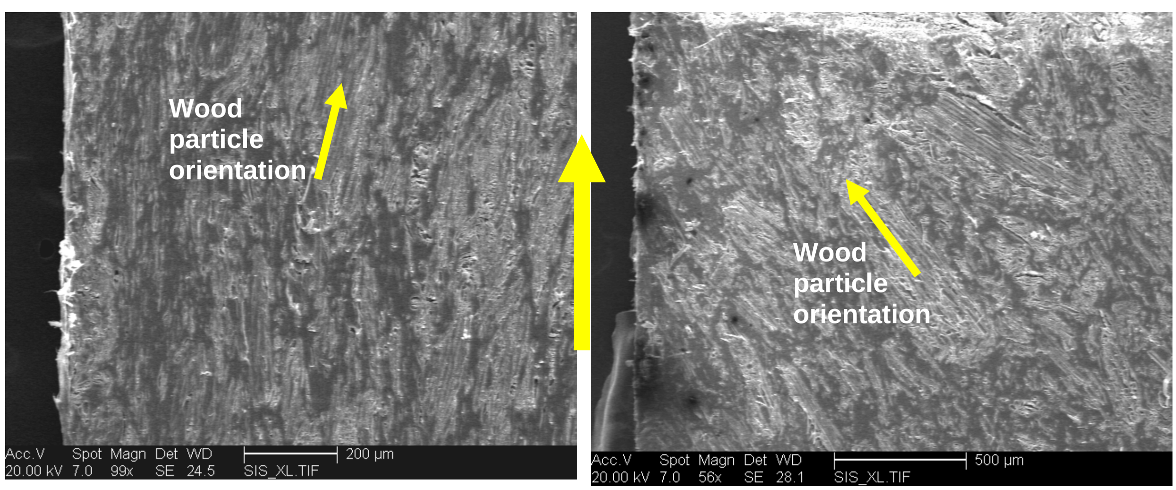

a b

Figure 5.10: SEM images of experimental composites; a) injection molding b) extrusion. Comparison of particle alignment in the 1-direction (arrow).

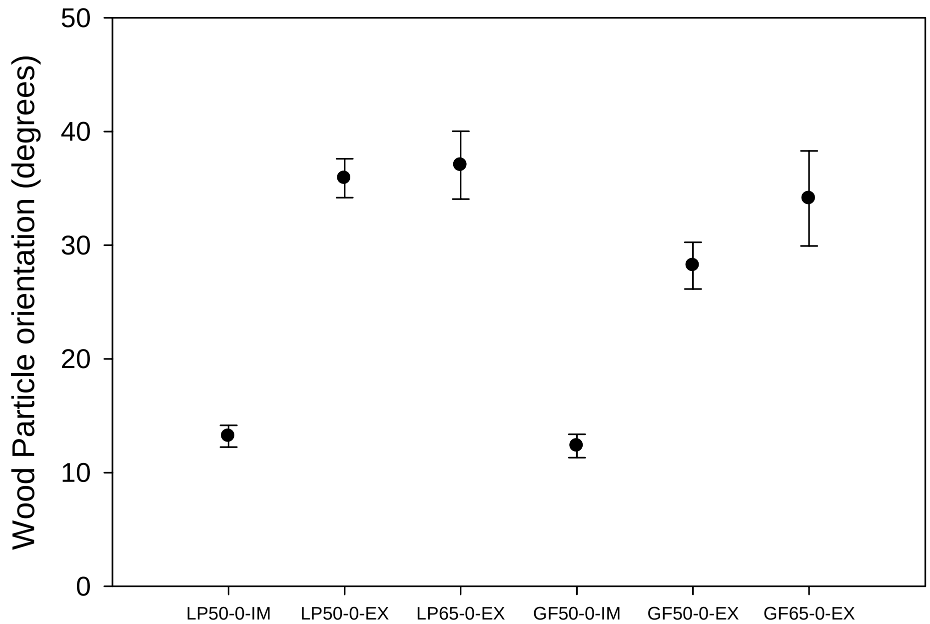

Figure 5.11: Mean value and 95% interval of confidence for wood particle alignment. Notation: LP65-0-IM is lodgepole pine, 50% wood – 0% coupling - injection molding process. GF65-0-EX is grand fir, 65% wood – 0% coupling – extrusion process.

CHAPTER 6
PROJECT SUMMARY AND CONCLUSIONS

In an experiment designed to analyze the physical interaction between a molten thermoplastic and solid wood, results showed a high correlation between the potential area for transverse flow and the interaction between HDPE and wood species. There was also a higher potential area for transverse flow as the interfacial area increased between phases. This potential area was determined based on the diameter and number of pits in or close to the cross field. This demonstrates the influence of anatomical features of wood species on thermoplastic mobility inside the cellular structure. Cell collapse in specific wood species was identified as a probable mechanism impeding mobility of the thermoplastic and thus the interpenetration and interfacial area.

In a creep test analysis, mechanical adhesion was quantified in composites made without additives, and an interphase factor affecting mechanical properties and toughness of the WPC was estimated. This factor represents the slippage between phases, which is determined by using a viscoelastic model and its parameters as an analogy. High correlation coefficients were determined for multiple regression models, used to predict the mechanical properties of experimental WPCs based on the slippage between phases and the interfacial area determined in previous experiments.

Another associated factor contributing to the final strength and variability of WPCs was the void content. A poor interpenetration of the molten thermoplastic into the cell lumens generates conditions for the free buckling of cell walls during extrusion, which finally results in an important source of void generation.

There is a potential reduction in the efficiency of natural fillers on WPC properties when they suffer degradation at the cellular level. This may decrease the constitutive mechanical properties. We explored this by using a methodology based on nanoscale measurements of the properties of the cellular filler before and after injection molding. There was a reduction in Young's modulus of the cell wall due to processing from 40% to 70%.

Based on these findings, we proposed an adapted rule of mixtures. In the new model for predicting the modulus in the 1-Direction, it was assumed that the TCL and bulk matrix had similar mechanical properties. The new model also introduced a modification factor affecting filler properties. This factor represents the modulus reduction in wood cells due to processing, and is expressed as a reduction in modulus in the 1-Direction, where the modulus of the natural filler in a composite was evaluated with nanoindentations.

Finally, we used this methodology to characterize wood species' effect on the extrusion process, where one goal was to evaluate wood particle alignment. We developed a more detailed prediction model based on these measurements, which provided very good approximations to experimental results in the modulus of elasticity for lodgepole pine and grand fir composites in coupled and uncoupled systems. We observed that WPC properties relate to type of wood particle, fiber alignment and void content. We also observed a probable thermo-mechanical degradation of wood during the process, which had a larger effect on double processed composites.

APPENDIX

A. WOOD FLOUR PREPARATION

Figure A.1: Corewood and outerwood boards obtained from logs of 12 inches diameter.

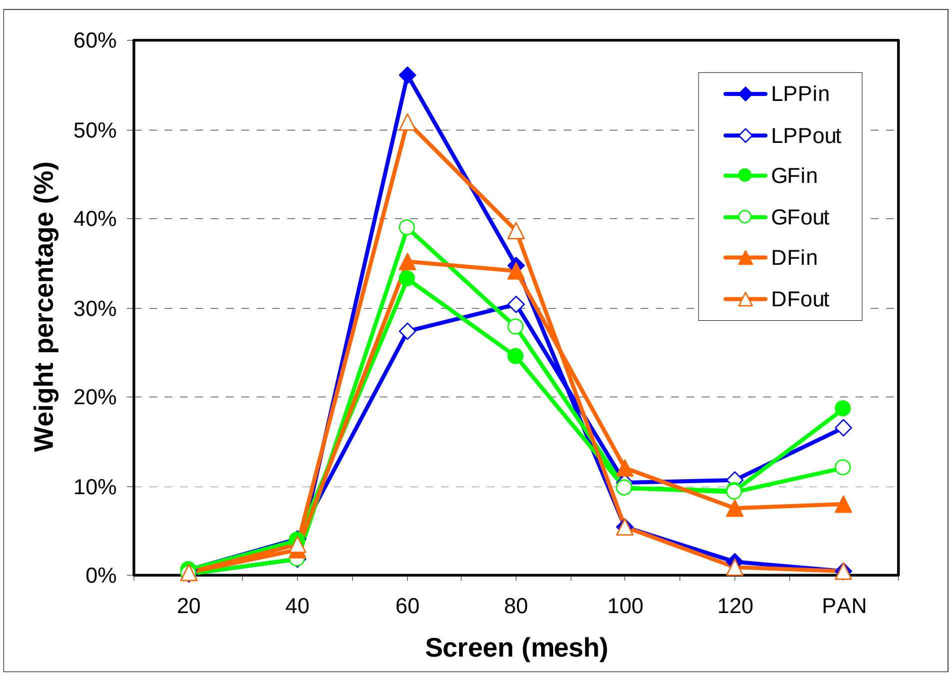

Figure A.2: Wood particle size distribution for lodgepole pine (LPP), garn fir (GF) and Douglas-fir (DF). Wood particles obtained from two locations into a log: corewood (in) and outerwood (out).

B. INJECTION MOLDING EXPERIMENTS AND NANOINDENTATIONS

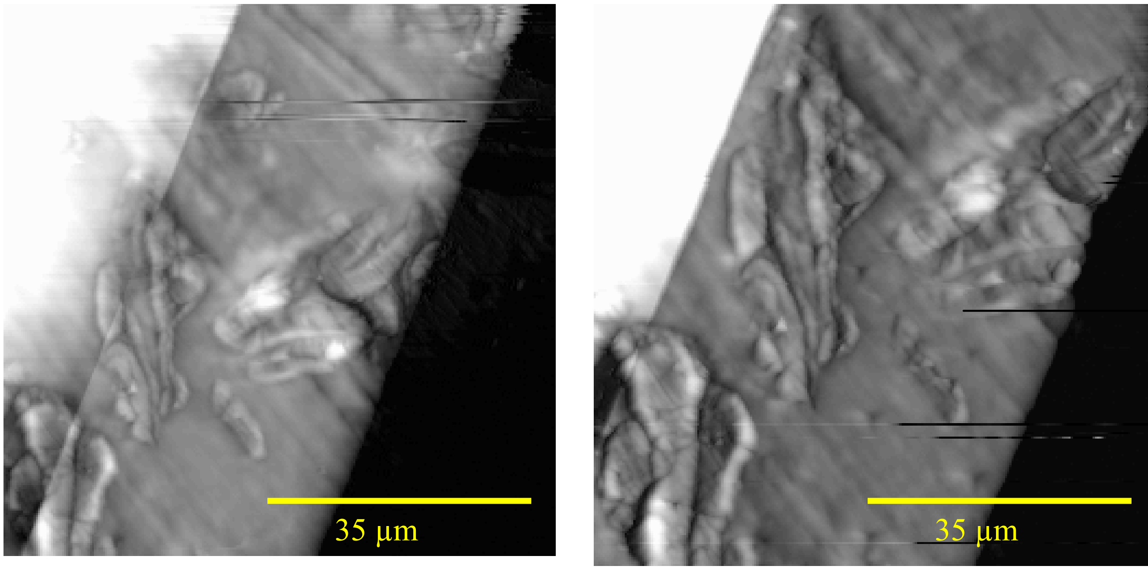

a **b**

Figure B.1: In situ scanning probe image. Cross section of a WPC made of grand for, before (a) and after indentations on cell walls, TCL and matrix.

C. EXTRUSION TRIALS

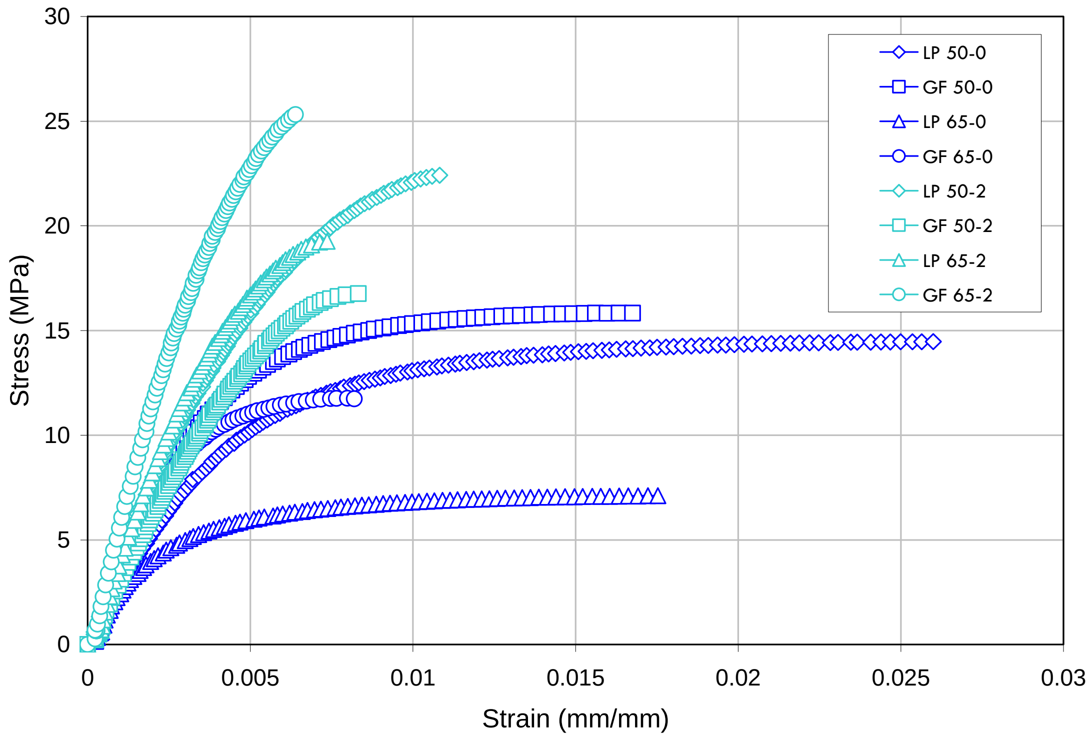

Figure C.1: Stress strain relation for extrusion trials.

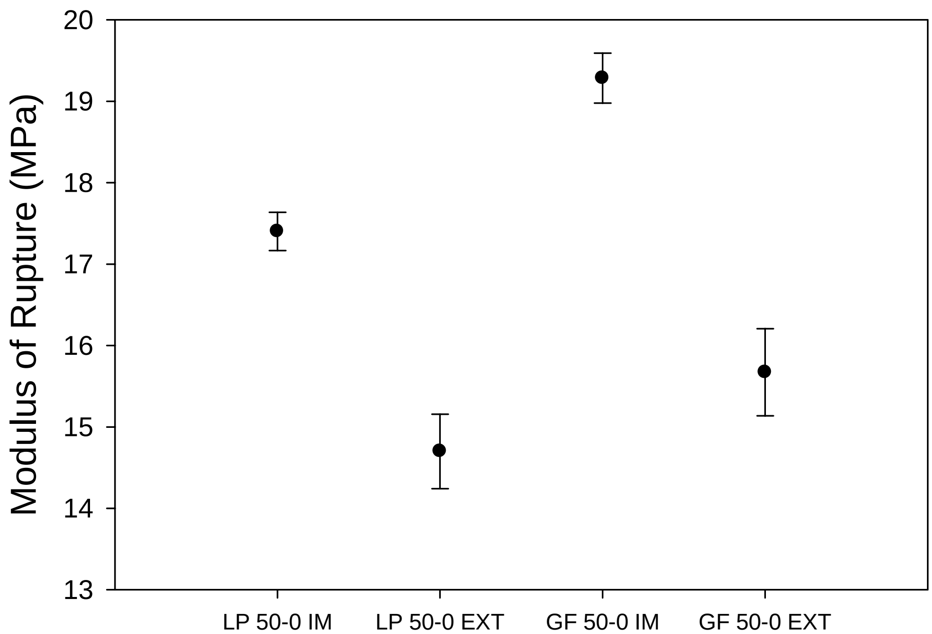

Figure C.2: Comparison of modulus of rupture. Injection molding vs. extrusion.

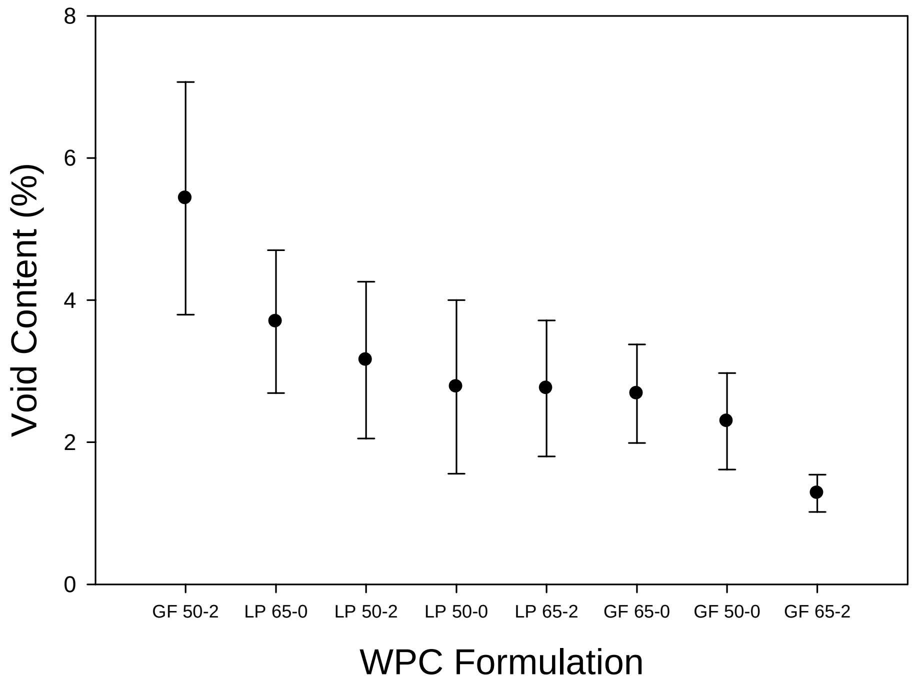

Figure A.C: Void content of composites. Process, extrusion.

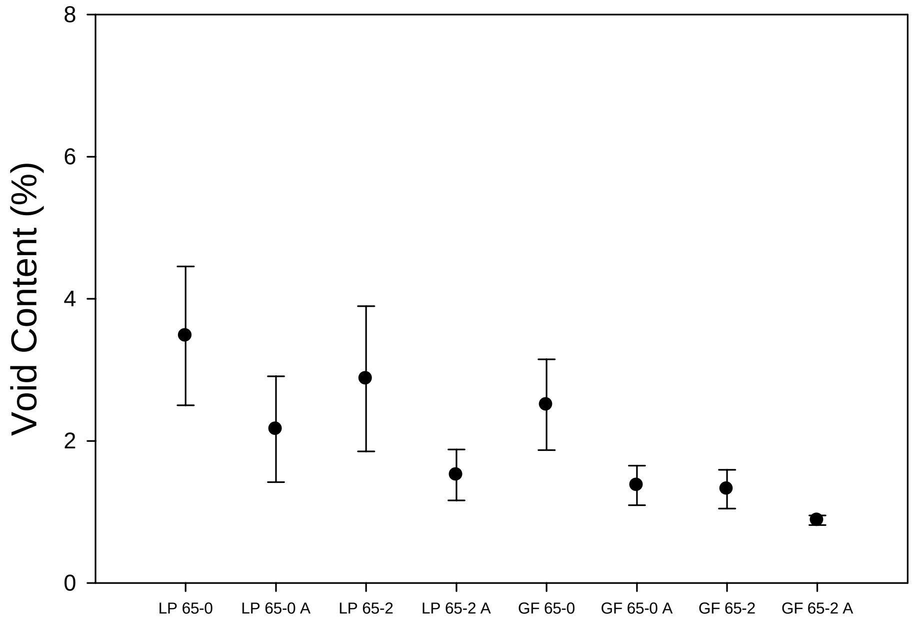

Figure C.4: Reduction of void content after tensile test. "A" represents the condition after testing. Process, extrusion.